COENZYME Q_{10} CONTENT, COMPOSITION, TEXTURE AND PHYSIOCHEMICAL CHARACTERISTICS OF PASTA FORTIFIED WITH FREEZE–DRIED BEEF HEART

A Dissertation

presented to

the Faculty of the Graduate School

at the University of Missouri–Columbia

In Partial Fulfillment

of the Requirements for the Degree

Doctor of Philosophy

---

by

KHWANKAEW DHANASETTAKORN

Dr. Ingolf U. Grün, Dissertation Co–Supervisor

Dr. Mengshi Lin, Dissertation Co–Supervisor

DECEMBER 2008

The undersigned, appointed by the Dean of the Graduate School, have examined the dissertation entitled

COENZYME Q_{10} CONTENT, COMPOSITION, TEXTURE AND PHYSIOCHEMICAL CHARACTERISTICS OF PASTA FORTIFIED WITH FREEZE–DRIED BEEF HEART

presented by Khwankaew Dhanasettakorn

a candidate for the degree of Doctor of Philosophy

and hereby certify that in their opinion it is worthy of acceptance.

Dr. Ingolf U. Grün, Food Science	Dr. Mengshi Lin, Food Science
Dr. Andrew D. Clarke, Food Science	Dr. Fu–Hung Hsieh, Food Science
Dr. Jason W. Cooley, Chemistry	Dr. Mark Ellersieck, Statistics

ACKNOWLEDGEMENTS

I would like to express my deepest and sincere gratitude to my advisor, Dr. Ingolf U. Grün, for his support, meaningful supervision and valuable suggestion during my study. Beyond his constructive and moral guidance, Dr. Grün has always supported me with his kindness and understanding, which enabled me to complete my work successfully. Similarly, my great appreciation is expressed to my co–advisor, Dr. Mengshi Lin, for his beneficial criticism and precious academic advice during my graduate work.

I am also grateful to my committee members, Dr. Andrew D. Clarke, Dr. Fu–Hung Hsieh, Dr. Mark Ellersieck, and Dr. Jason W. Cooley, for their constructive comments and helpful discussions that helped me to enhance the quality of my work.

My sincere thanks go to Mr. Lakdas Fernando and Mr. Harold Huff for their technical assistances and contributions in laboratory facilities. Without them, I would not have been able to work on my research efficiently.

I would like to express my thanks to all of my friends and all staff members in the Food Science program at the University of Missouri, especially JoAnn Lewis, for their kindness and friendliness since I have been here in the program.

Last but not least, I wish to express my truthful appreciation to my loving family, especially my grandfather, my parents, my sister and my aunt, for their love, understanding, and encouragement, both for strength and financial support during pursuing the doctoral degree in Food Science at the University of Missouri, Columbia.

TABLE OF CONTENTS

LIST OF ILLUSTRATIONS

Figure **Page**

LIST OF TABLES

Table **Page**

LIST OF ABBREVIATIONS

~	Approximately
°C	Degree Celsius
hr	Hour
i.e.	id est (that is)
Kg	Kilogram
μg	Microgram
mg	Milligram
mL	Milliliter
min	Minute
n.d.	No date

COENZYME Q_{10} CONTENT, COMPOSITION, TEXTURE AND PHYSIOCHEMICAL CHARACTERISTICS OF PASTA FORTIFIED WITH FREEZE–DRIED BEEF HEART

Khwankaew Dhanasettakorn

Dr. Ingolf U. Grün, Dissertation Co–Supervisor

Dr. Mengshi Lin, Dissertation Co–Supervisor

ABSTRACT

This study evaluated the feasibility of fortifying fresh pasta with beef heart, a beef by–product high in coenzyme Q_{10}. Incorporating freeze–dried beef heart into pasta significantly increased coenzyme Q_{10} and protein content, which were unaltered by cooking, but also significantly changed physical attributes, including texture and color, of the fortified pasta products. Alterations in pasta matrixes, after partially replacing durum wheat flour with freeze–dried beef heart, were evaluated at the molecular level using vibrational spectroscopic methods, FT–IR and Raman spectroscopy accompanied by multivariate statistical analyses. The results were deducted that lipid−protein interactions, β−sheet arrangement, the starch network, and cysteine thiol groups might contribute to hardness and chewiness of the pasta products. The lipid fraction and β−sheet alignment were possibly involved in pasta adhesiveness. Pasta firmness might be caused by β−sheet structure and the polysaccharide network. Pasta cohesiveness might be affected by the α−helical structures and hydrogen bonds in the gluten network. It was concluded that FT−IR and Raman Spectroscopy can be applied to evaluate physiochemical changes of pasta and showed a potential use for quality assessment in pasta products because of rapidly and non–destructively determining changes related to many food components, including protein, carbohydrate, and lipid, at one time measurement.

CHAPTER 1

INTRODUCTION

The growing concerns for general health, chronic disease preventing and aging have fueled consumer interest in healthy foods. The USDA Food Guide Pyramid (USDA 1996) recommends daily servings for each food group in order to get a proper balance of nutrients as follows:

- Six to eleven servings of bread, cereal, rice and pasta
- Three to five servings of vegetables
- Two to four servings of fruits
- Two to three servings of milk, yogurt or cheese
- Two to three servings of meat, poultry, fish, legumes, eggs and nuts

No one food group is more important than another. Therefore, to stay healthy, people need them all. Much of the current interest in healthy foods, however, has focused on bioactive ingredients, such as carotenoids, dietary fiber, fatty acids, phenols, plant sterols, soy proteins, and coenzyme Q_{10}. In addition, the 2004 Prepared Foods Survey O'Donnell (2004a) indicated that soy proteins and antioxidants would be the two most important additions to functional food formulations, and coenzyme Q_{10} would be part of a brighter future for antioxidants (O'Donnell 2004b). Furthermore, the reduced form of coenzyme Q_{10}, ubiquinol, is the only fat–soluble antioxidant synthesized in the human body that is involved in protecting cellular membranes and plasma lipoproteins from lipid peroxidation (Kishi and others 1999; Kagan and Quinn 2000). As a result, this study

focuses exclusively on coenzyme Q_{10} in terms of being a pharmacologically active agent because of its potentially very positive effects on health.

Increased consumption of coenzyme Q_{10} from a diet fortified with coenzyme Q_{10} might be an alternative to dietary supplements to sustain good health. Consequently, development of a healthy addition to our diet is the aim of this study in order to help consumers' achieve beneficial health effects. In order to formulate functional food products containing elevated level of coenzyme Q_{10}, pasta was chosen as the food vehicle because of its popularity and the large number of recommended serving (USDA 1996). The American Dietetics Association describes a serving of cooked pasta as the size of a tennis ball or one cup of cooked pasta made from 2 ounces of dry pasta (ADA's Public Relations Team 2004a, 2004b). Therefore, because of the potentially large amount of consumption, fortified pasta will provide more coenzyme Q_{10} than traditional cereal grain foods. In a comparison of new side dish products, including pastas, potato products, rice, and soup, which were launched in 2003, pastas came out on top (Roberts 2004).

Daily consumption of 30 – 200 mg coenzyme Q_{10} can promote and sustain good health (Weber and others 1994; Barbieri and others 1999; Hodges and others 1999; Langsjoen and Langsjoen 1999; Munkholm and others 1999; Overvad and others 1999). Nevertheless, the cost of coenzyme Q_{10} supplements is not cheap, approximately 15 – 45 dollars per month for healthy individuals. Moreover, for a patient whose recommended dose is larger than the one recommended for healthy people, the estimated cost is 3 – 10 dollars/day (UC Berkeley Wellness Letter 2003). Therefore, making coenzyme Q_{10} available for all people through less expensive coenzyme Q_{10} enriched diets might be another way to provided recommended amounts of coenzyme Q_{10}. Beef heart was chosen

as the source of coenzyme Q_{10} because using beef heart is obviously very economical. Although coenzyme Q_{10} is considered fairly stable, the effect of cooking on the compound was also of interest because coenzyme Q_{10} might be lost under household cooking conditions, which have not been investigated yet.

However, partial substitutions of a food component of any food may have unintended consequences. For example, partially substituting durum wheat flour with beef heart in home–made pasta might alter texture attributes in newly formulated pasta products. In order to understand the effects of beef heart addition on the pasta matrix, it is necessary to investigate the physicochemical changes at the molecular level. The outcome of this study can subsequently be applied for the quality assessment of pasta products.

1.1 Objectives of the study

The objectives of this study were as follows:

- To formulate pasta products containing elevated level of coenzyme Q_{10} by replacing durum wheat flour with beef heart.
- To investigate the effect of a common household cooking method, i.e. boiling, on coenzyme Q_{10} content in the newly formulated pasta products.
- To determine the effect of beef heart additions on texture attributes of the newly formulated fresh home–made pasta.
- To determine the effect of beef heart additions on the color of the newly formulated pasta.

- To examine proximate composition and cholesterol content of the cooked home–made pasta fortified with beef heart.
- To investigate physiochemical changes including changes of food component interactions and food structural conformations in cooked home–made pasta made with durum wheat flour and also in pasta made with additional beef heart using vibrational spectroscopic methods, FT–IR and Raman spectroscopy, combined with multivariate statistical analyses.

CHAPTER 2

LITERATURE REVIEW

2.1 Pasta

2.1.1 Overview

Pasta is a popular side dish and also one of the well–liked main dishes throughout a large part of the world. Recently, pasta consumption per capita in the US market has increased. The reasons, given by American consumers, are that pasta is healthy, easy to store at home, and simple to prepare (Kill 2001). Pastas are introduced worldwide in a large variety of shapes and sizes such as spaghetti, macaroni, lasagna and farfalle (bowties). Pasta could be categorized into two basic styles, fresh and dried pastas. However, whether classified as fresh or dried, whether appearing in different shapes and sizes, all pastas are prepared by a similar approach. The basic ingredients for making pasta are durum wheat flour (or semolina) and water. Thus, pasta is obviously a wheat flour–based product, which is low in protein, as well as some vitamins and minerals. To improve the nutritional quality of pasta, additional ingredients are usually included, such as eggs, vitamins, and natural colorants from spinach and tomato (Kill 2001). In order to create diversity of pasta products to support human nutritional needs and consumer food choices, many researchers have also incorporated various plant proteins, such as soy flour (Shogren and others 2006), corn germ flour (Lucisano and others 1984), legume flour (Zhao and others 2005), whey proteins (Schoppet and others 1976) or animal proteins, i.e. fish (Kim and others 1990) into pasta products.

2.1.2 Durum wheat

All types of wheat, which include wild and cultivated wheat, are members of the genus of *Triticum*. There are many criteria that have been used to classify the *Triticum* such as using physiology, morphology, cytogenetic, and cytology (Wiseman 2001). However, it is impractical to discuss all wheat types comprehensively in this section. Therefore, this literature review revolves the common questions of what durum wheat is and what the difference is between durum wheat flour and bread wheat flour.

Both durum wheat (macaroni wheat) and bread wheat (common wheat) belong to the genus *Triticum*. The scientific names of durum wheat and bread wheat are *Triticum durum* and *Triticum aestivum*, respectively. *T. durum* is commonly considered as being a larger grain with more elongated shape than *T. aestivum*, which is generally smaller and more ovate in shape (Wiseman 2001) (Figure 2.1). While durum wheat has a particularly hard endosperm that give coarse yellow semolina after milling, bread wheat has a starchy floury endosperm, which is more simply milled (Wiseman 2001). Nutritional values compared between durum wheat flour and common wheat flour are shown in Table 2.1.

Figure 2.1. Wheat characteristics: A.) *Triticum durum* (durum/macaroni wheat) and B.) *Triticum aestivum* (common/bread wheat) (Department of Horticulture and Crop Science, the Ohio State University n.d.)

Table 2.1. Nutritional values of durum wheat flour and common wheat flour (U.S. Department of Agriculture, Agricultural Research Service 2007)

Nutrient	**Units**	**Value per 100 grams**	
		Durum wheat	**Bread wheat**
Proximates			
Water	g	10.94	13.36
Energy	kcal	339	361
Protein	g	13.68	11.98
Total lipid (fat)	g	2.47	1.66
Ash	g	1.78	0.47
Carbohydrate, by difference	g	71.13	72.53

Table 2.1. Nutritional values of durum wheat flour and common wheat flour (U.S. Department of Agriculture, Agricultural Research Service 2007) (continued)

Nutrient	Units	Value per 100 grams	
		Durum wheat	Bread wheat
Minerals			
Calcium, Ca	mg	34	15
Iron, Fe	mg	3.52	0.90
Magnesium, Mg	mg	144	25
Phosphorus, P	mg	508	97
Potassium, K	mg	431	100
Sodium, Na	mg	2	2
Zinc, Zn	mg	4.16	0.85
Copper, Cu	mg	0.553	0.182
Manganese, Mn	mg	3.012	0.792
Selenium, Se	mcg	89.4	39.7
Vitamins			
Vitamin C	mg	0	0
Thiamin	mg	0.419	0.080
Riboflavin	mg	0.121	0.060
Niacin	mg	6.738	1.000
Pantothenic acid	mg	0.935	0.438
Vitamin B–6	mg	0.419	0.037
Folate, total	mcg	43	33
Vitamin B–12	mcg	0	0
Vitamin A	IU	0	2

The major functional characteristic of the *Triticum* grains, especially *Triticum durum* and *Triticum aestivum*, is contributed by the gluten proteins, consisting of gliadin and glutenin, which are essential components in the bread and pasta making process (Pasta 2004). These protein components, which are involved in the formation of the gluten matrix in wheat flours, are illustrated in Table 2.2. However, the production of bread and pasta is fairly dissimilar because bread is a leavened product, while pasta does not require any leavening time. Wheat flour used in bread production, therefore, has a different chemical composition than durum wheat flour, which is used in pasta production, in which dough leavening is not only dispensable but must be avoided. Thus native enzymes that can hydrolyze sugars contained in the grains, which are main factors in dough leavening, must be kept to a minimum in order to keep pasta dough from being leavened (Pasta 2004).

Table 2.2. Average protein content in wheat flours from the *Triticum* grains (Pasta 2004)

	Albumin	Globulin	Gliadin	Glutenin	Amino acid residue
Triticum durum	13.2	12.0	39.8	21.5	14.5
Triticum aestivum	16.2	9.4	34.2	37.6	5.5

2.1.3 Physical chemistry of pasta

According to Damodaran (1996), wheat protein consists of soluble and insoluble protein fractions. The soluble proteins (about 20% of the total proteins) are mainly albumin– and globulin–type enzymes as well as minor glycoproteins. These proteins are not involved in the dough–forming properties of wheat flour. The major protein of wheat for dough formation is gluten. Gluten is a heterogeneous mixture of proteins, primarily gliadins and glutenins, with limited solubility in water. The structures of glutenins and gliadins contributing to the gluten formation are presented in Figure 2.2. Kitts (n.d.) mentioned that one significant difference between gliadins and glutenins is that gliadins only have intra–molecular disulfide linkages while glutenins have both inter– and intra–molecular disulfide linkages. As a result, gliadins are more compact and have a globular shape and the glutenins are linear.

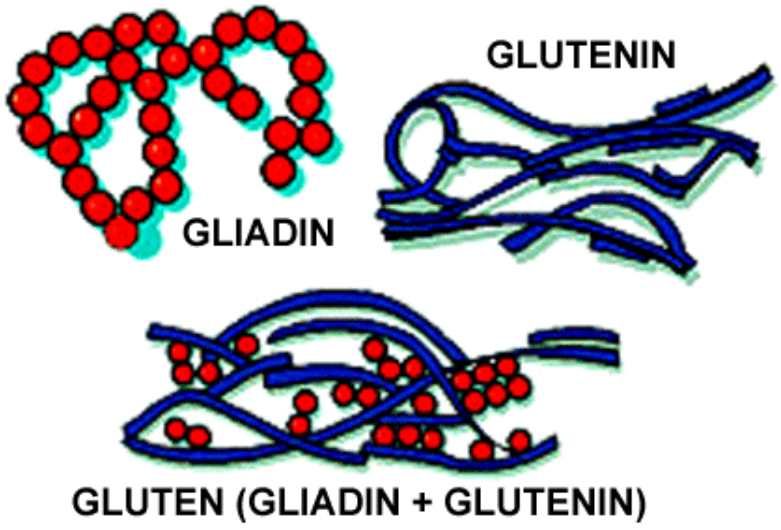

Figure 2.2. The structures of glutenins and gliadins contributing to gluten formation (Kitts n.d.)

Gluten has a unique amino acid composition, with glutamate/glutamine (Glu/Gln) and proline (Pro) accounting for more than 50% of the amino acid residues (Damodaran 1996). The low water solubility of gluten is attributable to its low content of lysine (Lys), arginine (Arg), Glu, and aspartic acid (Asp) residues, which together amount to less than 10% of the total amino acid residues (Damodaran 1996). About 30% of amino acid residues in gluten are hydrophobic and the residues contribute greatly to its ability to form protein aggregates by hydrophobic interactions and to bind lipids and other nonpolar substances (Damodaran 1996). Since gluten is formed in an aqueous media and gluten proteins contain several amino acids with hydrophobic side chains, such as alanine (Ala), leucine (Leu), phenylalanine (Phe), isoleucine (Ile), valine (Val), and Pro, from a thermodynamic point of view, these nonpolar groups tend to link with each other via hydrophobic interactions (Lasztity 1996). However, the high content of glutamine and hydroxyl amino acids (about 10%) in gluten is accountable for its water binding properties (Damodaran 1996). In addition, hydrogen bonds between glutamine and hydroxyl residues of gluten polypeptides contribute to its cohesion–adhesion properties (Damodaran 1996). Cysteine and cystine residues, which account for 2 – 3% of total amino acid residues in gluten, lead to sulfhydryl–disulfide interchange reactions, resulting in extensive polymerization of gluten proteins during dough formation (Damodaran 1996). The functional groups in the gluten protein are shown in Table 2.3.

Table 2.3. Functional groups in gluten protein (mmol/100 g protein) (adapted from Lasztity 1996)

Group	Gliadin	Glutenin	Amino acids
Acidic	27	36	Glu, Asp
Basic	39	52	Lys, Arg, His, Trp
Amide	309	266	Gln, Asn
Thiol and disulfide	12	12	Cys, Cystine
Total ionic	66	87	Acidic + basic
Total polar	381	365	Hydroxy + amide
Total nonpolar	390	301	

In the pasta making process, mixing and kneading durum wheat flour with water induces gluten formation. Under the applied shear and tensile forces, the gluten proteins gliadin and glutenin absorb water and partially unfold (Damodaran 1996). The partial unfolding of protein molecules facilitates hydrophobic interactions and sulfhydryl–disulfide interchange reactions (Damodaran 1996). The tentative model of the role of gliadins in the formation of disulfide bonds is presented in Figure 2.3.

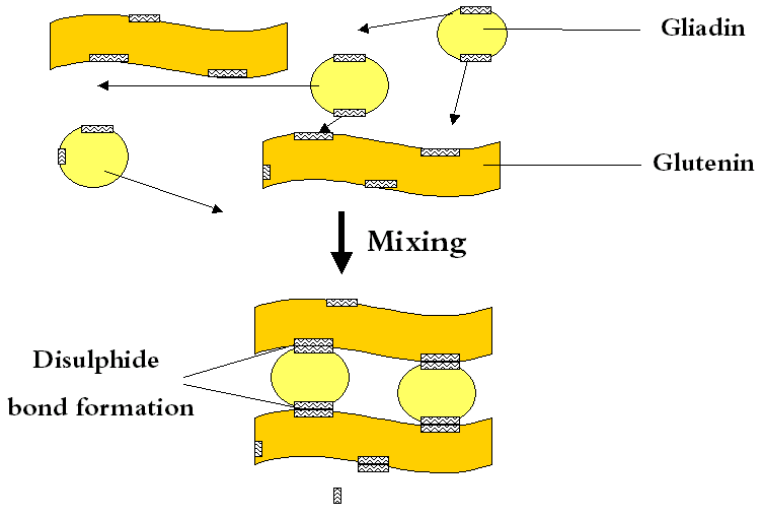

Figure 2.3. Tentative model of disulfide bond formation created between gliadin and glutenin (Anonymous 2005)

Weegels and others (1991) explained that at the beginning, hydrophobic gliadins would interact with hydrophobic sites on the C– and N–terminal ends of glutenins. This phenomenon could facilitate the –SH containing ends in disulfide bond formation. They believed that the non–covalent interactions of gliadins with glutenins take place first and covalent interactions occur subsequently. Therefore, disulfide bonds, hydrogen bonds, and hydrophobic interactions arising during development of gluten are the crucial interactions between wheat protein components, according to Lasztity (1996) and Damodaran (1996). In addition, the unique viscoelastic properties of wheat flour–based foods (such as bread, noodles, and pasta) are also caused by two gluten proteins, glutenin and gliadin (Wrigley 1996). The large polymers of glutenin create resistance to extension forces during dough–mixing (springiness), while at the same time, the gliadin monomers have a plasticizer functions (Wrigley 1996). According to Pezolet and others (1992) and Popineau and others (1994), alignments of β–sheets in gluten dough matrixes might

contribute to viscoelasticy in the dough because an increase of β–sheet contents, especially intermolecular β–sheets, together with a reduction of α–helix formation observed in a doughy hydrated state. The common protein secondary structures, which include parallel β pleated sheet, antiparallel β pleated sheet, and α–helix, are depicted in Figure 2.4.

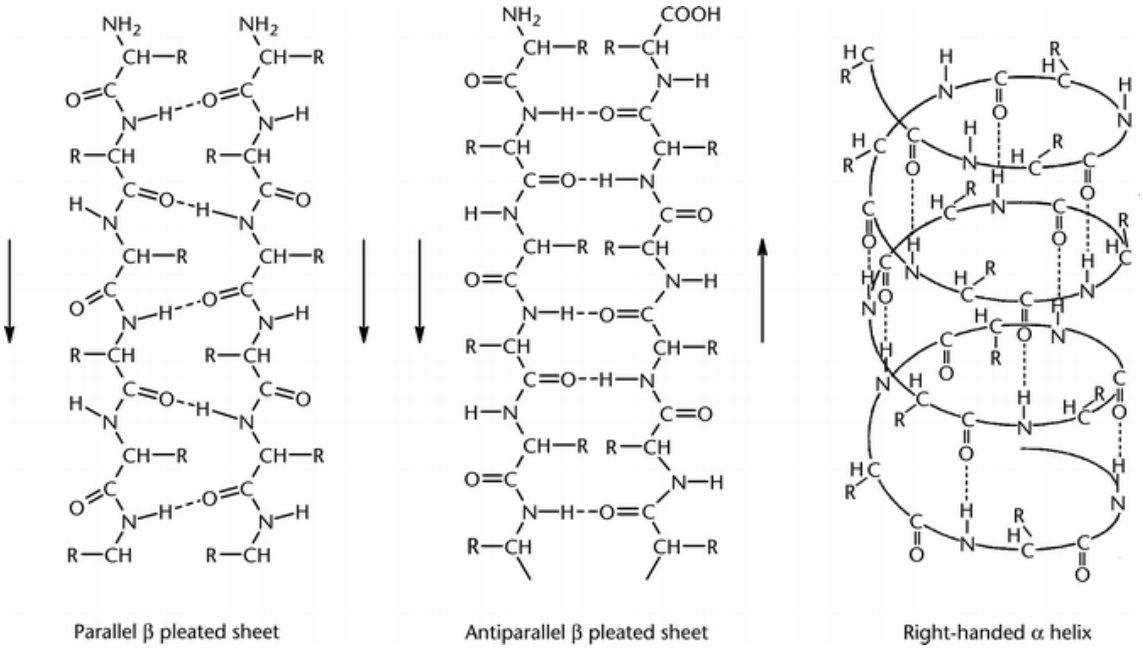

Figure 2.4. Secondary structures of proteins (Pietzsch n.d.)

The majority of protein–lipid complexes are measurable in dough as well (Lasztity 1996). The two models of the nature of protein–lipid interaction in the gluten network are depicted in Figure 2.5. Lasztity (1996) assumed that the protein–lipid complex is formed by electrostatic interactions between the numerous polar side chains of protein and polar phospholipids and/or glycolipids. In addition, hydrophobic

interactions are probably involved in the formation of the protein–lipid complex (Lasztity 1996).

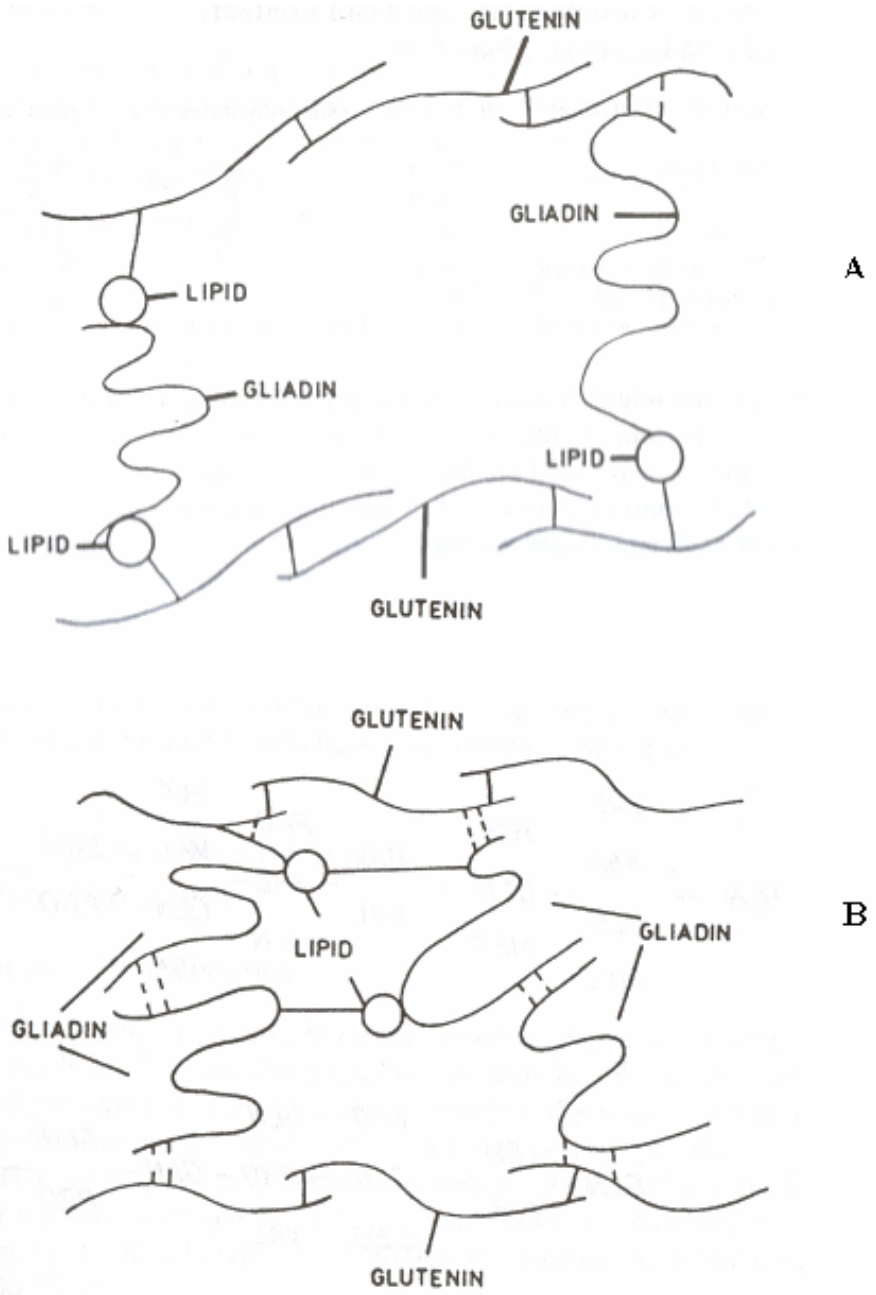

Figure 2.5. Possible location of lipids in the gluten network: A) lipid mediates the gliadin–glutenin interactions; B) lipid mediates the gliadin–gliadin interactions. (Lasztity 1996)

While covalent interactions, especially disulfide bonds formed during gluten development, are the conventional intermolecular connections, Weegels and others (1991) acknowledged that carbohydrates can also form covalent bridges between gluten proteins. At low temperature, such as room temperature, interactions between protein and starch are charge–charge (ionic) phenomena (Marshall and Chrastil 1992). However, upon heating with unlimited water being available, proteins can undergo extensive cross-linking, mainly through disulfide bond linkage to form a continuous protein network (Marshall and Chrastil 1992). In case of starch, high temperature with excess water leads to gelatinization. When protein and starch are in contact with each other, stable complexes can develop by formation of a protein–starch matrix, where hydrogen bonding and covalent bonding, in addition to charge interactions may be found (Marshall and Chrastil 1992). Lasztity (1996) reviewed that a minor portion of carbohydrate is bound by gliadin components and the major carbohydrate components are glucose, galactose, and mannose.

Walstra (2003) summarized that the structure of the dough consists of partially swollen starch grains and a continuous phase of homogeneous viscoelastic liquid that includes water, protein, other nonstarch solids and part of the amylose. As a result, a combination of protein–protein, protein–lipid, and protein–carbohydrate interactions could be contributing to the formation of pasta matrixes, according to Wrigley (1996) (Figure 2.6).

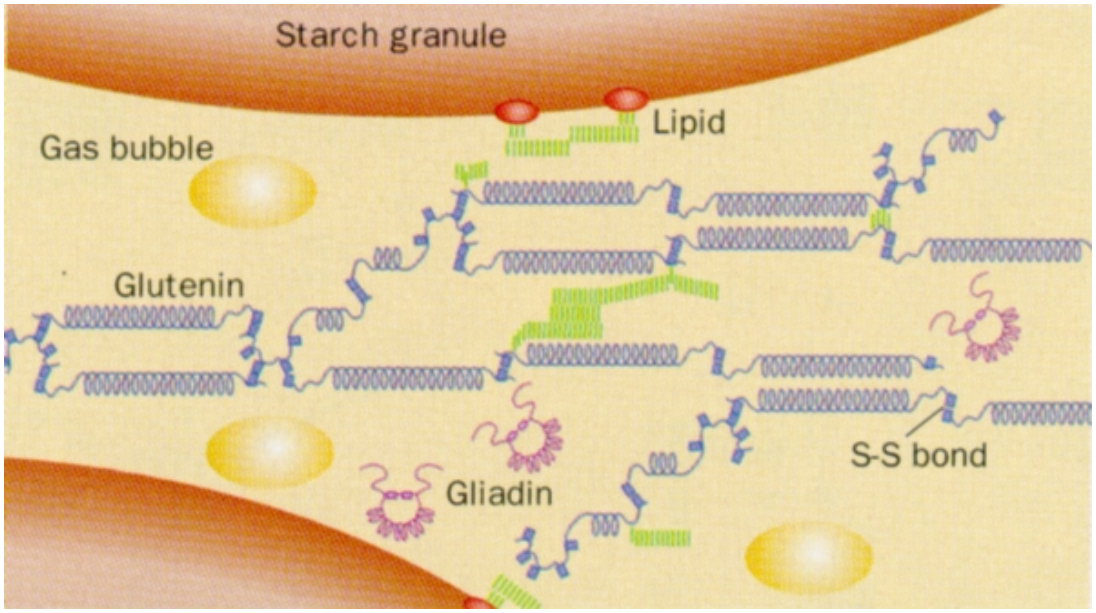

Figure 2.6. The disulphide–bonded polymeric structure of wheat glutenin, which forms the protein matrix between the starch granules and gas bubbles in dough (Wrigley 1996)

2.1.4 Nutritional benefits

Pasta has currently been recognized as part of a healthy diet because fat content in plain pasta is relatively low (Kill 2001). Nutritional values of three different types of pasta are shown in Table 2.4. Pasta is traditionally consumed together with a large variety of ingredients and sauces, such as meat balls and spaghetti sauce. As a result, additional sauces and/or ingredients in pasta could compensate some nutrients that are lacking in the grains.

Table 2.4. Nutritional values of three different types of cooked pasta (U.S. Department of Agriculture, Agricultural Research Service 2007)

Nutrient	Units	Value per 100 grams		
		Homemade pasta made without egg	Homemade pasta made with egg	Pasta with meatballs in tomato sauce
Proximates				
Water	g	68.86	68.71	77.84
Energy	kcal	124	130	103
Protein	g	4.37	5.28	4.32
Total lipid (fat)	g	0.98	1.74	4.08
Ash	g	0.66	0.73	1.47
Carbohydrate, by difference	g	25.12	23.54	12.29
Cholesterol	mg	0	41	8
Minerals				
Calcium, Ca	mg	6	10	11
Iron, Fe	mg	1.13	1.16	0.93
Magnesium, Mg	mg	14	14	14
Phosphorus, P	mg	40	52	46
Potassium, K	mg	19	21	165
Sodium, Na	mg	74	83	418
Zinc, Zn	mg	0.37	0.44	0.73
Copper, Cu	mg	0.060	0.056	0.085
Manganese, Mn	mg	0.193	0.183	0.156

Table 2.4. Nutritional values of three different types of cooked pasta (U.S. Department of Agriculture, Agricultural Research Service 2007) (continued)

Nutrient	Units	Value per 100 grams		
		Homemade pasta made without egg	Homemade pasta made with egg	Pasta with meatballs in tomato sauce
Vitamins				
Vitamin C	mg	0.0	0.0	3.0
Thiamin	mg	0.182	0.173	0.077
Riboflavin	mg	0.148	0.174	0.062
Niacin	mg	1.343	1.257	1.315
Pantothenic acid	mg	0.150	0.231	0.206
Vitamin B–6	mg	0.028	0.037	0.066
Folate, total	mcg	43	43	25
Vitamin B–12	mcg	0.00	0.10	0.23
Vitamin A	IU	0	58	198

2.2 Beef heart

While beef heart is a by–product of beef manufacture and commonly used in animal feed as an inexpensive source of protein, it could be a good protein source for human consumption. Besides, beef heart is widely known as a good source of riboflavin, vitamin B_{12}, selenium, and iron. Nutritional values of beef heart are shown in Table 2.5. Beyond its nutritive compounds, other non–nutritive ingredients are also relatively high in beef heart, such as coenzyme Q_{10} (Mattila and Kumpulainen 2001; Purchas and others 2004a), and creatine (Purchas and others 2004a).

Table 2.5. Nutritional values of beef heart (U.S. Department of Agriculture, Agricultural Research Service 2007)

Nutrient	Units	Value per 100 grams	
		Raw	Cooked
Proximates			
Water	g	77.11	65.67
Energy	kcal	112	165
Protein	g	17.72	28.48
Total lipid (fat)	g	3.94	4.73
Ash	g	1.10	0.97
Carbohydrate, by difference	g	0.14	0.15
Cholesterol	mg	124	212
Minerals			
Calcium, Ca	mg	7	5
Iron, Fe	mg	4.31	6.38
Magnesium, Mg	mg	21	21
Phosphorus, P	mg	212	254
Potassium, K	mg	287	219
Sodium, Na	mg	98	59
Zinc, Zn	mg	1.70	2.87
Copper, Cu	mg	0.396	0.559
Manganese, Mn	mg	0.035	0.033
Selenium, Se	mcg	21.8	38.9

Table 2.5. Nutritional values of raw beef heart (U.S. Department of Agriculture, Agricultural Research Service 2007) (continued)

Nutrient	Units	Value per 100 grams	
		Raw	Cooked
Vitamins			
Vitamin C	mg	2.0	0.0
Thiamin	mg	0.238	0.101
Riboflavin	mg	0.906	1.210
Niacin	mg	7.530	6.680
Pantothenic acid	mg	1.790	1.600
Vitamin B–6	mg	0.279	0.245
Folate, total	mcg	3	5
Vitamin B–12	mcg	8.55	10.80
Vitamin A	IU	0	0
Vitamin E (α−tocopherol)	mg	0.22	0.29

Beef heart is a low cost edible nutritious beef by–product (~ 65 dollars per 100 pound; U.S. Department of Agriculture, the Agricultural Marketing Service 2008). It has recently been incorporated in many protein–based food products, such as beef jerky (Miller and others 1988), surimi (Wang and Xiong 1998), and frankfurters (Desmond and Kenny 1998), in order to increase values of beef heart, to enhance nutrition values of newly formulated food products and also to reduce costs of productions. For example, Miller and others (1988) formulated beef heart jerky and were able to reduce final cost by 43%, in comparison to beef jerky prepared from top round.

2.3 Coenzyme Q_{10}

2.3.1 Chemical and physical properties of coenzyme Q_{10}

Coenzyme Q_{10} (also called ubiquinone, ubidecarenone, CoQ_{10} or Q_{10}) is a lipid soluble compound found naturally in plants and animals, as well as in microorganisms. The chemical structure of coenzyme Q_{10} consists of a quinone ring attached to an isoprene side chain (Figure 2.7). The number of isoprene units in the side chain varies with each species of plants and animals. Coenzyme Q_{10} in humans has 10 isoprene units, therefore, it is known as coenzyme Q_{10}. Coenzyme Q_{10} plays an important role in the mitochondrial electron transport chain as an electron carrier. It exists in two redox forms, an oxidized and a reduced form. The reduced form of coenzyme Q_{10}, ubiquinol, is the only endogenously synthesized fat–soluble antioxidant protecting cellular membranes and plasma lipoproteins from lipid peroxidation (Kishi and others 1999). Therefore, roles of coenzyme Q_{10} in the biological system could be categorized into two important purposes, one involving in the oxidative phosphorylation process to generate ATP and the other being involved in preventing lipid oxidation and scavenging superoxide.

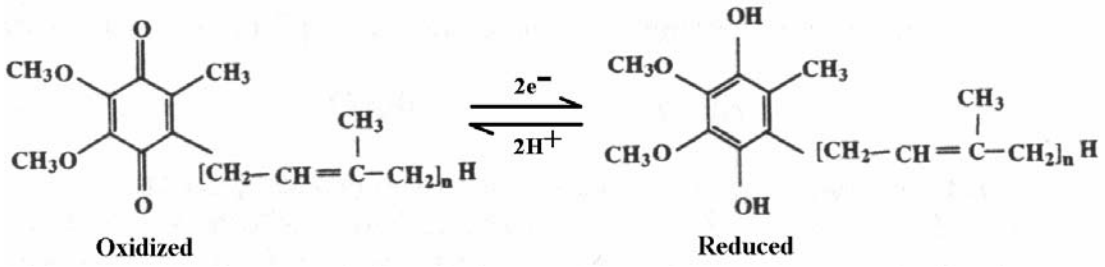

Figure 2.7. Oxidized and reduced forms of Coenzyme Q: In humans, the number of isoprene units (n) is 10. (Papas 1999)

2.3.2 Biosynthesis, distribution, and biotransformation of coenzyme Q_{10}

Overvad and others (1999) indicated that coenzyme Q_{10} is not only the most prevalent form in humans, but in most mammals as well. In addition, coenzyme Q_{10} is present in most animal tissues, but in varying amounts. In human, the average content of coenzyme Q_{10} is reasonably high in the heart, kidney, and liver, approximately 110, 70, and 60 μg/g tissue, respectively (Papas 1999; Overvad and others 1999). On the other hand, the lowest concentration is found in lung tissue, 8 μg/g (Overvad and others 1999). Coenzyme Q_{10} is not only concentrated in the mitochondria, Golgi apparatus, and lysosome of cells, but also found in all plasma membranes including low-density lipoprotein, LDL (Papas 1999). In human plasma, the coenzyme Q_{10} concentration is in the range of 0.75 – 1.0 μg/mL, of which 75% is in the reduced form (Overvad and others 1999). The total coenzyme Q_{10} content in the body is estimated to be in the range of 1.0 – 1.5 g, with the majority found in muscle cells due to the greater overall mass, and the level of coenzyme Q_{10} has been shown to decrease with age (Overvad and others 1999).

Kishi and others (1999) reviewed that coenzyme Q_{10} in nonmitochondrial membranes is serially synthesized through the enzymes in the endoplasmic reticulum–Golgi membrane system and is then translocated from this compartment to other cellular membranes and plasma lipoproteins by transfer vesicles. However, physiological roles of coenzyme Q_{10} in other cells other than mitochondria are still unclear. Coenzyme Q_{10} is a crucial component in the mitochondrial respiratory chain, which is localized within the inner mitochondrial membrane (Aguilaniu and others 2005; DiMauro and others 2007). Therefore, synthesis of coenzyme Q_{10} mainly takes place in mitochondria. NADH and $FADH_2$ are electron donors and donate electrons to either complex I or complex II in the

oxidative phosphorylation chain. Then, electrons from complexes I and II are transferred to coenzyme Q_{10}, complex III, and finally complex IV. In general, the biosynthesis of coenzyme Q_{10} consists of three important steps. They are synthesis of a quinonoid ring, synthesis of decaprenyl diphosphate (a long tail), and quinonoid ring modification (Choi and others 2005). In mammals, *para*-hydroxybenzoate (PHB) is a precursor of the quinonoid ring and is derived from tyrosine (Choi and others 2005). Decaprenyl diphosphate synthase produces a unique hydrophobic tail composed of ten isoprene units (Choi and others 2005). Prenylation is the first step of ring modification and then followed by other ring modification reactions, including decarboxylation, three hydroxylation and three methylation reactions (Choi and others 2005). DiMauro and others (2007) mentioned that decaprenyl diphosphate is synthesized by a heterotetrameric enzyme composed of prenyl-diphosphate synthase subunit 1 (PDSS1) and prenyl-diphosphate synthase subunit 2 (PDSS2) from mevalonate via farnesyl diphosphate and geranylgeranyl diphosphate and is attached to the *para*-hydroxybenzoate (PHB) ring by OH–benzoate polyprenyl transferase (COQ2). Subsequently, at least 6 more COQ enzymes (COQ3 – COQ8), catalyzing methylation, decarboxylation, and hydroxylation reactions, are needed to produce functional coenzyme Q_{10}. Coenzyme Q_{10} synthesis and the mechanism of coenzyme Q_{10} in the mitochondrial electron transport chain (ETC) are demonstrated in Figure 2.8.

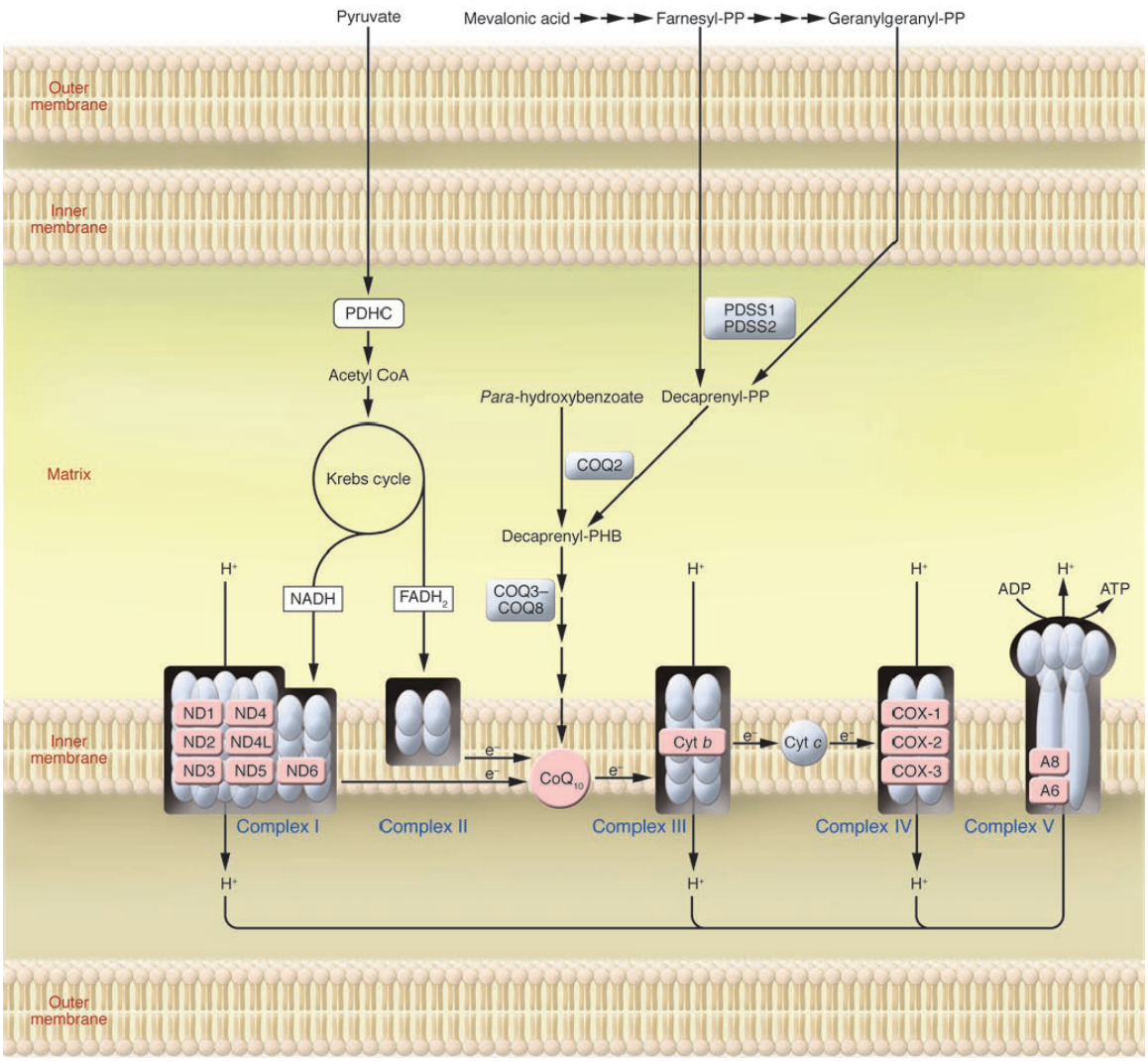

Figure 2.8. Biosynthesis of coenzyme Q_{10} and coenzyme Q_{10} in mitochondrial metabolism: A8, ATP synthase subunit 8; Cyt *b*, cytochrome *b*; FADH2, flavin adenine dinucleotide, reduced form; ND1 – 6, subunits 1 – 6 of NADH dehydrogenase; PP, diphosphate; PDHC, pyruvate dehydrogenase complex (DiMauro and others 2007)

Coenzyme Q_{10} is the coenzyme for three important enzymes in the mitochondrial respiratory chain. The coenzyme Q_{10}–dependent enzymes are NADH dehydrogenase (or NADH–ubiquinone oxidoreductase), succinate dehydrogenase (or succinate–coenzyme Q reductase), and ubiquinone–cytochrome c oxidoreductase. Coenzyme Q_{10} plays a role as the coenzyme because it is a freely–diffusible molecule that carries electrons from one

complex to the next complex (Complex I to Complex III and/or Complex II to Complex III). As seen in Figure 2.8, coenzyme Q_{10} plays an important role in the oxidative phosphorylation process to generate ATP. Coenzyme Q_{10} is an electron carrier in the electron transport chain by transferring electrons between Complex I to Complex III and/or Complex II to Complex III. The Complex I, II, and III are complexes of integral membrane proteins embraced in the inner mitochondrial membrane. Complex I (also called NADH dehydrogenase or NADH–ubiquinone oxidoreductase) is an enzyme complex and responsible for catalyzing the electron transfer from NADH to coenzyme Q_{10} (Nelson and Cox 2000; Marcotte 2005). In other words, reduced coenzyme Q_{10} is produced by Complex I and then distributes to Complex III, where coenzyme Q_{10} is oxidized to ubiquinone (Nelson and Cox 2000; Marcotte 2005). Complex II (also known as succinate–coenzyme Q reductase or succinate dehydrogenase) is an enzyme complex that catalyzes the transfer of electrons from succinate to FAD, then through Fe–S centers to ubiquinone (Nelson and Cox 2000; Marcotte 2005). Complex III is the cytochrome bc_1 complex, also called as ubiquinone–cytochrome c oxidoreductase (Nelson and Cox 2000; Marcotte 2005). It catalyzes the reduction of cytochrome *c* by oxidation of ubiquinol (Nelson and Cox 2000; Marcotte 2005). A summary of how coenzyme Q_{10} is involved in the three enzyme complexes in the electron transport chain is depicted in Figure 2.9.

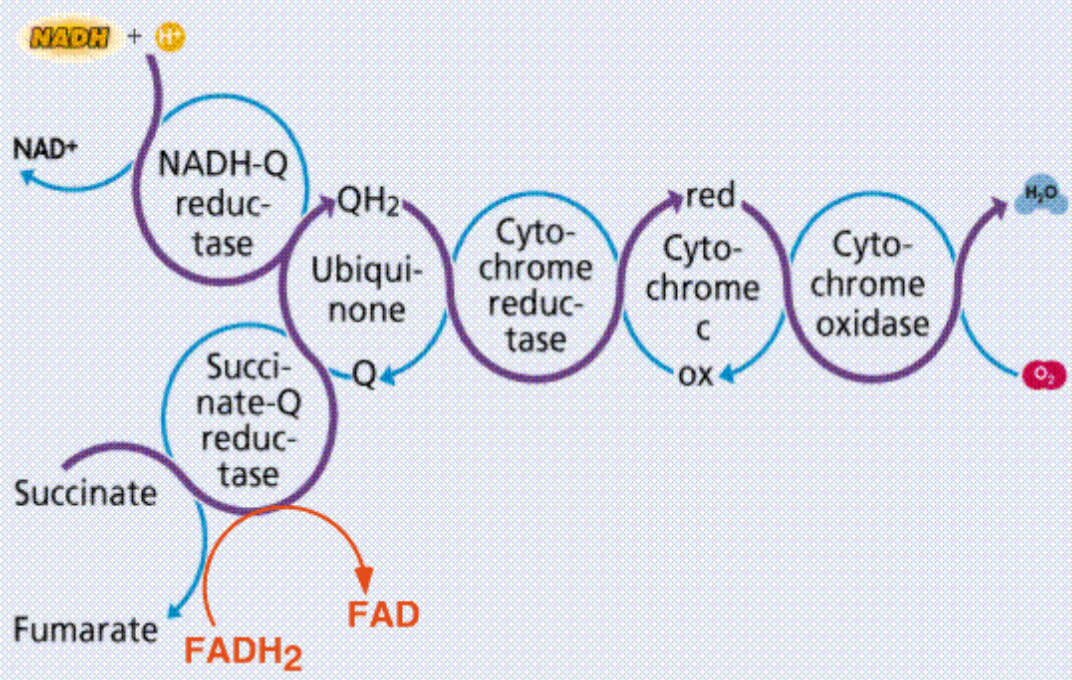

Figure 2.9. Coenzyme Q_{10} and the three enzyme complexes, including the NADH dehydrogenase complex, the succinate dehydrogenase complex, and the cytochrome c reductase complex (Anonymous 2007)

2.3.3 Coenzyme Q_{10} and health benefits

Coenzyme Q_{10} has been found in most human tissues but in varying amounts, including heart, kidney, and liver (Overvad and others 1999). Moreover, from accumulated data, many researchers found that coenzyme Q_{10} levels in human decrease with increasing age, with some chronic diseases, such as heart disease, cancer, AIDS, and with some genetic disease such as neurologic disease and myopathies (Cupp and Tracy 2003; Papas 1999; Overvad and others 1999). Therefore, consumption of exogenous coenzyme Q_{10} from food sources and/or supplements might be an alternative way to sustain good health. Effects of coenzyme Q_{10} treatment in human are shown in Table 2.6.

Table 2.6. Effects of coenzyme Q_{10} treatment in human

References	Subjects	Study Design	Gender (n)	Age (y)	Treatment	Results
Barbieri and others 1999	Hepatitis B vaccinated volunteers	Randomized single-blind and placebo controlled	3 groups 1. F (10), M (11) 2. F (9), M (12) 3. F (13), M (8)	20–66	Capsule administration for 90 d (1. placebo, 2. 90 mg/day, 3. 180 mg/day)	The dose of 180 mg/day increase antibody response in humans vaccinated against hepatitis B with up to 57% (p = 0.011)
Munkholm and others 1999	Sinus rhythm and suffered from ischemic heart disease or dilated cardiomyopathy	Randomized double-blinded placebo controlled	Not indicated (22)	43–75	Coenzyme Q_{10} in soya oil (200mg/d for 12w)	A significant decrease in pulmonary artery pressure (PAP) and stroke index at rest, and pulmonary capillary wedge pressure (PCWP) and stroke index at work
Weber and others 1994	Healthy young volunteers	Not indicated	F (13), M (9)	25.9±2.6	Oral administration (coenzyme Q_{10} 90 mg/day for 2 weeks)	The level of TBARS decrease during the week of coenzyme Q_{10} ingestion

2.3.3.1 Cardiovascular disease

Yalcin and others (2004) indicated a relation between low plasma coenzyme Q_{10} concentration and coronary artery disease because they found that plasma coenzyme Q_{10} concentrations in patients with coronary artery disease (0.43 μmol/L) were lower than that in control groups (0.77 μmol/L). Munkholm and others (1999) treated patients suffering from congestive heart failure with coenzyme Q_{10} 200 mg/day and found that the treatment caused an improvement in left ventricular performance, which indicated that coenzyme Q_{10} could reduce the risk of cardiovascular disease (CVD). Langsjoen and Langsjoen (1999) suggested that maintaining plasma coenzyme Q_{10} levels (> 3.5 μg/mL) together with using coenzyme Q_{10} supplements could improve heart function.

2.3.3.2 Immune function

Coenzyme Q_{10} also has an ability to boost the immune system. Barbieri and others (1999) found that antibody titer was significantly higher in the subject groups treated daily with 90 and 180 mg of coenzyme Q_{10} compared with the placebo group. In an animal study, the administration of 150 – 750 μg coenzyme Q_{10} to mice enhanced phagocytic activity and improved antibody titers (Hodges and others 1999). Significantly decreased blood coenzyme Q_{10} levels have been documented in patients with Acquired Immune Deficiency Syndrome, AIDS (Papas 1999; Zhang and others 1997). In contrast, Human Immunodeficiency Virus (HIV)–positive people without symptoms still have normal blood coenzyme Q_{10} levels that lower the disease progress as AIDS Related Complex (ARC), and further decline as they develop

AIDS. Zhang and others (1997) suggested that supplementations with coenzyme Q_{10} could delay the progress from ARC to AIDS and probably had positive result on the T4/T8 lymphocyte ratio. Based on these findings, therefore, coenzyme Q_{10} can enhance immune functions in both the healthy and deficient people.

2.3.3.3 Cancer

Hodges and others (1999) believed that coenzyme Q_{10} is important for normal cell respiration and function. Any deficiency in its availability or biosynthesis probably interrupts normal cellular function. Consequently, abnormal cell divisions, which induce an oncogenic response, might be observed. In their literature review, Hodges and others (1999) also found that coenzyme Q_{10} levels in patients with breast cancer, lung cancer, and pancreas cancer were lower than those in healthy people. Therefore, administering coenzyme Q_{10} might have therapeutic potential for cancer treatment. In addition, Conklin (2000) suggested that during chemotherapy, patients should be provided coenzyme Q_{10} supplementation to prevent doxorubicin–induced cardiotoxicity. The doxorubicin effects include (Conklin, 2000):

- Reduction of coenzyme Q_{10} content of mitochondrial membranes
- Inhibition of respiratory chain coenzyme Q_{10}–dependent enzymes, interfering with the aerobic generation of ATP
- Inhibition of mitochondrial synthesis of coenzyme Q_{10}

2.3.3.4 Antioxidant function

Weber and others (1994) studied the effect of an oral dose of 90 mg/day of coenzyme Q_{10} on the antioxidant status in healthy young subjects. They found that ingestion of coenzyme Q_{10} could reduce the rate of oxidative reaction. According to Papas (1999), two possible mechanisms of antioxidant functions of coenzyme Q_{10} have been proposed as follows:

- The reduced form of coenzyme Q_{10} (ubiquinol, CoQH) functions independently as a chain breaking antioxidant and reduces peroxyl (ROO*) and alcoxyl radicals.

$$CoQH + ROO^* \rightarrow Q^* + ROOH$$

- Ubiquinol interacts with vitamin E radicals (TO*) via a redox reaction and consequently regenerates vitamin E the same as vitamin C does.

$$CoQH + TO^* \rightarrow Q^* + TOH$$

While the free radical scavenging ability of coenzyme Q_{10} in vivo is less efficient than that of vitamin E, the role of coenzyme Q_{10} as an antioxidant that regenerates vitamin E is realistically been more important in vivo (Papas 1999). Quinn and Fabisiak (1999) proposed the potential role of coenzyme Q_{10} in vitamin E regeneration taking place in the electron transport chain as shown in Figure 2.10.

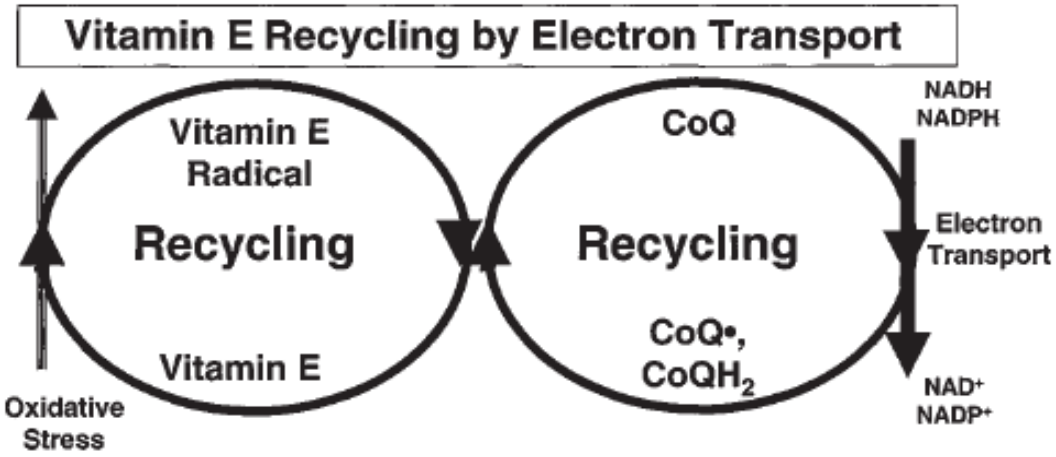

Figure 2.10. Linkage of vitamin E regeneration to electron transport pathways via coenzyme Q (Quinn and Fabisiak 1999)

2.3.3.5 Coenzyme Q_{10} deficiency

In case of coenzyme Q_{10} deficiency, exogenously administered coenzyme Q_{10} probably reestablishes disturbed electron/proton translocation activities (Kagan and others 1996). Viscosity of mitochondrial membranes would increase with aging and the coupled electron/proton shuttle diffusion activity of coenzyme Q_{10} might become rate limiting (Kagan and others 1996). Kagan and others (1996) acknowledged that administering coenzyme Q_{10} can overcome this limitation not only by increasing the number of electron carriers but also by direct physical effects on membranes as a result of its antioxidant function. Coenzyme Q_{10} deficiency could lead to many serious problems at the cellular level. For example, because coenzyme Q_{10} is one of the key parameters in the electron transport chain of cell membranes, particularly in the respiratory chain located in the inner membranes of mitochondria, the depletion of coenzyme Q_{10} can cause an increase of reducing equivalents in both mitochondria and cytosol, e.g. elevated NADH/NAD ratios, or a decrease in mitochondria ATP

production, or an increase of monovalent reduction of oxygen resulting in superoxide formation, or the functional impairment of many metabolic pathways requiring respiratory chain function, e.g. the tricarboxylic acid cycle and the β-oxidation (Rustin and others 2004). Rustin and others (2004) also pointed out three major clinical problems from coenzyme Q_{10} depletion as the following:

- A myopathic form characterized by epilepsy exercise intolerance, mitochondria myopathy, myoglobinuria, epilepsy and ataxia
- A generalized infantile variant with severe encephalopathy and renal disease
- An ataxic form, dominated by ataxia, seizures and either cerebral atrophy or anomalies of the basal ganglia

Coenzyme Q_{10} deficiency is rare and probably treatable by providing high doses of coenzyme Q_{10} from oral supplements and/or food sources. In patients with the myopathic variant and in patients with an atypical ataxic form, a daily dose of 300 mg for adults has been reported to improve most symptoms such as CK and lactic values, and muscle weakness (Rustin and others 2004). Patients with coenzyme Q_{10} deficiency syndrome dominated by cerebella ataxia and atrophy, or presenting a pseudo-Leigh syndrome in adulthood also responded to coenzyme Q_{10} supplementation at a dosage of 300 – 800 mg/day (Rustin and others 2004). Consumption of 5 mg coenzyme Q_{10} daily could stimulate respiration and fibroblast enzyme activities in patients with severe encephalomyopathy and renal failure (Rustin and others 2004).

DiMauro and others (2007) found in a literature review that of at least nine genes that are presumably involved in coenzyme Q_{10} biosynthesis and suspected of causing primary coenzyme Q_{10} deficiency, three, including PDSS1, PDSS2, and COQ2 have been found guilty. As a result, people suffering from dysfunction of genes involved in coenzyme Q_{10} biosynthesis need to get more coenzyme Q_{10} from supplements or from their diet. In addition, Choi and others (2005) recommended that coenzyme Q_{10} could be used as a supplement to statins, which are inhibitors of 3–hydrox–3–methylglutaryl coenzyme A (HMG CoA) reductase, because statins competitively inhibit the biosynthesis of cholesterol and coenzyme Q_{10}, as shown in Figure 2.11. Consequently, patients who were taking statin drugs, such as Lovastatin and Provastatin, for lowering blood cholesterol would have a depletion of coenzyme Q_{10} content in serum or tissue as well.

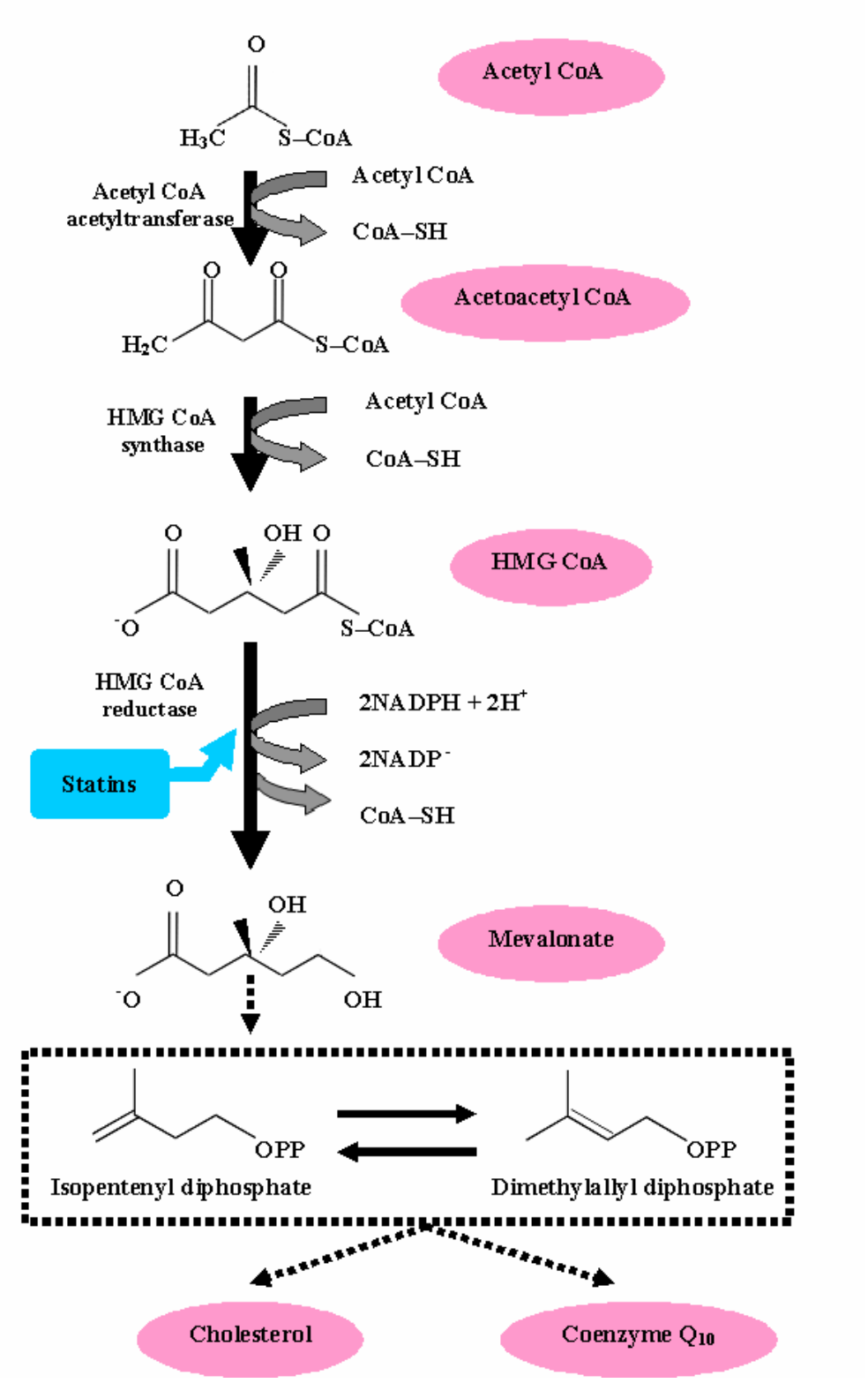

Figure 2.11. Inhibition of cholesterol and coenzyme Q_{10} biosynthesis by statin drugs in human (altered from Choi and others 2005)

2.3.4 Sources of coenzyme Q_{10} and typical coenzyme Q_{10} intakes

Although coenzyme Q_{10} is synthesized endogenously, dietary intake is a significant contributor of coenzyme Q_{10} in humans. Meat, poultry, and fish are good sources of dietary coenzyme Q_{10} since these muscle tissues contain high amount of mitochondria (Weber 2001). The contents of coenzyme Q_{10} in meat, poultry, and fish are 8 – 200, 17 – 21, and 4 – 64 μg/g food, respectively (Weber 2001). Mattila and Kumpulainen (2001) determined coenzyme Q_{10} in foods and found that reindeer meat (157.9 μg/g fresh wt), pork heart (126.8 μg/g fresh wt), beef heart (113.3 μg/g fresh wt), and beef liver (39.2 μg/g fresh wt) were the richest sources of coenzyme Q_{10}.

Overvad and others (1999) reviewed that the total coenzyme Q_{10} content in human is estimated to 1 – 1.5 g and found mostly in muscle cells. The coenzyme Q_{10} content in human plasma is in the range of 0.75 – 1 μg/mL (Overvad and others 1999). Coenzyme Q_{10} in the body typically stems from endogenous synthesis as well as from dietary intake and from oral supplement (Overvad and others 1999). Few studies have investigated the average daily coenzyme Q_{10} intake, but it has been estimated to be 3 – 5 mg/day, primarily derived from meat and poultry, while cereal fruit, edible fats, and vegetable were minor contributors (Weber and others 1997a). Another study showed the average coenzyme Q_{10} intake to be 5.4 mg/day for men and 3.8 mg/day for women (Mattila and Kumpulainen 2001). Because coenzyme Q_{10} is not regarded as an essential nutrient, there is currently no Dietary Reference Intake (DRI) or other formal recommendation for coenzyme Q_{10} published (National Academy of Sciences, 1997 – 2005). However, Papas (1999) recommended that an

intake of 10 – 30 mg coenzyme Q_{10} daily is a common dose used in supplements and therapeutic dosages for severe conditions range from 200 – 400 mg/day.

2.3.5 Effect of food processing and cooking methods on coenzyme Q_{10} content

Weber and others (1997a) observed the effect of cooking on coenzyme Q_{10} content and found 14 – 32% destruction of coenzyme Q_{10} by frying, however, there was no detectable destruction by boiling. Purchas and others (2004a) found that after cooking lambs at 70°C for 90 min, the higher coenzyme Q_{10} content was found in the cooked lambs. They suggested that the higher content of coenzyme Q_{10} in cooked than raw meat might be due to cooking facilitating the coenzyme Q_{10} extraction procedure. However, Purchas and others (2004b) found that coenzyme Q_{10} content in beef steaks decreased significantly after grilling at 200°C but there was no significant difference in the content of coenzyme Q_{10} in steaks that were cooked to two different final internal temperatures, which were 60 and 80°C. Processing of dried whole soybean to boiled beans, natto (fermented soybeans), and kinako (roasted and ground soybeans) had little effect on coenzyme Q_{10} content of the products (Kamei and others 1985). These results indicated that processing, such as boiling, fermentation, and heat treatment, do not cause a reduction of coenzyme Q_{10} in soy beans due to effusion or destruction.

2.3.6 Determination of coenzyme Q_{10} content

Two basic methods that have been used for extraction of coenzyme Q_{10} from biological tissues and foods are direct extraction and saponification before extraction. Weber and others (1997a) reported that an incorporation of a mixture of ethanol–hexane in the extraction procedure provided equivalent results to the procedure that included the saponification step. As a result, the direct solvent extraction has been broadly employed for food samples because of its simplicity, effectiveness, and being less time consuming (Weber and others 1997a; Mattila and others 2000; Purchas and others 2004a; Strazisar and others 2005; Souchet and Laplante 2007). Souchet and Laplante (2007) acknowledged that while saponification could provide better results by removing impurities, such as triglycerides, and releasing coenzyme Q_{10} bound to proteins in the mitochondrial membrane, it could also cause destruction of coenzyme Q_{10}, which is sensitive to alkali, and lead to formation of artifacts (ethoxy substitutions in the quinone ring and formation of ubichromenol). Nevertheless, the integration of a saponification step has still been widely employed in the extraction procedure, especially for high-fat content samples (Kamei and others 1985; Mattila and Kumpulainen 2001).

2.4 Texture profile analysis (TPA)

Bourne (1978) reported that a major breakthrough in texture profile analysis came with the improvement of the General Food Texturometer. The Texturometer applied a small flat–ended plunger to compress a bite–size piece of food sample with 75% compression. Two cycles of compression were used to imitate the action of human bites and the stress developed in the food during the compression was recorded over time in the form of a force–time curve as shown in Figure 2.12. Rosenthal (1999) explained that after the first bite, while the flat–ended cylinder was drawn away from the food surface, any tension due to stickiness was observed. The second–compression cycle then hit the food sample again and allowed it to relax for a second time. The resistance during the food deformation was observed throughout the two–bite cycle.

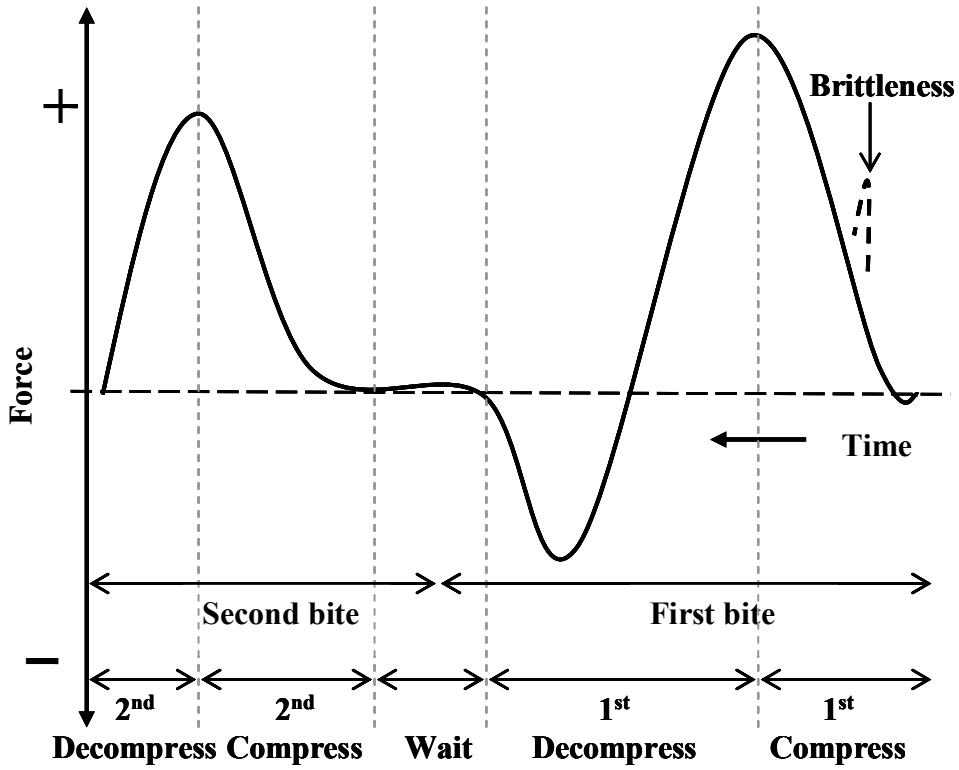

Figure 2.12. A typical texture profile analysis (TPA) curve (based on figures obtained from Bourne 1978; Rosenthal 1999)

Seven textural parameters can be derived from the texture profile analysis (TPA) curve (Bourne 1978). Five parameters, including hardness, springiness, adhesiveness, cohesiveness, and brittleness, can be measured and extracted directly from the TPA curve while the other two parameters, chewiness and gumminess, can be calculated from the measured parameters. The extraction and definition of texture profiles, consisting of hardness, springiness, adhesiveness, cohesiveness, brittleness, chewiness, and gumminess, are described in Table 2.7.

Table 2.7. Parameters measured by TPA (Bourne 1978; Rosenthal 1999)

Parameter	Sensorial definition	Instrumental definition
Hardness	Force required to compress a food between the molars	The height of the force peak on the first compression cycle ("first bite") 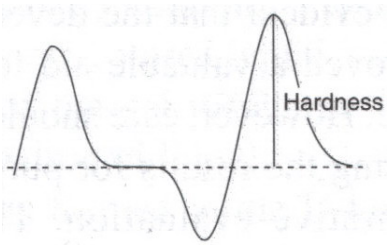
Springiness (elasticity)	The extent to which a compressed food returns to its original size when the load is removed	The height that food recovers during the elapsed time between the end of the first bite and the beginning of the second bite 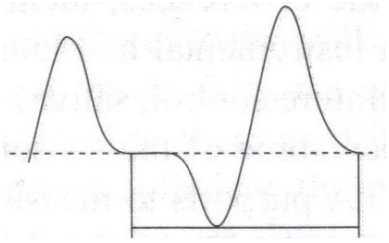 Cycle = Second contact – First contact Elasticity = Cycle for inelastic material – Cycle for food
Adhesiveness	The work required to pull the food away from a surface	The negative force area of the first bite which represents the work necessary to pull the compressing plunger from the sample 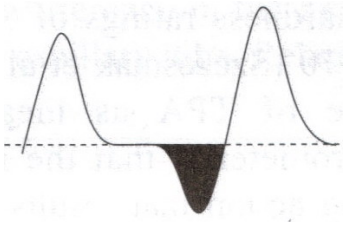

Table 2.7. Parameters measured by TPA (Bourne 1978; Rosenthal 1999) (continued)

Parameter	Sensorial definition	Instrumental definition
Cohesiveness	The strength of the internal bonds making up the food	The ratio of the positive force areas during the second compression to that during the first compression 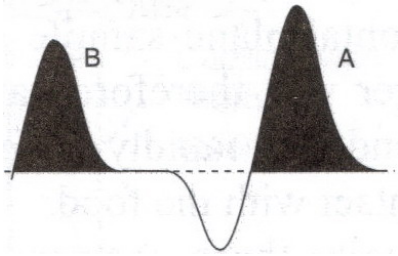 Cohesiveness = B/A
Brittleness (fracturability)	The force at which the material fractures. Brittle foods are never adhesive.	The force at the first significant break in the curve 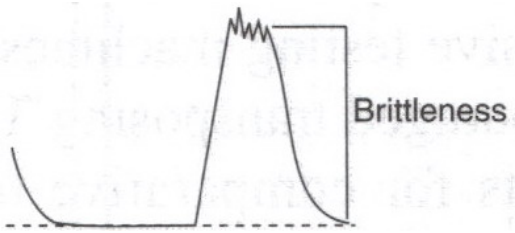
Chewiness	The energy required to chew a solid food until it is ready for swallowing	Chewiness = Hardness × Cohesiveness × Springiness
Gumminess	The energy required to disintegrate a semisolid food so that it is ready for swallowing	Gumminess = Hardness × Cohesiveness

A common mistake that has been mostly overlooked when texture profile analysis results are reported is that chewiness and gumminess should not be reported for the same food (Bourne 2002a). According to the sensorial definitions of chewiness and gumminess by Rosenthal (1999), chewiness is only used for characterizing a solid food sample while gumminess is only used for defining a semi–solid food sample. Therefore, chewiness is not commonly included with gumminess because a food sample is either a solid or a semi–solid but cannot be both.

2.5 Vibrational spectroscopy

According to Jones (2004), spectroscopy is an analytical technique arising from an interaction of a species with electromagnetic radiation; i.e. the electromagnetic radiation absorbed, emitted or scattered by a molecule is analyzed. The radiation in the vibrational region of the electromagnetic spectrum in terms of a unit is described as a wavenumber ($\bar{\nu}$ or cm^{-1}) rather than wavelength (μ or μm) because wavenumbers are directly proportional to energy: a higher wavenumber corresponds to a higher energy (Pavia and others 2001). Wavenumbers can be converted to wavelengths or vice versa by using the following equations:

$$cm^{-1} = \frac{1}{(\mu m)} \times 10{,}000 \qquad \text{and} \qquad \mu m = \frac{1}{(cm^{-1})} \times 10{,}000$$

In general, a beam of radiation from a source (such as a laser) is passed through a sample and only radiation that exits the sample is considered. For example, in vibrational absorption spectroscopy, by varying radiation frequencies, a spectrum is produced and intensities of the exiting radiation for each frequency then appear. This spectrum will show which frequencies of radiation are absorbed after molecules are raised to the higher vibrational energy states. Since each molecule has its own typical spectrum, spectroscopy is widely used in analytical chemistry. In addition, the major advantage of vibrational spectroscopic methods is that the samples can be analyzed non–destructively and in real time.

2.5.1 Infrared (IR) in comparison to Raman spectroscopy

Infrared (IR) and Raman spectroscopy are both techniques subcategorized under vibrational spectroscopic methods (Li–Chan and others 1994). IR spectroscopy involves the absorption of radiation in the IR region of the electromagnetic spectrum while Raman spectroscopy involves the inelastic scattering of radiation, usually in the visible region but also in the ultraviolet and near infrared (NIR) regions (Li–Chan and others 1994). The inelastic scattering takes place when photons and molecules exchange energy, which lead to an emission of another photon with a different frequency to the incident photon (Jones 2004). The relationships between IR absorption and Raman scattering are illustrated in Figure 2.13.

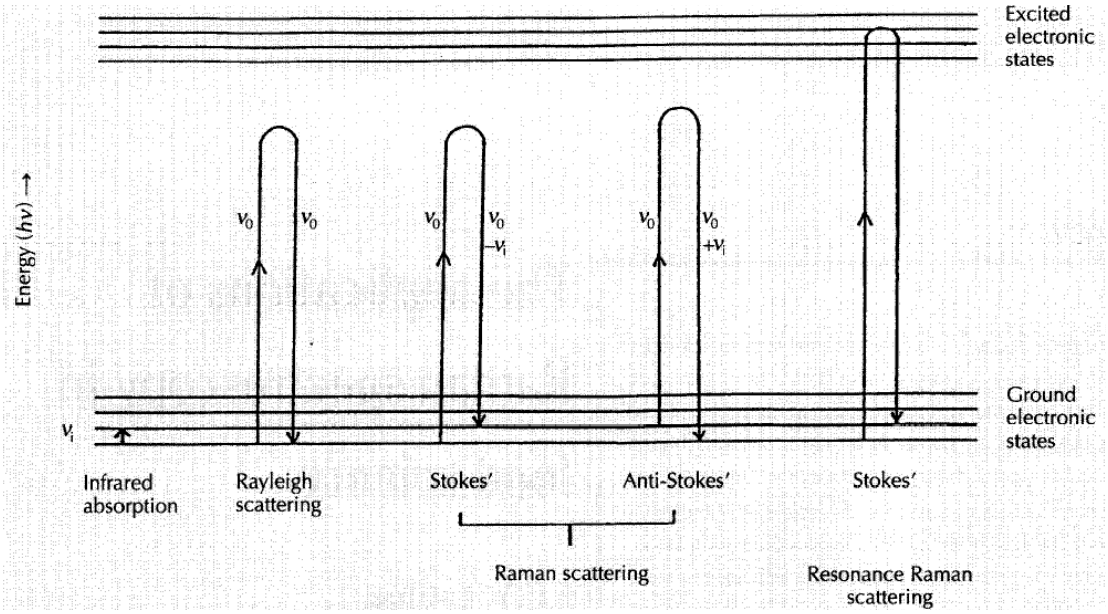

Figure 2.13. The relationships between infrared absorption and Raman scattering (Li–Chan 1996)

Using Figure 2.13, Li–Chan (1996) explained that in IR spectroscopy, the absorption of incident electromagnetic radiation at a particular frequency (ν_i) in the IR region is related to a specific vibrational excitation energy ($\Delta E = h\nu_i$). On the other hand, in Raman spectroscopy, the exciting or incident light beam is at a frequency (ν_0) that may correspond to the visible, UV or NIR region of the electromagnetic spectrum. The inelastic scattering of the incident radiation, which results in a Raman shift ($\Delta\nu = \nu_i$), is related to the energy of a vibrational transition within a sample molecule. Stokes' transitions are those in which the molecule is excited by the radiation whereas anti-stokes' transitions are those in which the molecule is de-excited. Because the lowest vibrational level is the most energetically favorable, there is a higher frequency of occurrence, and consequently stronger signal intensity during Raman scattering corresponding to Stokes' transitions. Therefore, Raman

spectroscopic studies usually report data corresponding to Stokes' rather than anti-stokes' transitions. In the particular branch of Raman spectroscopy known as resonance Raman spectroscopy, the incident photon energy corresponds to an electronic absorption mode that allows a transition to an excited electronic state, followed by inelastic scattering to produce Stokes' and anti–Stokes' resonance Raman bands.

Both IR absorption and the Raman scattering process involve vibrational energy levels of sample molecules, which are related primarily to stretching or bending deformations of bonds (Li–Chan and others 1994; Li–Chan 1996). Therefore, a Raman spectrum is obtained by plotting the intensity of scattered light as a function of the Raman shift, $\Delta\nu$ in cm^{-1}, and gives information based on stretching and bending vibrational modes, similar to that provided by an IR spectrum, of the absorption or transmission of energy as a function of the frequency (Li–Chan 1996). A comparison of Raman and IR spectra is shown in Figure 2.14. However, IR absorption requires a change in the intrinsic dipole moment with molecular vibration, while Raman scattering depends on changes in the polarizability of the molecule (Li–Chan and others 1994; Li–Chan 1996). They suggested that IR spectroscopy and Raman spectroscopy are complementary rather than substitutes for each other because polar functional groups, such as C=O, C≡N, O–H, N–H and C–H, normally have strong IR stretching vibrations, while intense Raman lines are associated with nonpolar groups, such as C=C, S–S, C–C and N=N. Besides, an important advantage of Raman spectra over IR is that water does not cause interference, consequently, Raman spectroscopy can be applied for aqueous solutions (Skoog and others 1998).

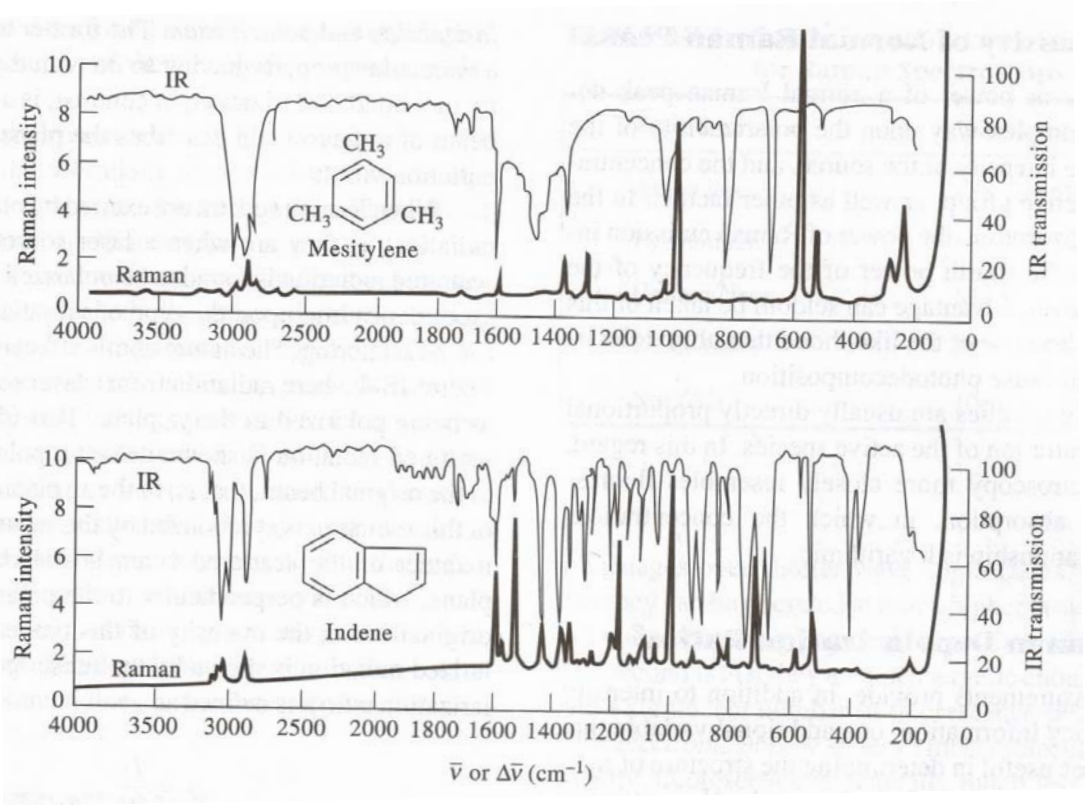

Figure 2.14. Comparison of Raman and IR spectra (Skoog and others 1998)

2.5.2 FT–IR and its applications in food science

According to Pavia and others (2001), a Fourier transform infrared spectrometer (FT–IR) is an IR spectrophotometer that is operated by using a mathematical operation known as a Fourier transform (FT). The advantages of FT–IR are that it acquires an interferogram (a wave–like pattern signal containing all frequencies that make up the IR spectrum) in less than a second, collects dozens of interferogram from the same samples, and provides a spectrum with a great signal–to–noise ratio (Pavia and others 2001).

Nowadays, FT–IR is widely used in food analyses. For example, FT–IR has been used in the study of the degree of tenderization in beef (Iizuka and Aishima 1999), in the discriminant analysis of edible oils and fats (Yang and others 2005), and for investigating structural changes in sweet potato flour after modifications (Ramesh Yadav and others 2007). Moreover, FT–IR has been used to investigate interactions between proteins and other food components and the changes of secondary structures in gluten (Leon and others 2000; Wellner and others 2005; Georget and Belton 2006). The major FT–IR bands that are usually applied for the interpretation of physiochemical changes in foods are shown in Table 2.8.

Table 2.8. Tentative assignment of major bands in the FT–IR spectra*

Wavenumber (cm^{-1})	**Tentative assignment**
~ 3400	O–H stretch of water
~ 2925	Asymmetric stretches of methylene group
~ 2856	Symmetric stretch C–H of methylene groups
~ 1740	C=O stretching vibrations of ester functional groups (primarily from lipids and fatty acids)
1700 – 1600	Amide I: C=O stretch weakly coupled with C–N stretch and N–H bending
~ 1682	β sheets
~ 1668	β turns
~ 1650	α helices and random coils
~ 1630	Antiparallel β sheets
1600 – 1500	Amide II: C–N stretch strongly coupled with N–H bending
~ 1400	Symmetric deformation of CH_3 and CH_2 of proteins, and symmetric stretch of C–O of COO^- groups
1350 – 1200	Amide III: N–H in plane bending coupled with C–N stretching and also includes C–H and N–H deformation vibrations
1200 – 900	C–O–C stretching vibrations of polysaccharides
~ 1020	C–O–H bending and deformation

* References: Georget and Belton 2006; Lin and others 2005; Liu and others 2002; Singh 2000

2.5.3 Raman spectroscopy and its applications in food science

For the Raman spectra, peak intensities are based on the number of repeating vibrational units in a given chemical environment and on the change in molecular polarizability associated with the vibration (Spiro and Gaber 1977). Both peptide backbone and amino acid side chains are directly associated to the vibrational modes (Spiro and Gaber 1977). Some of the Raman modes that are useful in the interpretation of physical chemistry of foods are shown in Table 2.9. In Raman spectroscopy, the different types of interactions can be differentiated from one another by wavenumber shift (cm^{-1}). For example, the presence of disulfide bonds can be detected by Raman spectroscopy due to the intense band assigned to the disulfide (S–S) stretching vibration in the region of 550 – 500 cm^{-1}. Stretching vibration due to the S–H group of cysteinyl residues appears in the area of 2580 – 2550 cm^{-1}. Tyrosine–residue vibration modes can be used to detect the hydrogen bond formation (Li–Chan and others 1994).

Table 2.9. Tentative assignment of major bands in the Raman spectra*

Wavenumber (cm^{-1})	**Tentative assignment**
~ 3060	=CH stretching
3000 – 2800	C–H stretching
2580 – 2550	S–H stretching
1750 – 1700	C=O stretch of COOH or COOR
~ 1685	Amide I (Disordered structure: non–hydrogen–bonded)
1670 $\pm$ 3	Amide I (Antiparallel β–pleated sheet)
1665 $\pm$ 3	Amide I (Disordered structure)
1655 $\pm$ 5	Amide I (α–helix)
~ 1465, ~ 1450	C–H bending
1430 – 1400	C=O stretch of COO^-
~ 1409	Histidine
~ 1360, ~ 880, ~ 760	Tryptophan
~ 1340	CH vibrations of carbohydrates
>1275	Amide III (α–helix)

* References: Li–Chan and others 1994; Li–Chan 1996; Bulkin and others 1987; Synytsya and others 2003; Howell and others 1999; Thygesen and others 2003; Spiro and Gaber 1977

Table 2.9. Tentative assignment of major bands in the Raman spectra* (continued)

Wavenumber (cm^{-1})	**Tentative assignment**
~ 1260	α–helix
1245 $\pm$ 4 (broad)	Amide III (Disordered structure)
1235 $\pm$ 5 (sharp)	Amide III (Antiparallel β–pleated sheet)
~ 1235	Amide III (Disordered structure: non–hydrogen–bonded)
~ 1121	C–C vibrations of carbohydrates
~ 1087	C–O vibrations of carbohydrates
1120 – 1040	C–N and C–C stretching
~ 1006	Phenylalanine
~1005	β–pleated sheet
945 – 935	C–C stretching (α–helix)
850/830	Tyrosine
745 – 700, 670 – 630	C–S stretching
~ 545, ~ 525, ~ 510	S–S stretching
~ 480	Skeletal mode of starch

* References: Li–Chan and others 1994; Li–Chan 1996; Bulkin and others 1987; Synytsya and others 2003; Howell and others 1999; Thygesen and others 2003; Spiro and Gaber 1977

Raman bands that relate to the amide I, amide III and skeletal stretching modes can be used to characterize backbone conformation in polypeptides or proteins (Li–Chan 1996). A review by Li–Chan and others (1994) indicated that, in general, protein with high α–helical contents show an amide I band centered in a range of 1645 – 1657 cm^{-1} and a weak amide III band located in a broad region of 1260 cm^{-1} to 1300 cm^{-1}, which overlaps with the area assigned for β–turns. In case of proteins with high β–sheet structures, an amide I band centered around 1665 cm^{-1} to 1680 cm^{-1} and an amide III band near 1238 – 1245 cm^{-1} have been observed. Proteins containing a high proportion of undefined or random coil structures show an amide I band at 1660 and an amide III transition close to 1250 cm^{-1}. The distinctive areas of amide I and amide III corresponding to protein conformations (comprising of α–helix, β–sheet, β–turn, and random coil) are depicted in Figure 2.15.

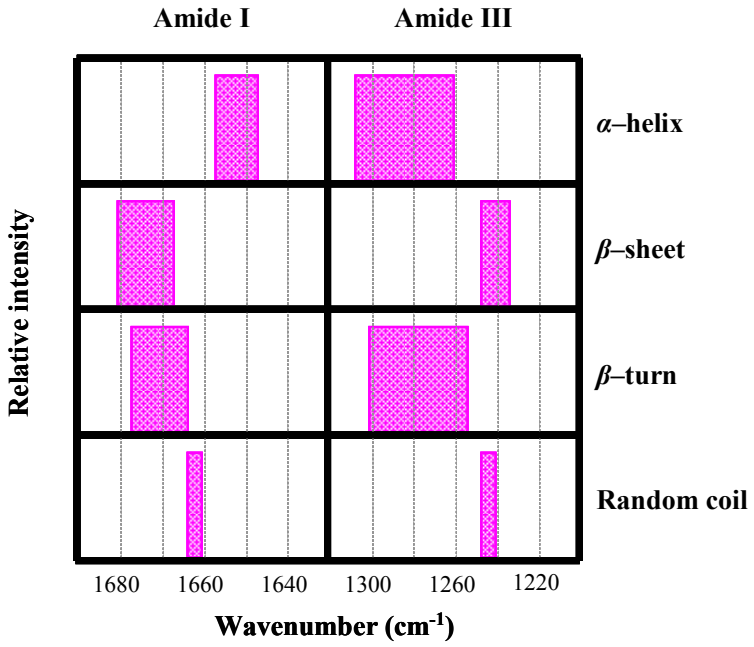

Figure 2.15. The typical locations of amide I and amide III vibrations corresponding to different types of protein conformation (modified from Li-Chan and others 1994)

A major advantage of Raman spectroscopy is that tested samples are not required to be optically clear (Li–Chan 1996). As a result, Raman spectroscopy is practical for molecular studies in aqueous solutions, nonaqueous solutions, fibers, films, powders, precipitates, gels and crystals. Since Raman scattering is physically weak and intensities of the Raman signal are in the order of 1×10^{-9} to 1×10^{-6} of those of elastic or Rayleigh scattering, reasonably high concentrations of the targets are required in samples (Li–Chan 1996). Therefore, the sample should usually contain protein or nucleic acid concentrations in the range of 2 – 20 mg/mL or approximately 0.03 – 0.1 M, expressed with respect to the concentration of peptide or nucleotide groups (Li–Chan 1996). Protein concentrations are positioned in an appropriate range in many food systems such as fluid milk, egg white, and meat systems, which contain approximately 3%, 10% and 15 – 20% protein, respectively (Li–Chan 1996). Therefore, Raman spectroscopy can be used for direct *in situ* analysis of food proteins and only small amounts of the food samples are required. However, for macromolecular constituents, such as proteins or polysaccharides, which are the structural substances of many food systems, the large number of functional groups and their diverse microenvironments usually result in overlapping broad spectral bands (Li–Chan 1996). To avoid the problem of overlapping bands, second derivative transformations can be performed.

Recently, Raman spectroscopy has become a popular method to determine the conformational changes of food proteins during gelation, coagulation, and emulsification. For example, Raman spectroscopic determination has been used for investigating effects of buffer conditions and heat treatments on the conformation of

common buckwheat globulin (Choi and Ma 2007) and on the whey protein structure (Alizadeh–Pasdar and others 2002). In addition, Raman spectroscopy has been reported as a tool to determine the degree of O-esterification in food proteins, specifically acetylated soy protein isolates, by investigating the C=O vibration band at 1737 cm^{-1} (Yu and others 2004).

Not only has Raman spectroscopy been employed in studies of physiochemical changes in protein–based foods, it has also been used in the analyses of carbohydrates (Bulkin and others 1987; Arboleda and Loppnow 2000; Synytsya and others 2003; Fechner and others 2005) and lipids (Strehle and others 2006). In addition, Raman spectroscopy has been lately applied for evaluating changes in macromolecular interactions, such as protein–protein interactions (Howell and others 1999), protein–lipid interactions (Meng and others 2005), and protein–carbohydrate interactions (Alizadeh–Pasdar and others 2002) in food systems. For example, Sultanbawa and Li–Chan (2001) employed Raman spectroscopy to investigate effects of frozen storage on structural changes of proteins in a natural actomyosin matrix and a surimi matrix.

CHAPTER 3

EFFECT OF FREEZE–DRIED BEEF HEART ADDITION ON COMPOSITION AND TEXTURE CHARACTERISTICS OF HOMEMADE FRESH PASTA

3.1 Abstract

The objective of this study was to investigate the effect of adding freeze–dried beef heart to fresh pasta on texture profiles, firmness, color and composition of the cooked pasta. Fresh pasta was prepared from durum wheat flour with substitution levels of 0%, 10%, 30% or 50% freeze–dried beef heart. Pasta dough did not form at 50% freeze–dried beef heart substitution. The addition of beef heart at 30% significantly increased the hardness, adhesiveness, chewiness, and firmness of the pasta. Partly replacing durum wheat flour with freeze–dried beef heart led to significant changes in lightness, redness, and yellowness of cooked fresh pasta. In addition, the protein content of the pasta increased considerably by partial incorporation of freeze–dried beef heart. Addition of freeze–dried beef heart to pasta might have the potential to increase the nutritional value of pasta while simultaneously increasing the value of beef heart, which currently is a by–product of beef manufacture.

Keywords: pasta; beef heart; texture; color; proximate composition

3.2 Introduction

Pasta is a popular side dish throughout a large part of the world. Pasta is commonly made from durum wheat flour mixed with water. Thus, pasta is categorized as a wheat flour–based product, which is low in protein, as well as some vitamins and minerals. To improve the protein quality of pasta, many researchers have incorporated various plant proteins, such as soy flour (Shogren and others 2006), corn germ flour (Lucisano and others 1984), legume flour (Zhao and others 2005), whey proteins (Schoppet and others 1976) or animal proteins such as fish (Kim and others 1990) into pasta.

Beef heart is a by–product of beef manufacture and commonly used in animal feed as an inexpensive source of protein. Because of its high nutritional quality, beef heart could be a good protein source for human consumption. In addition, beef heart is high in riboflavin, vitamin B_{12}, and iron. Beyond its nutritive compounds, other non–nutritive components have also been shown to be relatively high in beef heart, such as coenzyme Q_{10} (Mattila and Kumpulainen 2001; Purchas and others 2004a), and creatine (Purchas and others 2004a). Thus, partially replacing durum wheat flour in pasta with freeze–dried beef heart may not only add value to beef heart but also increase the nutritional value of pasta products. However, incorporation of freeze–dried beef heart into homemade pasta may cause changes of other quality attributes. Specifically, partial replacement of durum wheat flour with freeze–dried beef heart may negatively affect texture, flavor, and color characteristics of the pasta. Among those attributes, appearance and texture are considered to be of greater importance to consumers' acceptance of pasta products than flavor attributes (Cole 1991). Sensory evaluation and instrumental

assessment are contemporary methods for investigating quality attributes of food products. Tang and others (1999) investigated the correlation between instrumental analysis and sensory descriptive evaluation of physical attributes of cooked wheat flour–based products, such as cooked wheat noodles. Their observations showed a reasonably good association of texture and color attributes obtained through instrumental methods with sensory assessments. In other words, the results obtained from both instrumental and sensory analysis of physical quality attributes of cooked wheat flour–based products are quite representative of one another. Instrumental analysis was chosen in this study as the analytical tool to investigate the effects of freeze–dried beef heart on texture profiles, firmness, and color in cooked fresh pasta because it is less expensive, less time–consuming, and provides reliable results.

The main objective of this study was to determine effects of incorporating freeze–dried beef heart on physical attributes including texture profiles, firmness, and color in fresh homemade pasta products. Proximate composition and cholesterol content of the cooked homemade pasta were also examined in this study.

3.3 Materials and Methods

3.3.1 Freeze–dried beef heart preparation

Beef hearts were obtained from the meat laboratory of the University of Missouri, Columbia. After cleaning the beef hearts with distilled water and removing the connective tissue sheaths and any non–edible portions, the beef hearts were chopped into small pieces. The beef hearts were then homogenized in a general–purpose electric blender (Osterizer, Oster Corporation, Wis.) and freeze–dried in a freeze–dryer

(LabConCo Corp., Kansas City, Mo.) for ~ 48 h. Afterwards, the freeze–dried beef hearts were blended into fine powders and placed into a plastic bag which was purged with nitrogen gas and then stored in a freezer at –20°C until use.

3.3.2 Pasta preparation

Fresh pasta was prepared in a home–made style with three replications. The formulations of fresh pasta are shown in Table 3.1.

Table 3.1. Fresh pasta formulations

Percentage of added freeze–dried beef heart pasta	Ingredients		
	Durum wheat flour (g)	Freeze–dried beef heart (g)	Water (mL)
0%	180	0	120
10%	162	18	120
30%	126	54	120
50%	90	90	120

The dry ingredients including durum wheat flour (semolina) (Bob's Red Mill Natural Foods, Milwaukie, Ore.) and freeze–dried beef heart were mixed well before being poured onto a clean smooth work area. A well was made at the center of the flour mixture and 120 mL of tap water was slowly poured into the well. The mixture of durum wheat flour and freeze–dried beef heart was gradually mixed with the water by drawing the dry

mixture from the inside walls of the well with a fork until the dough became thick enough to stick to the fork. The flour was continually incorporated in the pasta dough by slowly drawing the flour by hand to form the dough ball. The pasta dough was further kneaded by hand for 10 min. until a smooth and elastic dough was obtained. During the kneading process, the pasta dough was pressed with the heels of the hands thereby thinning the dough. The dough was then folded back and the kneading process was repeated. When the dough became too sticky, a thin layer of flour was sprinkled on the dough while kneading. After 10 min, the smooth and elastic dough ball that was obtained was wrapped with a plastic film and left to rest in a refrigerator at 5ºC for 60 min. After resting, the pasta ball was divided into 4 small pieces. One piece of the dough was flattened and then fed into a rolling machine (Al Dente from Villaware ®, Cleveland, Ohio) starting at the widest setting (number 7). The flattened dough exiting from the rolling machine was folded and repeatedly fed through the machine at consecutively narrower settings (numbers 6, 5, 4 and 3, respectively) to get a thin pasta sheet, which was finally cut by passing it through the spaghetti cutter attachment. The long thin pasta strands (Figure 3.1) were then dried at room temperature on kitchen towels for 90 min before use.

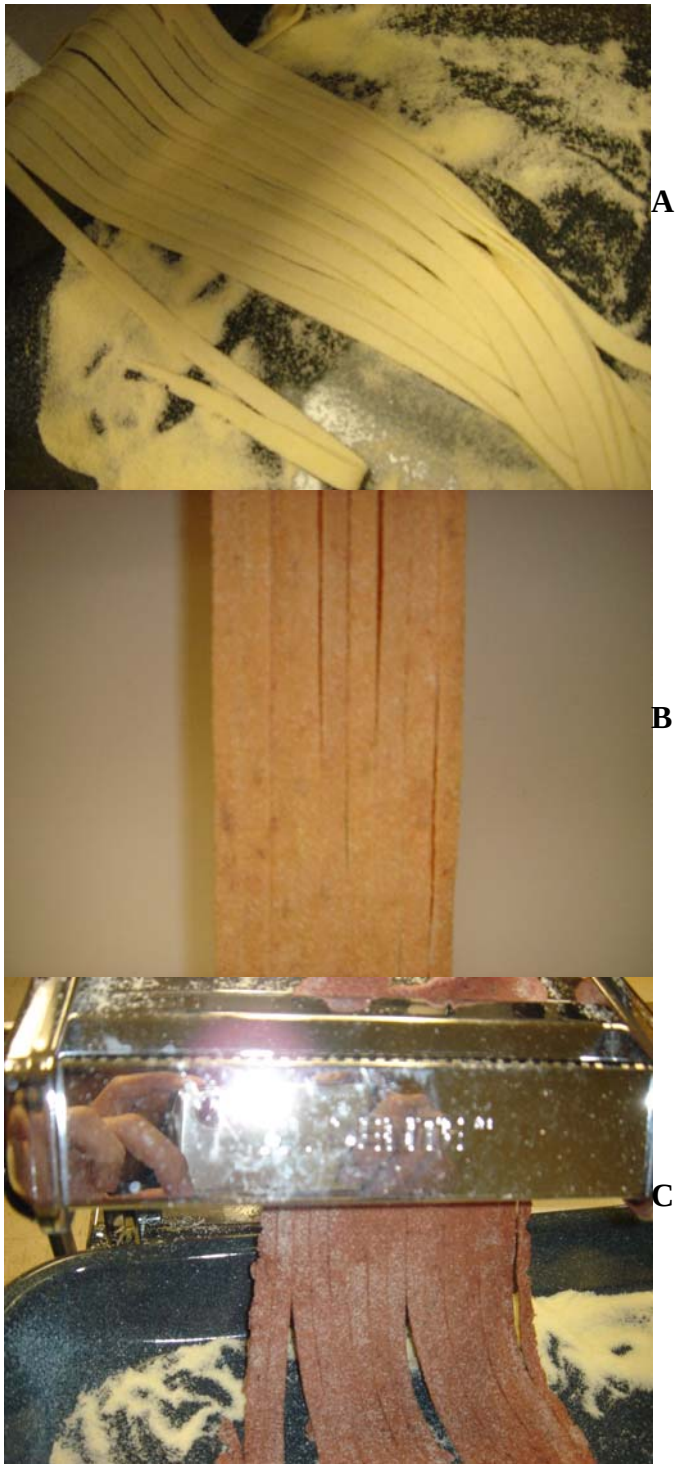

Figure 3.1. Newly formulated pasta strands made up of durum wheat flour and freeze–dried beef heart at the levels of A) 0%, B) 10%, and C) 30% additions

3.3.3 Cooking condition

Fifty grams of pasta strands were cooked in 1 L of boiling water for 2 min. After draining, the pasta was rinsed with tap water. The cooked pasta was either kept in a Ziploc bag until further analysis or immediately used for texture and color attribute determinations.

3.3.4 Texture measurement

Texture profiles and firmness of cooked formulated pasta were determined by a slightly modified method of that used by Tang and others (1999) for determining texture profiles and firmness of cooked wheat noodles. The measurement was done in triplicate for each replication of cooked pasta from the same sample formulas. The texture profile analysis (TPA) and firmness test were accomplished by using a TA–HDi® texture analyzer (Texture Technologies Corp., Scarsdale, N.Y.). The extraction and definitions of texture profiles including hardness, cohesiveness, adhesiveness, springiness, and chewiness have been described by Bourne (1978) (Table 3.2). Texture profile analysis was conducted by placing a pasta strand on a sample holder, which was attached to a surface serrated by 90 ºvee grooves, 1.5 mm deep, spaced at 3.6 mm. A flat cylindrical plexiglass plunger (25 mm in a diameter) with a 5 Kg load cell was connected to the texture analyzer. A strand of the cooked pasta samples was compressed to 70% fixed strain (referred to as the distance that the cylinder probe traveled as a percentage of the sample height) using a cross head speed of 0.2 mm/s. The compression was done twice to better replicate the action of human bites. For the firmness test, a pasta strand was placed on a sample holder and then compressed with a plexiglass blade instead of a flat

cylindrical plexiglass plunger (Figure 3.2), also using a 5 Kg load cell. A strand of the cooked pasta samples was sheared crosswise by the blade to 75% fixed strain using a cross head speed of 0.2 mm/s. While firmness is a result derived from the shear test, texture profiles are values extracted and calculated from the force–time curve. All data obtained from the texture measurements were collected using Texture Expert Exceed (version 2.61, Texture Technologies Corp., Scarsdale, N.Y.).

Table 3.2. Physical attributes in texture profile analysis (Bourne 1978)

Attributes	Definition
Hardness	The height of the force peak on the first compression cycle (“first bite”)
Cohesiveness	The ratio of the positive force areas during the second compression to that during the first compression
Adhesiveness	The negative force area of the first bite which represents the work necessary to pull the compressing plunger from the sample
Springiness (or elasticity)	The height that food recovers during the elapsed time between the end of the first bite and the beginning of the second bite.
Chewiness	Hardness × Cohesiveness × Springiness

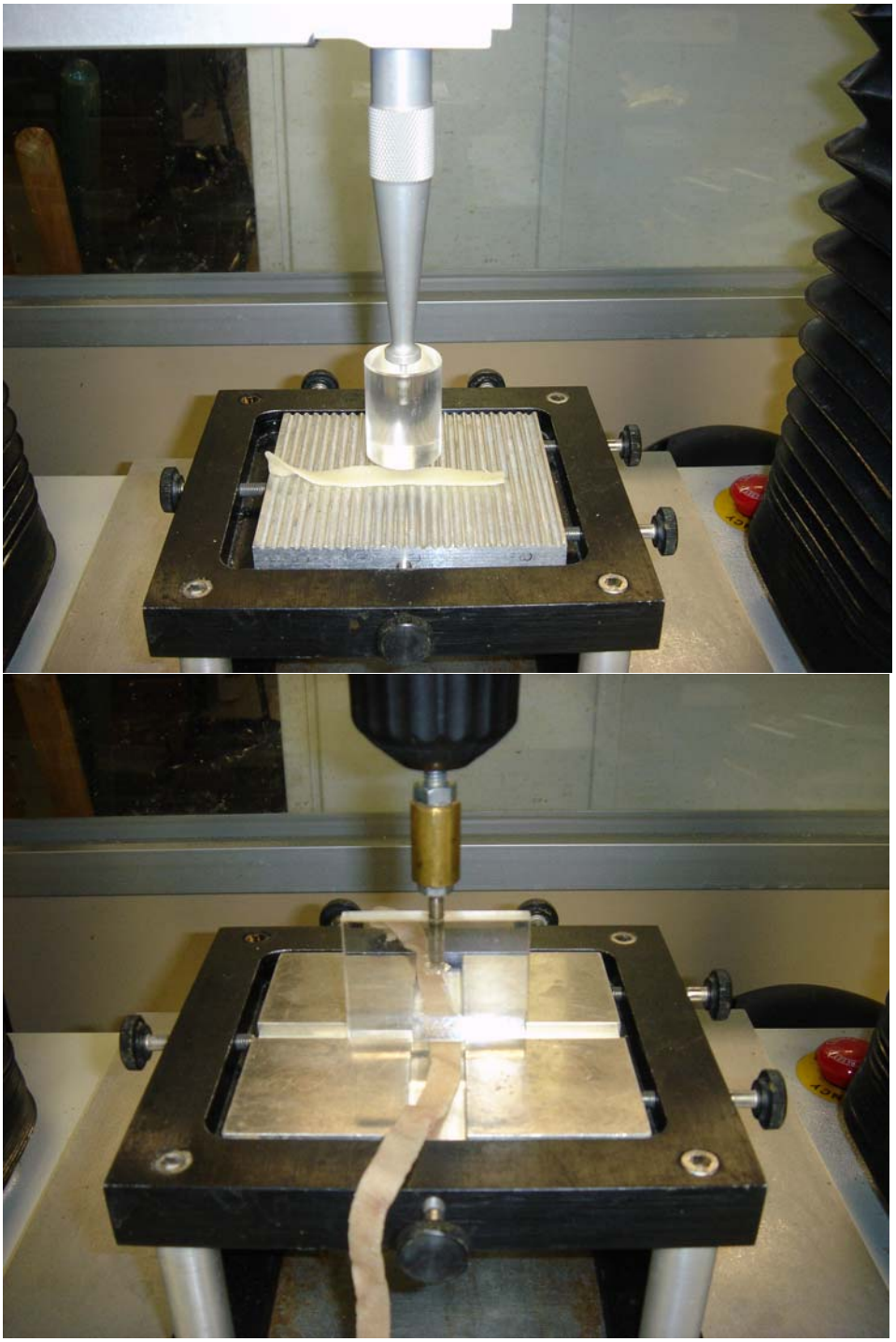

A

B

Figure 3.2. A flat cylindrical plexiglass plunger (A) against a plexiglass blade (B)

3.3.5 Color measurement

The color of ingredients (durum wheat flour and freeze–dried beef heart), and cooked fresh pasta was determined using a hand–held Konica Minolta Chromameter (Model CR–410, Sensing Inc., Japan). The values obtained from the color measurement were reported as the values of L* (assigned for lightness), a* (for redness when positive and greenness when negative), and b* (for yellowness when positive and blueness when negative). The color was measured in triplicate for each replication.

3.3.6 Proximate composition and cholesterol content

Proximate compositions and cholesterol content were analyzed by AOAC International Official Methods (2006). Moisture content was determined by AOAC Method 934.01 using a vacuum oven. Crude fat was determined by ether extraction, which is AOAC Official Method 920.39. Ash determination was done by AOAC Method 942.05, and crude protein was done by the AOAC Kjeldahl Method 984.13. Total carbohydrate content was determined by subtraction of the sums of the percentages of moisture, crude fat, ash, and crude protein from 100. Cholesterol content was determined using gas liquid chromatography, AOAC Method 994.10.

3.3.7 Data analysis

Statistic analysis was conducted using the SAS® for Windows^{TM} version 9.00 (SAS Institute Inc., Cary, N.C.). Significant differences among cooked pasta samples were determined using analysis of variance (ANOVA) at $p<0.05$ in the general linear models (GLM) procedure of the SAS® software program. The ANOVA was analyzed as a Randomized Complete Block Design. Fisher's least significant difference (LSD) was performed as a mean separation method. SAS inputs are illustrated in Appendix 1 (1.1–1.3).

3.4 Results and Discussion

In preliminary experiments, homemade pasta was fortified with freeze–dried beef heart up to 50%. However, substituting half of the durum wheat flour with freeze–dried beef heart prevented dough formation, which might be due to interference of the heart tissue proteins with the formation of the gluten network and the interactions between starch granules and gluten proteins. Thus, Table 3.3 only shows the texture characteristics and firmness of cooked fresh pasta prepared with three different levels (0%, 10%, and 30%) of freeze–dried beef heart. There was a tendency but no significant increase in hardness, adhesiveness, and chewiness between the 0% and the 10% freeze–dried beef heart addition. However, significant increases for those attributes were observed at the 30% beef heart level. The characteristics of cooked pasta are shown in Figure 3.3.

Table 3.3. Texture profiles and firmness of cooked fresh pasta

Characteristics	Percentage of freeze–dried beef heart content in cooked pasta		
	0% (Control)	10%	30%
Hardness (g)	1186.44 ± 228.75 [b]	1680.27 ± 373.42 [b]	3867.55 ± 349.69 [a]
Cohesiveness	0.46 ± 0.03 [ab]	0.42 ± 0.02 [b]	0.47 ± 0.01 [a]
Adhesiveness (g.s)	-121.45 ± 32.56 [b]	-86.90 ± 44.67 [b]	-12.65 ± 14.25 [a]
Springiness	0.87 ± 0.09 [a]	0.88 ± 0.04 [a]	0.90 ± 0.07 [a]
Chewiness	482.89 ± 130.58 [b]	621.71 ± 143.53 [b]	1643.04 ± 183.32 [a]
Firmness (g)	66.83 ± 12.70 [b]	89.93 ± 19.28 [b]	248.45 ± 66.22 [a]

Values are means ± SD of three replications (n = 3).

Values in the same row with the same superscript letters are not significantly different at $p<0.05$.

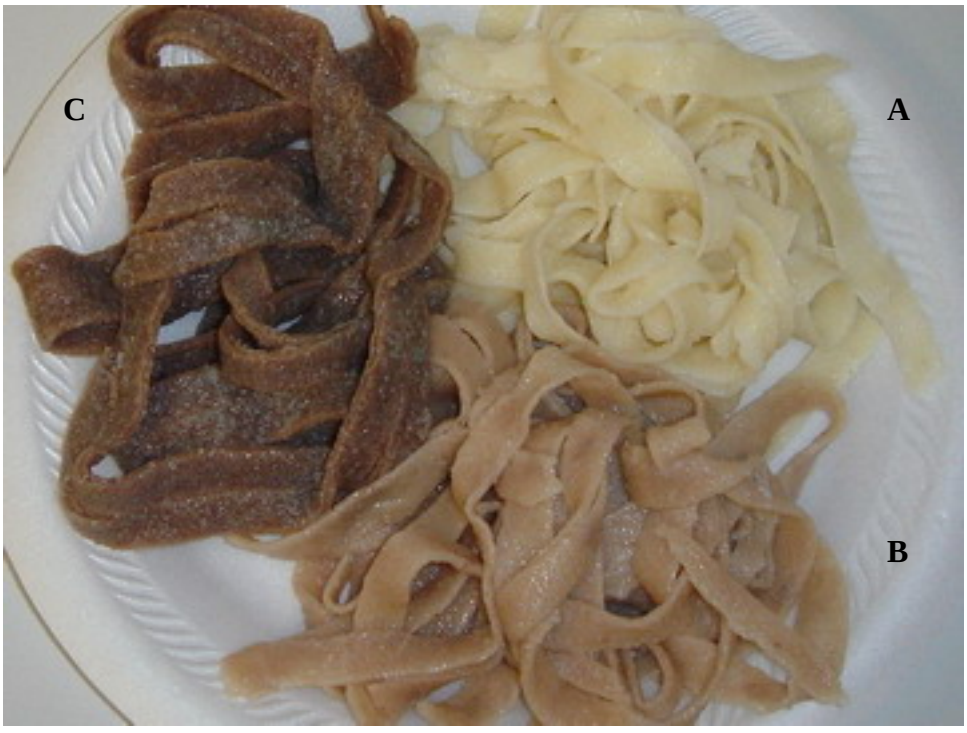

Figure 3.3. Characteristics of cooked pasta; A) 0%, B) 10%, and C) 30% added beef heart pasta

Olivera and Salvadori (2006) considered that the greater hardness of pasta made with whole wheat was a result of interactions between the gluten network and the fiber, which strengthened the dough and increased its resistance to breakdown instead of weakening it. Muscle proteins, such as in striated skeletal and heart muscles (Foegeding and others 1996) are fibrous in nature, as well, and may interact with the gluten network in a similar fashion, especially considering that protein–protein interactions, such as in gluten and muscle proteins, are even more likely than protein–carbohydrate interactions, such as in gluten and dietary fibers. Thus, cardiac fibers might have been integrated in the gluten matrix, which lead to increased hardness in cooked pasta containing higher amounts of freeze–dried beef heart. The observation that other proteins may increase the hardness of a dough product was made by Gujral and Pathak (2002), who showed that the addition of caseinate, which is milk protein, to chapati dough, in addition to increasing the extensibility of the dough, increased the force necessary to fracture the unleavened bread.

Springiness, also called elasticity, of cooked fresh pasta was not significantly different among the three levels of freeze–dried beef heart addition. However, cohesiveness of cooked pasta was significantly different between cooked pasta samples with 10% and 30% freeze–dried beef heart addition. Adhesiveness of cooked pasta showed a rising tendency with increasing level of freeze–dried beef heart and was significantly increased at the 30% replacement level. The decrease in cohesiveness in 10% added freeze–dried beef heart pasta compared with cooked pasta without added freeze–dried beef heart, might be because freeze–dried beef heart could function similarly to shortening. Shortening of gluten strands can be achieved by lipids or with surface–

active ingredients (Knightly 1981). However, lipids, in addition to imparting decreased cohesiveness, also decrease the hardness of shortened products, such as in cakes compared to breads. Thus, it is unlikely that beef heart proteins “shorten” the dough in a lipid–like fashion because the hardness of the dough increased due to the beef heart proteins. Considering that beef heart muscle proteins have emulsifying activities (Parkington and others 2000), the added beef heart proteins in “shortening” the gluten strands in the pasta is more likely similar to that of surface–active ingredients, which might shorten gluten strands and decrease cohesiveness but not affect hardness as the way lipids do. Adding 30% freeze–dried beef heart into pasta, on the other hand, could possibly strengthen gluten strands in the matrixes. This finding might be caused by soluble proteins and/or polar lipids in beef heart incorporated in pasta at 30% level could promote stability of the gluten network. Changes in texture attributes especially in cohesiveness and adhesiveness of pasta products after partial addition of freeze–dried beef heart might also be due to hydroxyl groups on the surface of cardiac proteins that could interfere with the hydrogen bonding in the gluten network. Hydrogen bonding between glutamine and hydroxyl residues of gluten polypeptides contributes to cohesion–adhesion properties of food products (Damodaran, 1996). In addition, hydrogen bonds play an important role in the stabilization of protein secondary structures, which are β–sheets and α–helices (Koning and Visser, 1992). Accordingly, partially incorporating beef heart into pasta could interrupt hydrogen bond formation and lead to changes of texture attributes in the pasta matrixes. These explanations correspond to observations made during the washing of pasta dough in order to get gluten balls (results not shown). When no freeze–dried beef heart was added, the gluten matrix was well developed,

specifically gluten strands were bonded together, and the gluten balls exhibited great elasticity. However, gluten balls obtained from the dough with 10% added freeze–dried beef heart pasta tended to fall apart during washing, unlike the gluten balls that originated from the pasta dough containing 0% freeze–dried beef heart. The gluten balls from the 30% added beef heart, on the other hand, showed a gluten structure that was as cohesive as that of the 0% control.

Chewiness is a parameter derived from the multiplication of hardness, cohesiveness and springiness (Table 3.2), and because all three of these parameters are significantly higher for the 30% added beef heart pasta compared to the 0% and 10% pasta, it is obvious that the difference between the 10% and the 30% beef heart pasta for the derived parameter, chewiness, will be greatly amplified. Similar to hardness, adhesiveness, and chewiness, the firmness of cooked fresh pasta tended to increase with increasing amounts of freeze–dried beef heart and significantly increased at the 30% substitution level, which again might be explained by the reinforcement of the pasta matrix by cardiac muscle tissue. On the other hand, Kim and others (1990) found a significant decrease in the firmness of cooked pasta with added animal proteins. However they fortified the pasta with a different protein source, namely surimi, and considered that the interference of the fish muscle protein with the gluten matrix lowered the firmness of cooked pasta.

Color attributes are shown in Table 3.4. The L* values (lightness) of cooked fresh pasta decreased significantly with an increase in the percentage of added freeze–dried beef heart. While durum wheat flour and pasta without beef heart were significantly lighter than other treatments, there was no significant difference in lightness between

freeze–dried beef heart and the pasta with 10% added freeze–dried beef heart, indicating that adding freeze–dried beef heart has a considerable influence on lightness of cooked fresh pasta. Adding freeze–dried beef heart into fresh pasta also caused significant increases in a* values among cooked pasta samples, indicating that freeze–dried beef heart had a substantial effect on redness of cooked fresh pasta. Unlike L* and a* values, b* values decreased significantly with an increase of freeze–dried beef heart addition to fresh pasta products, which indicates a lowering of the yellow color due to beef heart addition. The b* values of freeze–dried beef heart and 30% added freeze–dried beef heart pasta were not significantly different. Partially adding freeze–dried beef heart into pasta products caused observable color changes in the newly formulated pasta from the original one. However, many differently colored food products, such as pink lemonade and green spinach pasta that were introduced into the marketplace, have been successfully accepted by consumers. Lawless (1995) indicated that success of alternated–colored food products in the marketplace stemmed from an expansion of dietary selections by consumers, such as a shift from white bread to whole wheat bread, and consequently broadened the selection of food ingredients offered by food manufactures.

Table 3.4. Color values of ingredients and cooked fresh pasta

Samples	Color		
	L*	a*	b*
Durum wheat flour	83.50 ± 0.82 [a]	-1.37 ± 0.09 [d]	23.23 ± 0.33 [a]
Freeze–dried beef heart	49.91 ± 2.44 [c]	11.79 ± 0.88 [a]	7.06 ± 0.60 [d]
0% Freeze–dried beef heart addition	75.70 ± 2.16 [b]	-2.14 ± 1.04 [d]	19.76 ± 1.24 [b]
10% Freeze–dried beef heart addition	51.54 ± 0.83 [c]	8.72 ± 0.52 [b]	13.53 ± 1.00 [c]
30% Freeze–dried beef heart addition	36.13 ± 1.80 [d]	6.87 ± 0.86 [c]	6.90 ± 0.75 [d]

Values are means ± SD of three replications (n = 3).

Values in the same column with the same superscript letters are not significantly different at $p<0.05$.

The proximate composition and cholesterol contents of cooked pasta fortified with three different levels of freeze–dried beef heart are shown in Table 3.5. The moisture content of cooked pasta tended to decrease and was significantly reduced in the pasta with 30% freeze–dried beef heart addition. Similarly, fat content and ash content tended to increase when pasta was fortified with freeze–dried beef heart and showed significant differences at the 30% level, but there was no significant difference in carbohydrate content among pasta samples. Partially replacing durum wheat flour with freeze–dried beef heart boosted protein content in cooked pasta significantly. Like the protein content, cholesterol levels of cooked pasta increased significantly with higher substitution. Although incorporating freeze–dried beef heart into pasta led to higher cholesterol contents in cooked homemade pasta, freeze–dried beef heart could be an alternate ingredient to egg, which is a classic ingredient usually added to homemade pasta

products. Evidently, homemade pasta made with egg contains higher levels of cholesterol than homemade pasta made without egg. According to the USDA national nutrient database for standard reference (2007), one hundred grams of cooked homemade pasta made with egg contains 41 mg of cholesterol, which is 40% higher than what we found with a 30% beef heart addition. However, research is needed to answer the general question how important slight changes in color and texture of pasta produced by partially adding beef heart might be for consumer acceptance if people know that the newly formulated pasta is healthier.

Table 3.5. Proximate composition and cholesterol content of cooked fresh pasta

Composition	Percentage of freeze–dried beef heart content in pasta		
	0%	10%	30%
Moisture (%)	69.54 ± 1.68 [a]	67.96 ± 2.96 [a]	62.36 ± 1.13 [b]
Crude fat (%)	0.16 ± 0.10 [b]	0.33 ± 0.18 [b]	1.30 ± 0.75 [a]
Ash (%)	0.22 ± 0.02 [b]	0.28 ± 0.03 [b]	0.61 ± 0.10 [a]
Crude protein (%)	4.95 ± 0.25 [c]	7.10 ± 0.32 [b]	13.37 ± 0.99 [a]
Total carbohydrate* (%)	25.13 ± 1.52 [a]	24.33 ± 2.48 [a]	22.36 ± 1.55 [a]
Cholesterol (mg/100g)	0.25 ± 0.43 [c]	7.12 ± 0.45 [b]	28.27 ± 4.07 [a]

Values ± SD in the same row with the same superscript letters are not significantly different at $p<0.05$.

3.5 Conclusion

Addition of freeze–dried beef heart in fresh pasta significantly influenced texture attributes and firmness of cooked fresh pasta products at 30% substitution level. However, no significant differences in texture and color attributes were observed when only 10% of the flour was replaced with beef heart. These changes in physical attributes after partially replacing durum wheat flour with freeze–dried beef heart are likely due to interferences of the gluten development, as well as the development of the gluten–starch interactions by the cardiac muscle proteins. In addition, direct interactions of these cardiac proteins with the gluten proteins may very well contribute to these changes in physical attributes. Moreover, freeze–dried beef heart had a major effect on lightness, redness, and yellowness of cooked fresh pasta by increasing the darkness, enhancing the red color and also lowering the yellow color of cooked products. While pasta is obviously a carbohydrate–rich food, replacing durum wheat flour with freeze–dried beef heart could be a way to lower carbohydrate levels and increase protein levels, making it more appealing to people who follow an Atkins–type or South Beach–type diet. In addition, the use of freeze–dried beef heart in pasta would be an avenue to add additional value to beef heart, as well as enhance the nutritional value of pasta products.

CHAPTER 4

VALUE–ADDED HOMEMADE PASTA FORTIFIED WITH FREEZE–DRIED BEEF HEART CONTAINING COENZYME Q_{10}

4.1 Abstract

The objectives of this study were to develop pasta containing elevated levels of coenzyme Q_{10} and to determine effects of household–type cooking on coenzyme Q_{10} content of the newly formulated pasta. The measurement of coenzyme Q_{10} was performed using direct solvent extraction and a high performance liquid chromatograph (HPLC) equipped with an ultraviolet (UV) detector. The coefficient of variance (*CV*) for testing the precision of the coenzyme Q_{10} extraction procedure was 11.66%. Repeatability of the HPLC and the data handling system for the coenzyme Q_{10} analysis was acceptable (*CV* = 8.45%). Coenzyme Q_{10} recovery was 99.36 ± 3.17%. Freeze–drying before extraction is recommended to be included in the analytical procedure. A saponification step, which is often incorporated in the procedure, was found to possibly degrade coenzyme Q_{10} in food matrixes. The content of coenzyme Q_{10} in beef heart was around 70 μg/g (dry basis). Fortifying pasta with beef heart significantly increased the content of coenzyme Q_{10} in the pasta. No significant change in coenzyme Q_{10} content was observed in the pasta after cooking. Although the content of coenzyme Q_{10} in the formulated pasta was lower than that generally found in commercially available supplements, beef heart still has a high potential as a source of coenzyme Q_{10} because, as a by–product, its use is economical.

Keywords: pasta; beef heart; coenzyme Q_{10}; ubiquinone; ubiquinol; ubidecarenone

4.2 Introduction

Currently, there is a growing interest among consumers to buy healthy functional foods that are fortified with various bioactive compounds. Therefore, much of the interest in developing novel healthy foods has been focused on bioactive ingredients, such as carotenoids, dietary fiber, fatty acids, phenols, plant sterols, soy proteins, and antioxidants, including coenzyme Q_{10}. Coenzyme Q_{10} (ubiquinone or ubidecarenone) is of particular interest among these bioactive compounds because of its unique characteristics. It is a lipid soluble compound found naturally in plants and animals, as well as in microorganisms. The reduced form of coenzyme Q_{10}, ubiquinol, is the only endogenously synthesized fat–soluble antioxidant protecting cellular membranes and plasma lipoproteins from lipid peroxidation (Kishi and others 1999; Kagan and Quinn 2000). Coenzyme Q_{10} has been found in varying amounts in most human tissues, including heart (~ 110 μg/g tissue), kidney (~ 70 μg/g tissue), and liver (~ 60 μg/g tissue) (Overvad and others 1999). However, many researchers have observed that coenzyme Q_{10} was lowered in people with some chronic diseases, such as heart disease, cancer, AIDS, and the elderly, including in some genetic diseases, such as neurologic diseases and myopathies (Papas 1999). Therefore, consumption of exogenous coenzyme Q_{10} from food sources has been proposed as a way to sustain good health (Mattila and Kumpulainen 2001) and also as a potential approach to maintain serum coenzyme Q_{10} in the human blood circulation system (Weber and others 1997b).

While coenzyme Q_{10} is synthesized endogenously, dietary intake is a significant contributor of coenzyme Q_{10} in humans. Mattila and Kumpulainen (2001) determined coenzyme Q_{10} in foods and found that reindeer meat (157.9 μg/g fresh wt), pork heart

(126.8 μg/g fresh wt), beef heart (113.3 μg/g fresh wt), and beef liver (39.2 μg/g fresh wt) were the richest sources of coenzyme Q_{10}. Beef heart is an edible and nutritious muscle, which is rarely used for human consumption because many people view it as an organ that is more similar to other innards than to skeletal muscle. Thus it is used mainly as a beef by–product in pet foods. It has recently been incorporated in animal protein–based foods, such as surimi (Wang and Xiong 1998) and frankfurters (Desmond and Kenny 1998), in order to increase the economic value of beef heart and also to enhance the nutritional value of newly formulated food products. However, no publication could be found on incorporating beef heart into gluten protein–based foods such as pasta yet. In 2005, the average pasta intake of the U.S. population was 19.52 pounds per person and tended to increase in successive years (Business Trend Analysis 2006). Therefore, pasta was chosen in this study as the vehicle to provide more coenzyme Q_{10} than that found in traditional cereal grain products because of its popularity and the potentially large amounts of consumption.

To date, there is no Dietary Reference Intake (DRI) for coenzyme Q_{10} (National Academy of Sciences 1997–2005). However, accumulated data (Weber and others 1994; Barbieri and others 1999; Hodges and others 1999; Langsjoen and Langsjoen 1999; Munkholm and others 1999; Overvad and others 1999) show that consumption of 30 − 200 mg/day of coenzyme Q_{10} can promote health. The current dietary intake of 3 − 5 mg/day of coenzyme Q_{10} (Weber and others 1997a) is far below these unofficial recommendations obtained from scientific experiments. Consumption of coenzyme Q_{10} from fortified foods might be an alternative to dietary supplements for maintaining good health. In addition, Weber and others (1997b) reported that ingestion of coenzyme Q_{10}

either from meals or capsules could significantly increase plasma coenzyme Q_{10} concentrations in human and there is no significant difference between administration of coenzyme Q_{10} from foods and supplements on the coenzyme Q_{10} absorption.

The objective of this study was, therefore, to formulate pasta products containing elevated levels of coenzyme Q_{10}. Although most research has shown good stability of coenzyme Q_{10} during food processing, the effect of household cooking on coenzyme Q_{10} content in the newly formulated pasta was also examined in this study because it has not yet been investigated. In order to quantify coenzyme Q_{10}, a direct hexane–ethanol extraction was used in the analytical method. Direct solvent extraction and a saponification step before extraction are generally used in the extraction of coenzyme Q_{10} from food samples. Weber and others (1997a) reported that incorporating a mixture of ethanol–hexane in the extraction procedure provided equivalent results to a procedure that included the saponification step. As a result, the application of the direct solvent extraction has been commonly used for food matrixes because of simplicity, effectiveness, and being less time consuming (Weber and others 1997a; Mattila and others 2000; Purchas and others 2004a; Strazisar and others 2005; Souchet and Laplante 2007). Nevertheless, saponification is still widely employed, specifically for high fat content samples (Kamei and others 1985; Mattila and Kumpulainen 2001).

4.3 Materials and methods

4.3.1 Freeze–dried beef heart preparation

Beef hearts were obtained from the meat lab at the University of Missouri, Columbia. The beef hearts were cleaned with distilled water. The beef hearts were then chopped into small pieces and the connective tissue sheaths, as well as any non–edible portions, were removed. The beef hearts were then homogenized in an electric blender (Osterizer, Oster Corporation, Milwaukee, Wis.) and freeze–dried (LabConCo Corp., Kansas City, Mo.) for approximately 48 hr. Afterwards, the freeze–dried beef hearts were blended into a fine powder. The freeze–dried beef heart powders were stored in plastic bags under nitrogen gas and kept at –20°C until use.

4.3.2 Pasta preparation

Three different formulas of homemade pasta were prepared in three replications as shown in Table 4.1. Dry ingredients, including durum wheat flour (Bob's Red Mill Natural Foods, Milwaukie, Ore.) and freeze–dried beef heart, were gradually mixed with 120 mL of tap water. The pasta dough was continually kneaded by hand for approximately 10 min until a smooth and elastic dough was obtained. The dough was folded back and repeatedly kneaded to form a ball of dough. After a smooth and elastic ball was obtained, it was wrapped with a plastic film and placed in a refrigerator for 60 min. After resting, the pasta ball was divided into 4 small pieces. A piece of the dough was flattened by feeding through a rolling machine (Al Dente from Villaware®, Cleveland, Ohio) at the widest setting, number 7. The flattened dough was repeatedly rolled at increasingly narrower settings of 6, 5, 4, and 3, respectively, to get a thin pasta

sheet. That pasta sheet was then cut by passing it through the spaghetti cutter attachment. The long thin pasta strands were then dried at room temperature on white kitchen towels for 90 min. Afterwards, fifty grams of the pasta strands were cooked in 1 L of boiling water for 2 min. After draining, the pasta was rinsed with tap water. The cooked pasta was then freeze–dried and kept in a bag under nitrogen until use.

Table 4.1. Formulas of fresh pasta

Percentage of added freeze–dried beef heart in pasta (W/W)	**Ingredients**		
	Durum wheat flour (g)	**Freeze–dried beef heart (g)**	**Water (mL)**
0% (control)	180	0	120
10%	162	18	120
30%	126	54	120

4.3.3 Moisture content determination

The moisture content of the samples was measured by the AOAC Official Method 934.01, a vacuum oven method (AOAC International 2006). An aluminum pan containing a small glass stirring rod with sand was dried in a vacuum oven (Model 3640, National Appliance Co., Portland, Ore.) overnight at 100°C. The sand pan was removed and allowed to cool in a desiccator. Approximately 3 − 5 g of sample were accurately weighed and then mixed well with the sand. The sample was dried in the oven at 100°C

for 2 hr. The sample pan was then removed, cooled down in a desiccator, and weighed. The pan was returned to dry in the oven until a constant weight was obtained by reweighing every 30 min. For the freeze–dried samples, instead of an aluminum pan with sand, an aluminum dish with a lid was used. Determination of the moisture content was performed in duplicate and the differences were less than 10%.

4.3.4 Coenzyme Q_{10} analysis: Saponification procedure

Initially, prior to coenzyme Q_{10} extraction, a saponification process was performed according to Mattila and Kumpulainen (2001) with slight alterations. However, because the saponification appeared to destroy coenzyme Q_{10}, in subsequent sample analysis, this step was omitted. For the saponification step, two milliliters of 2% ascorbic acid solution (L–ascorbic acid from Sigma, St Louis, Mo.) and 5 mL methanol (Fisher Scientific, Fairlawn, N.J.) were added to a screw cap tube that already contained approximately 1 − 3 g sample. The mixture was sonicated for 10 min and then refluxed with 0.5 mL of 50% KOH solution (Potassium hydroxide, pellets, from Fisher Scientific, Fairlawn, N.J.) in boiling water for 10 min. The mixture was vortexed after 5 min of boiling. Afterwards, the mixture was allowed to cool and 10 mL 0.15 M NaCl (Fisher Scientific, Fairlawn, N.J.) was added into the mixture to prevent emulsion formation. After saponification, coenzyme Q_{10} was then extracted using a hexane/ethanol mixture as stated in the section of coenzyme Q_{10} extraction below.

4.3.5 Coenzyme Q_{10} analysis: Coenzyme Q_{10} extraction

As mentioned, the saponification step was later omitted from the procedure and coenzyme Q_{10} was extracted directly from freeze–dried samples using a solvent extraction method (Weber and others 1997a) with some modifications. Approximately 1 − 3 g of sample was accurately weighed into a screw cap tube and then homogenized (ice cooled) with 10 mL 0.15 M NaCl by using a sonicator (FS 20, Fisher Scientific, Fairlawn, N.J.) for 10 min. A volume of 3 mL ethanol (Chemical Stores, University of Missouri, Columbia) was then added to the mixture. Afterwards, the mixture was continuously sonicated for 10 min and further mixed vigorously for 10 min by using a shaker (Burrell, Wrist Action, Burrell Corp. Pittsburgh, Pa.). Fifteen mL of hexane (Fisher Scientific, Fairlawn, N.J.) were added into the mixture, which was again sonicated for 10 min and then shaken for another 10 min. The layers were allowed to separate and the combined hexane/ethanol layer was collected. The mixture was re–extracted twice with 1 mL ethanol and 5 mL hexane. The combined hexane/ethanol layers were washed with 6 mL saline and trace water was removed with Na_2SO_4 (Fisher Scientific, Fairlawn, N.J.). After filtration (Whatman #4, Whatman International Ltd., England), the solvent was purged to dryness with nitrogen gas. The residue was redissolved in a known amount of 2–propanol (Fisher Scientific, Fairlawn, N.J.). The volume of 2–propanol for redissolving extracts of coenzyme Q_{10} obtained from freeze–dried beef heart were 2, 1, and 0.5 mL for 30% added beef heart pasta, 10% added beef heart pasta samples, and 0% added beef heart pasta samples, respectively. Before injection into the HPLC, the solution was filtered through a 0.45 μm Millex (Milllipore

Corporation, Bedford, Mass.) filter. The sample extracts were kept refrigerated in a brown bottle until analysis.

4.3.6 Coenzyme Q_{10} analysis: HPLC analysis

Twenty microliters of sample extracts were injected into a high performance liquid chromatograph (Series 410, Perkin–Elmer, Norwalk, Conn.) equipped with an LC–95 ultraviolet (UV)/visible spectrophotometer detector (Perkin–Elmer, Norwalk, Conn.) and a Zorbax® 300SB–C18 column (3.5 μm, 4.6 × 150 mm, RTI Rockland Technologies, Inc., York, Pa.) fitted with a Zorbax® 300SB–C18 guard column (5 μm, 4.6 × 12.5 mm, RTI Rockland Technologies, Inc., York, Pa.) was used for separation. Mobile phase was prepared in the ratio of 53:24:21:2, consisting of methanol, ethanol, 2–propanol, and 1 M ammonium acetate buffer (see appendix 2 for its preparation recipe), pH 4.4 (Ammonium acetate from Sigma–Aldrich, Inc., St. Louis, Mo.), respectively. The flow rate of the mobile phase was 0.8 mL/min. Identification and quantification of coenzyme Q_{10} was done using an external standard curve at the absorbance wavelength of 275 nm. Coenzyme Q_{10} (Sigma–Aldrich, Inc., St. Louis, Mo.) was analyzed at room temperature and quantification was based on peak area. The analysis was performed in duplicate and the difference within the same samples was less than 10%.

4.3.7 Method reliability test

Linearity of the coenzyme Q_{10} standard curve was determined. Recovery tests were conducted by the standard addition method, which is adding known amounts of coenzyme Q_{10} into samples before extraction. The reproducibility of the extraction method was evaluated by determining coenzyme Q_{10} content of nine separate extractions of the same sample. To determine the precision of the HPLC and the data handling system, ten repeated measures of the coenzyme Q_{10} content from the same extract were examined. The results obtained from the methodology checks were then used for calculating coefficients of variation (*CV*), 100 times the standard deviation of response values divided by the mean of the response values.

$$CV = 100 \times \left(\frac{\sigma}{\mu} \right)$$

Duplicate analyses were done on all samples. The percentages of differences between the duplicates were calculated and varied by no more than 10%. In addition, a system check sample was prepared, which consisted of a beef heart sample that was analyzed multiple times during the study, specifically at times when conditions changed that may have affected the analysis, such as the preparation of fresh mobile phase, etc.

4.3.8 Statistical analysis

Statistical analysis was conducted using SAS® for Windows™ version 9.00 (SAS Institute Inc., Cary, N.C.). Differences of coenzyme Q_{10} content between cooked and uncooked pasta and also among the pasta products were determined using analysis of variance (ANOVA) at $p<0.05$ in the general linear models (GLM) procedure of the

SAS® software program. The ANOVA was analyzed as a Randomized Complete Block Design in which the treatments were arranged in a 2×2 design. While the design was originally arranged as 3×2, the content of coenzyme Q_{10} in the control group was undetectable. Fisher's least significant difference (LSD) was performed as a mean separation method. SAS input is exemplified in Appendix 1.4.

4.4 Results and discussion

Measurements of coenzyme Q_{10} contents in foods have been reported using analytical methods in which coenzyme Q_{10} was extracted by organic solvents, either with or without saponification. In this study, direct extraction of coenzyme Q_{10} using ethanol–hexane mixtures without saponification was chosen as the analytical method. Preliminary results indicated that coenzyme Q_{10} was destroyed by the saponification process (Figure 4.1). When coenzyme Q_{10} was spiked into samples prior to saponification, no peak was observed in the chromatogram after subsequent extraction, whereas a spike after the saponification step but before extraction showed a peak size identical to that of the standard. A possible reason for the loss of coenzyme Q_{10} in the saponification step is the detrimental effects of the high temperature accompanied by an alkaline condition. Souchet and Laplante (2007) also preferred to employ direct extraction for coenzyme Q_{10} determination. They concluded that, while saponification could possibly provide more accurate results by removing impurities, such as triglycerides, and releasing coenzyme Q_{10} bound to proteins in the mitochondrial membrane, it may also cause destruction of coenzyme Q_{10}, which is sensitive to alkali, and may lead to formation of artifacts due to ethoxy substitutions in the quinone ring and formation of ubichromenol.

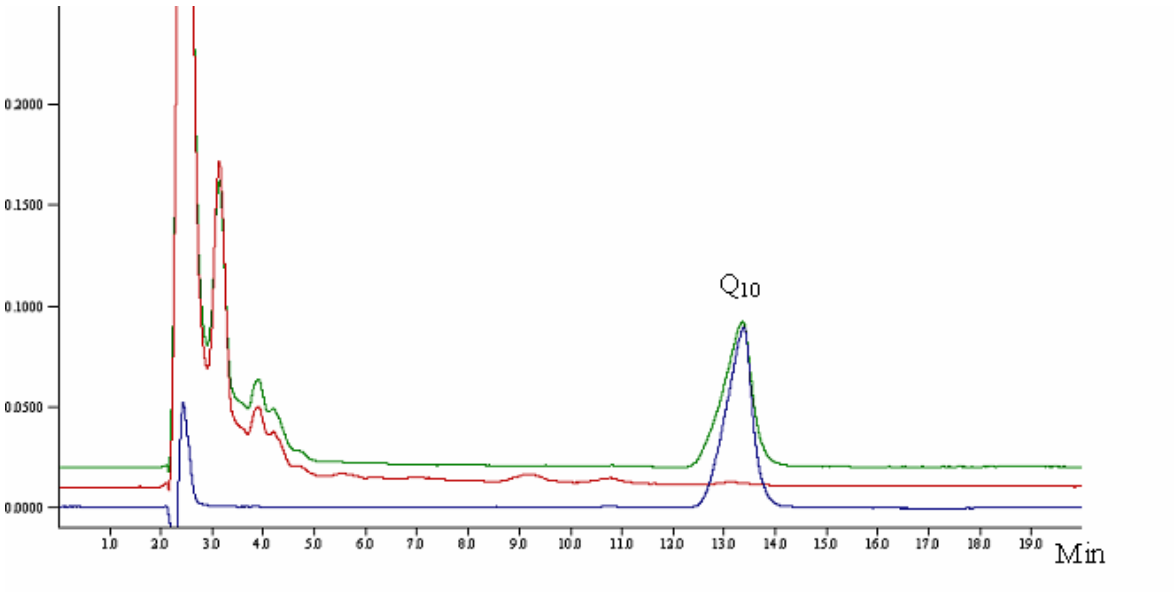

Figure 4.1. HPLC chromatograms of beef heart extract spiked with coenzyme Q_{10} standard after the saponification stage (top line), beef heart extract spiked with coenzyme Q_{10} standard prior to the saponification step (middle line), and coenzyme Q_{10} standard (bottom line)

In preliminary experiments, all pasta samples used for coenzyme Q_{10} analysis were fresh samples. As a result, the amounts of coenzyme Q_{10} was below detection limits in pasta samples with 10% beef heart addition and was close to detection limits in 30% added beef heart pasta samples before cooking and after cooking. The contents of coenzyme Q_{10} in the fresh uncooked and cooked pastas made with 30% level of beef heart were 3.38 ± 0.24 and 3.48 ± 1.97 μg/g dry weight, respectively. The quantitation limit of this methodology was 100 ng on column with a signal/noise ratio of 5:1, while the detection limit was set at a signal/noise ratio of 3:1. In addition, the percentages from the recovery tests in fresh pasta samples showed relatively high variations, ranging from 78 to 105%. These findings indicated that freeze–drying was a critical step in facilitating

extraction of coenzyme Q_{10} from food matrixes. The low moisture content of freeze–dried pasta samples might allow greater penetration of hexane–ethanol mixtures into the food matrixes, which will allow more coenzyme Q_{10} to be released from the food matrixes and dissolved in the organic solvents. Many researchers incorporated a freeze–drying step before the analysis of coenzyme Q_{10} (Mattila and Kumpulainen 2001; Purchas and others 2004a). However, many studies using fresh samples also yielded excellent results (Mattila and others 2000; Souchet and Laplante 2007).

The linearity of the coenzyme Q_{10} standard curve (Figure 4.2), ranging from 100 to 800 ng/injection, was shown by a coefficient of determination (R^2) of 0.98.

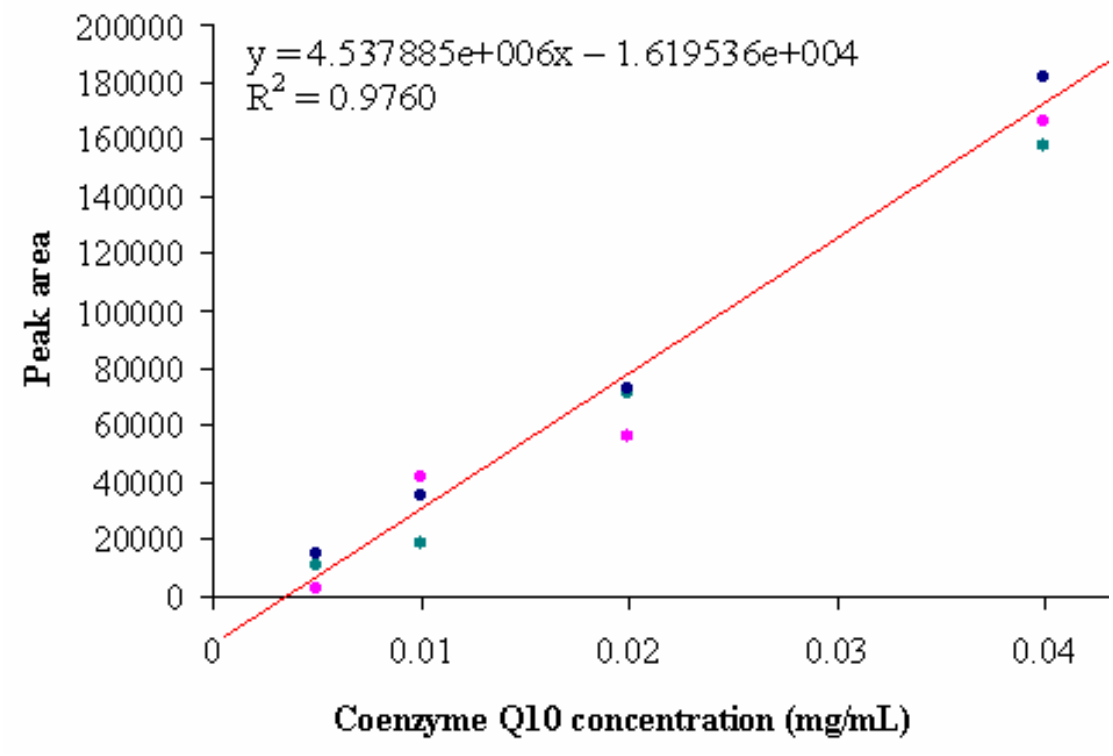

Figure 4.2. A calibration curve obtained from external coenzyme Q_{10} standard analysis

The precision of the HPLC and the data handling system for the coenzyme Q_{10} analysis was an acceptable *CV* of 8.45%. Reliability tests of the extraction method for coenzyme Q_{10} were also determined and showed a *CV* of 11.66%, which was not surprising since it included the variation of the extraction in addition to the variation due to the HPLC and data handling system. The recovery tests, which were done by spiking known amounts of coenzyme Q_{10} into freeze–dried samples, showed 99.36 ± 3.17% recovery. The retention time of coenzyme Q_{10} was rather sensitive to the mobile phase composition, and varied between 13 − 15 min. Sample chromatograms obtained from coenzyme Q_{10} standards compared to those of the pasta samples are illustrated in Figure 4.3.

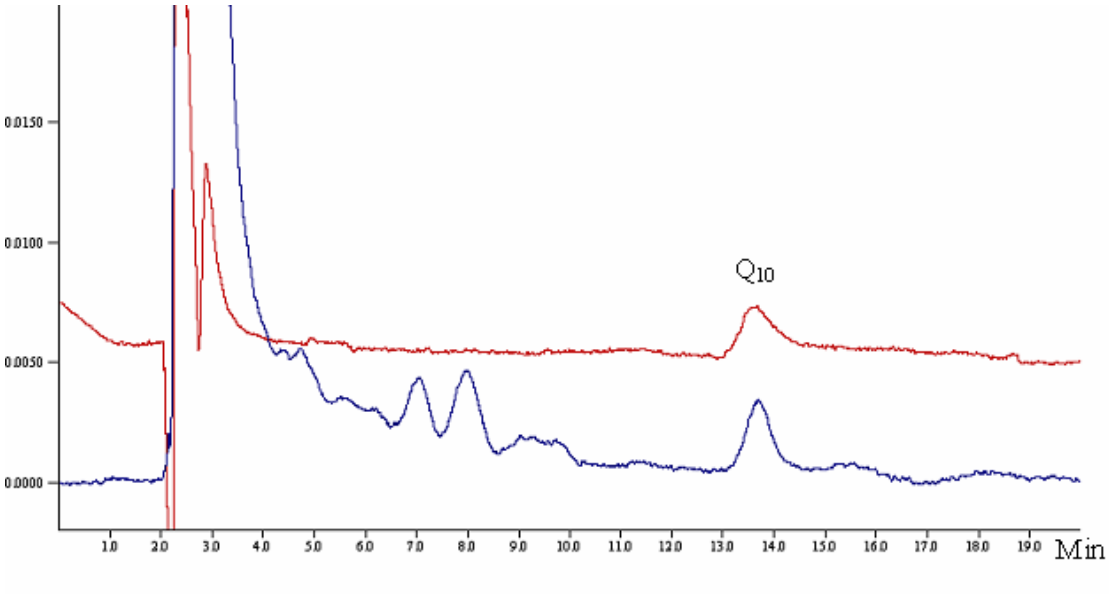

Figure 4.3. HPLC chromatograms of coenzyme Q_{10} standard (top line) and cooked pasta with 30% added beef heart pasta (bottom line)

Coenzyme Q_{10}, as reported in this study, was analyzed in the oxidized state. According to Weber and others (1997a), no coenzyme Q_{10} was detected in its reduced state at the end of the direct solvent extraction procedure. In agreement with the result by Kamei and others (1985), no coenzyme Q_{10} was detectable in the durum wheat flour. The content of coenzyme Q_{10} in beef heart was 69.11 ± 19.93 μg/g dry basis (15.69 μg/g fresh weight), which was lower than the results obtained from other studies. Mattila and Kumpulainen (2001), by applying a saponification step in the extraction procedure, detected 113.3 μg/g fresh weight of coenzyme Q_{10} in beef heart. By using the direct solvent extraction for coenzyme Q_{10} analysis, Purchas and others (2004a) found that beef heart contained 60.5 μg coenzyme Q_{10} /g fresh sample and also observed that Q_{10} content in animal tissues varied between muscles, animals, and with cooking. While the contents of coenzyme Q_{10} in beef heart reported in this study were less than in some other studies, the system check sample indicated there was no change in the performance of the method to quantify coenzyme Q_{10} during the whole experiment.

By incorporating freeze–dried beef heart into pasta, the coenzyme Q_{10} content in the newly formulated pasta increased significantly compared to the unfortified pasta and tended to only slightly decrease after cooking (Table 4.2).

Table 4.2. Coenzyme Q_{10} contents in cooked and uncooked pasta samples

Percentage of added freeze–dried beef heart in pastas	Coenzyme Q_{10} content (μg/g dry weight)	
	Before cooking	After cooking
0%	n.d.	n.d.
10%	4.71 ± 0.78^{b}	4.26 ± 0.50^{b}
30%	12.08 ± 2.36^{a}	11.29 ± 2.47^{a}

n.d. stands for not detected.

Values are means ± SD of three replications (n = 3).

Values in the same row and in the same column with the same superscript letters are not significantly different ($p<0.05$).

However, the decrease was not significant. Purchas and others (2004b) found that coenzyme Q_{10} content in steaks decreased significantly after grilling at 200°C but showed no significant difference between two final internal temperatures, 60 and 80°C. In this study, the reason why the loss of coenzyme Q_{10} in the formulated pasta after cooking was not significant might be due to the lower temperature used in the cooking process, shorter cooking time, and because boiling is an indirect thermal processing method. Nevertheless, the content of coenzyme Q_{10} of the newly formulated pasta was lower than expected calculated values, which were 20.73 and 6.91 μg/g dry basis for 30% added beef heart pasta and 10% added beef heart pasta, respectively based on the amount of coenzyme Q_{10} in the added beef heart. Percentages of coenzyme Q_{10} recovered from cooked pasta at 30% substitution, uncooked pasta at 30% substitution, cooked pasta at 10% substitution, and uncooked pasta at 10% substitution were 54.43, 58.24, 61.68, and 68.17% on a dry basis, respectively. The reason why the coenzyme Q_{10} in the newly formulated pasta was lower than expected might be due to a loss of beef heart during

making pasta. In addition, long time exposure of pasta to an environment (oxygen and light) during pasta making process might cause a destruction of coenzyme Q_{10}. This assumption was confirmed by measuring the content of coenzyme Q_{10} in freeze–dried beef heart samples that were left outside at room temperature overnight and consequently the result showed that no coenzyme Q_{10} was detected in the samples.

4.5 Conclusions

Currently, several dietary coenzyme Q_{10} supplements are commercially available. Most dietary supplement manufacturers add coenzyme Q_{10} in varying amounts from 30 to 100 mg/tablet. Common doses usually used for supplementation, and therapeutic dosages for diseases, range from 10 − 30 mg/day and 200 − 400 mg/day, respectively (Papas 1999). Coenzyme Q_{10} contents in one serving of cooked pasta (100 g) of the newly formulated pasta was much lower than that available in the commercial supplements. Nevertheless, this study is one of the first potential approaches to incorporate greater amounts of coenzyme Q_{10} into a regular food by using a natural and inexpensive source of coenzyme Q_{10}. In addition, the use of beef heart as a potential commercial source of coenzyme Q_{10} could enhance the value of this meat by–product.

CHAPTER 5

USING VIBRATIONAL SPECTROSCOPY TO STUDY PHYSIOCHEMICAL CHANGES IN PASTA MATRIXES

5.1 Abstract

Two vibrational spectroscopic methods (Fourier transform infrared (FT–IR) and Raman spectroscopy) were used as rapid and non–destructive tools for studying physiochemical changes of pasta after cooking, including changes of secondary structure of durum wheat proteins. A FT–IR band at 1630 cm^{-1} in cooked pasta exhibited weakened hydrogen bonds in proteins after cooking. Cooking led to significant alterations in the Raman spectra of pasta in the regions of 2910, 1460, and 1340 cm^{-1}. An existence of Raman peaks around 1673 and 1005 cm^{-1}, and an absence of the band at 1260 cm^{-1} indicated the development of β–structures in pasta matrixes and concurrent reduction of α–helical contents, which corresponded to the observation from FT–IR analysis. The spectral results demonstrated that vibrational spectroscopy could investigate physiochemical changes in pasta matrixes rapidly and non–destructively and allow determining the changes related to many food components, including protein, carbohydrate, and lipid, at one time measurement.

Keywords: FT–IR; Raman; vibrational spectroscopy; pasta; gluten; durum wheat flour

5.2 Introduction

FT–IR and Raman spectroscopy are analytical techniques subcategorized under vibrational spectroscopic methods. The major advantage of these spectroscopic methods is that the samples can be analyzed non–destructively and in real time. Vibrational spectroscopy provides useful information on the vibrational states or motions of molecules in a variety of ways. For example, FT–IR collects mid infrared vibrational spectra based on performing a mathematical Fourier transform on the sample signals, which rely on a modification of the intrinsic dipole moment with molecular vibration, while Raman spectroscopy studies molecular vibrations by light scattering, and the Raman effect requires an alternative in the polarizability of the molecule. Similar to infrared absorption, the Raman scattering mode depends on vibrational energy levels of the molecules, which are mainly associated with stretching or bending deformations of molecular bonding. Infrared spectroscopy and Raman spectroscopy are complementary rather than substitutes for each other because polar functional groups, such as C=O, C≡N, O–H, N–H and C–H, usually have strong infrared stretching vibrations, while intense Raman lines are associated with nonpolar groups, such as C=C, S–S, C–C and N=N (Li–Chan and others 1994; Li–Chan 1996). However, an important advantage of Raman spectra over infrared is that water does not cause interference in Raman spectra; consequently, the Raman method can be applied in aqueous systems (Skoog and others 1998).

FT–IR and Raman spectroscopy have recently been used in food analysis for both qualitative and quantitative measurements of food matrixes. For instance, FT–IR has been used studying the degree of tenderization (Iizuka and Aishima 1999), in the

discriminant analysis of edible oils and fats (Yang and others 2005), and for investigating structural changes in sweet potato flour after modifications (Ramesh Yadav and others 2007). Moreover, FT–IR has been used to investigate physical chemistry of gluten, but the experiments have been conducted only in model food systems, or for wheat protein fractions, or for isolated gluten (Leon and others 2000; Wellner and others 2005; Georget and Belton 2006). Lately, Raman spectroscopy has also been used in food analyses to study carbohydrates (Bulkin and others 1987; Arboleda and Loppnow 2000; Synytsya and others 2003; Fechner and others 2005) and lipids (Strehle and others 2006), to evaluate changes of interactions such as protein–protein interactions (Howell and others 1999), protein–lipid interactions (Meng and others 2005), and protein–carbohydrate interactions (Alizadeh–Pasdar and others 2002) in food systems. For example, Sultanbawa and Li–Chan (2001) employed Raman spectroscopy to investigate effects of frozen storage on structural changes of proteins in a natural actomyosin matrix and a surimi matrix. However, publicly available data on application of vibrational spectroscopy in real and complex food systems is still limited.

Real food matrixes are more complicated than model food systems. For example, in the pasta making process, mixing and kneading durum wheat flour with water induces gluten formation. Under the applied shear and tensile forces, the gluten proteins gliadin and glutenin absorb water and partially unfold, while the starch in the flour gelatinizes as temperature is increased (Damodaran 1996). Consequently, stable complexes can develop due to the formation of a protein–starch matrix, where hydrogen bonding and covalent bonding, in addition to charge interactions, are found (Marshall and Chrastil 1992). Since gluten is formed in aqueous media and gluten proteins contain several amino acids with

hydrophobic side chains, these nonpolar substances tend to link with each other via hydrophobic interactions, including interaction with lipids and other nonpolar substances (Damodaran 1996; Lasztity 1996). As a result, a combination of protein–protein, protein–lipid, and protein–carbohydrate interactions are contributing to the formation of pasta matrixes. Although changes of secondary structures of gluten proteins have been studied fairly extensively (Lee and others 1990; Pezolet and others 1992; Wellner and others 2005; Georget and Belton 2006), studies on real and complex food matrixes in the form in which they are consumed, are still rare. Little is known about any changes in food component interactions such as protein–starch, protein–protein and protein–lipid interactions, or about the secondary structures of proteins during the formation of these complex food matrixes.

The objective of this study was to use FT–IR and Raman spectroscopy to investigate physiochemical changes in pasta matrixes. Changes of interactions and structures from the native state of durum wheat flour to the modified state of the flour in pasta products, and the effect of cooking on physiochemical changes in homemade pasta were also investigated using these two vibrational spectroscopic methods combined with multivariate statistical analyses.

5.3 Materials and methods

5.3.1 Pasta preparation

Durum wheat flour (180 g) or semolina from Bob's Red Mill (Bob's Red Mill Natural Foods, Milwaukie, Ore.) was poured on a clean and smooth work area. A well was made at the center of the pile of the durum wheat flour and 120 mL of tap water was slowly poured into the well. The durum wheat flour was gradually mixed with the water. A smooth and elastic dough was obtained by slowly drawing the flour by hand and kneading for 10 min. The dough ball was then wrapped with plastic film and stored in a refrigerator at 4ºC for 60 min. After resting, the dough was flattened and fed into a rolling machine (Al Dente from Villaware®, Cleveland, Ohio) starting at the widest setting of number 7. The flattened dough coming out from the rolling machine was folded and fed back through the machine at consecutively narrower settings (numbers 6, 5, 4 and 3, respectively) of the pasta rolling machine to get a thin sheet of pasta. Finally, the thin pasta sheet was cut by passing it through the spaghetti cutter attachment. The long thin pasta strands were then dried at room temperature on kitchen towels for 90 min. Fifty grams of the pasta strands were cooked in 1 L boiling water for 2 min, then drained and rinsed with tap water. As the white opaque core of the pasta strands was not observed, the cooking time used in this study could achieve complete gelatinization of starch in the pasta matrixes (Gelencsér and others 2008). Fresh pasta was prepared in triplicate in a homemade style. The pasta samples, both before and after cooking, were cut into small pieces before measurement using FT–IR and Raman spectroscopy. Durum wheat flour, purchased from three different local grocery stores, was analyzed directly without any preparation.

5.3.2 Moisture content determination

The AOAC Official Method 934.01, a vacuum oven method, was used in the determination of moisture content of tested samples (AOAC International 2006). An aluminum pan that contained a small glass stirring rod and sand was baked at 100°C in a vacuum oven (Model 3640, National Appliance Co., Portland, Ore.) overnight. Then, the sand pan was removed and allowed to cool in a desiccator. Approximately 3 – 5 g of pasta samples were accurately weighed and consequently mixed well with the sand. The sample was dried in the oven at 100°C for 2 hr. Later, the sample pan was removed from the oven and cooled down in a desiccator before weighing. The pan was returned to dry in the oven until a constant weight was obtained by reweighing every 30 min. For the durum wheat flour samples, an aluminum dish with a lid was used rather than an aluminum pan with sand. The measurement of moisture content was done in duplicate and the difference was less than 10%.

5.3.3 FT–IR spectroscopy measurements

FT–IR analysis was carried out using a Thermo Nicolet 380 FT–IR Spectrometer (Thermo Electron Corporation, Madison, Wis.) at room temperature. For taking the measurements, the durum wheat flour and pasta samples were placed directly onto the ATR diamond crystal. FT–IR spectra were obtained in the range of 4000 to 400 cm^{-1} and recorded as absorbance units at a resolution of 4 cm^{-1}. Each measurement was the average value of 64 separate scans. Spectral data were collected using OMNIC^{TM} software, version 7.0 (Thermo Electron Corporation, Madison, Wis.). Measurements were done in duplicate.

5.3.4 Raman spectroscopy measurements

A Renishaw RM1000 Raman Spectrometer System (Renishaw Ramascope from Renishaw plc, UK) equipped with a Leica DMLB microscope from Leica Microsystems (Wetzlar, Germany) was used. A diode laser with a power of 300 mW at 785 nm coupled with an integral plasma filter was used as a laser source. Tested samples were placed on a gold coated micro slide (Thermo Electron Corporation, Madison, Wis.) and viewed through the Leica DMLB microscope with a 50× objective at room temperature. Spectral data were collected with 10 sec exposure time by the Renishaw WiRE 1.3 software (Renishaw plc, UK). Raman spectra were obtained in the Raman shift range from 3200 to 2000 cm^{-1} and from 1800 to 300 cm^{-1} in the extended mode. Each sample was measured in triplicate and average results were obtained.

5.3.5 Spectral pretreatment

Spectra obtained from the FT–IR and Raman analyses were preprocessed by correcting baseline shifts and normalizing the scale using OMNIC version 7.3 (Thermo Electron Inc., Waltham, Mass.). Normalized FT–IR spectra were further analyzed using the Delight software, version 3.2.1 (D–Squared Development Inc., LaGrande, Ore.), including smoothing with a Gaussian function over 6 cm^{-1}, binning with the width of 2 cm^{-1} and second derivative transformation over the gap value of 12 cm^{-1}.

5.3.6 Data analysis

Principal component analysis (PCA), a technique of reducing a data set to its most dominant features, was performed using the Delight software with 5 latent variables. The least squares techniques were used for performing linear fitting to a series of orthogonal eigenvectors (loadings). An array of vectors obtained from a data set, which is a set of spectra, is extracted to find the best fit product of scores (s) and loadings (L), and then present the best reproduction of the sample from the reduced data set. To avoid confounding effects of water stretching vibrations in the FT–IR dataset, the region of 4000 – 2000 cm^{-1} was excluded from the PCA analysis.

Unlike PCA in which unknown scores and loadings were integral into a modeling data, partial least square analysis (PLS) employed actual values to create components during data compression using the Delight software with 5 latent variables. In order to validate the best fit model of FT–IR spectral data at specific wavenumber (3600 – 3000 cm^{-1}) and actual values (moisture content), the optimum number of latent variables was evaluated by the lowest root mean square error cross validation (RMSECV). The coefficient of determination (the square of the correlation coefficient, R^2) for the predicted vs. actual values of the constituent and the root mean square error of predication (RMSEP) were accounted to evaluate the PLS model performance.

5.4 Results and discussion

5.4.1 FT–IR analysis

The FT–IR spectra of durum wheat flour and the pasta samples before and after cooking are illustrated in Figure 5.1.

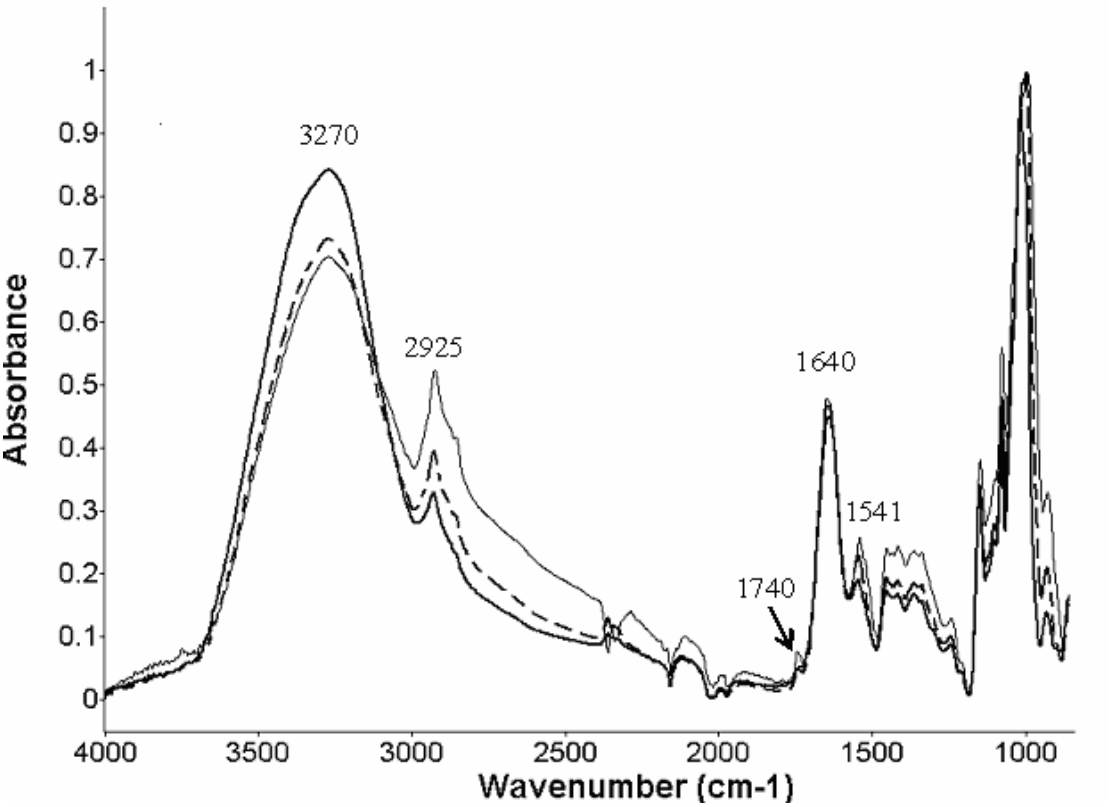

Figure 5.1. FT–IR spectra of durum wheat flour (—), pasta before cooking (---), and pasta after cooking (▬)

The prominent and wide peaks around 3600 – 3000 cm^{-1}, which stem from the O–H stretch of water, were observed in all samples. The higher intensity of the peaks at 3600 – 3000 cm^{-1} in cooked pasta might be caused by the higher moisture content (64%) of the cooked pasta compared to the uncooked pasta (30%) or the durum wheat flour (12%). In order to confirm that the peak centered around 3270 cm^{-1} was originated from an

influence of moisture content, a correlation between the selected spectral region in the FT–IR spectra and measured values of moisture content was verified using partial least squares analysis (PLS) (Figure 5.2). The coefficient of determination (R^2 = 0.96) indicated that the relationship between spectral data in the region of 3600 – 3000 cm^{-1} and measured moisture content was strong and provided the best performing model with two latent variables (LV). A root mean square error of cross validation (RMSECV) and that of prediction (RMSEP) were 6.51 and 5.43, respectively.

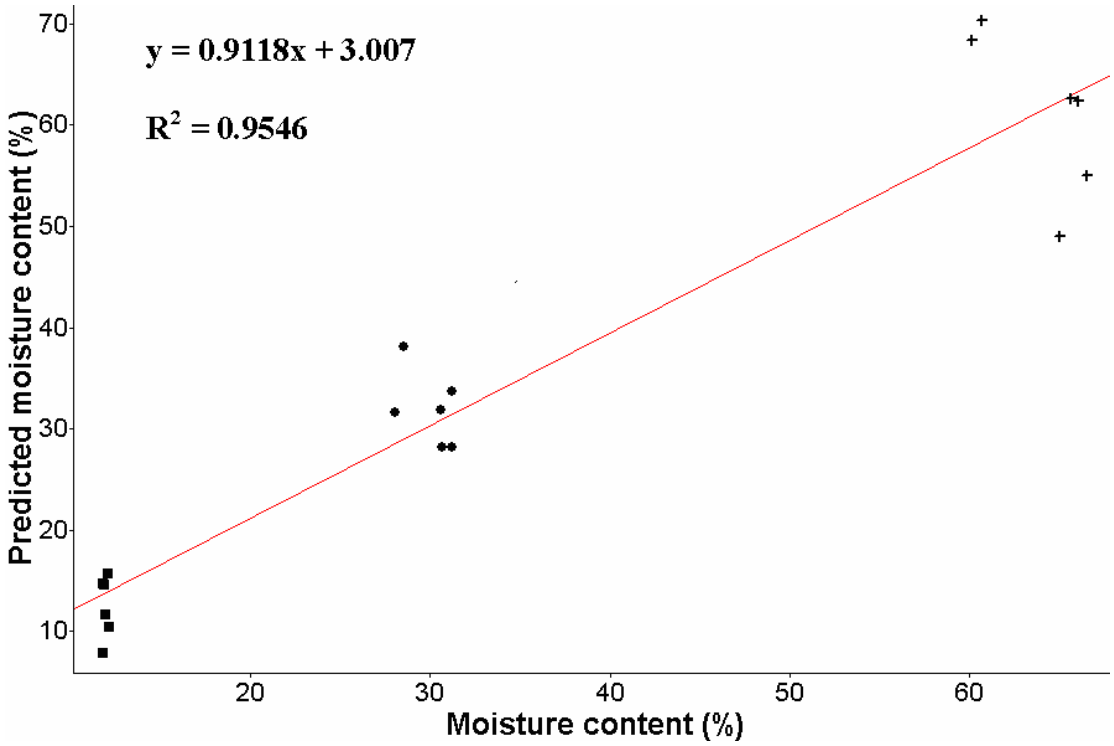

Figure 5.2. Moisture content of the tested samples, including durum wheat flour, uncooked pasta, and cooked pasta, versus predictions for the moisture content analysis based on the region of 3600 – 3000 cm^{-1} in the FT–IR spectra (n = 3)

The highest intensity of the band around 2925 cm^{-1} (asymmetric stretches of methylene groups) was observed in durum wheat flour, followed by uncooked pasta and cooked pasta, respectively. However, changes in this region could not be interpreted directly because the changes might originate from methylene groups of protein, carbohydrate, and lipid components in pasta matrixes. Weak signals in the FT–IR spectra of the samples were also observed at ~ 1740 cm^{-1}, indicating C=O stretching vibrations of ester groups mainly from lipids and fatty acids. These peaks were detected because the durum wheat flour used was not defatted, which agrees with the results reported by Georget and Belton (2006) who found that non–defatted hydrated gluten exhibits a peak at ~ 1740 cm^{-1}. The intensity of the 1740 cm^{-1} band obtained from pasta samples was lower than that obtained from durum wheat flour, which could be explained by the interactions between lipids and proteins during pasta processing. Mohamed and others (2005) explained that phospholipid–gluten interactions could occur at the interface in aqueous systems and were important factors for effective dough formation.

Strong bands located in the amide I region (~ 1640 cm^{-1}) and amide II region (~ 1541 cm^{-1}) were observed in all samples. These spectral ranges including amide I and II have been widely used to investigate the secondary structure of proteins based on vibrational features of C=O, C–N, and N–H groups of peptide bond. The amide I region has been previously used to investigate the protein structures because of its strong signal. It was, however, not straightforward for determining the protein structures in durum wheat flour and pasta samples in this study because the protein amide I peak at 1650 cm^{-1} (α–helices and random coils) was possibly disturbed by the band of water at 1640 cm^{-1} (Singh 2000). To solve this problem, the second–derivative transformation was

conducted (Figure 5.3). In this study, the emergence of bands at 1630 – 1610 cm^{-1} (antiparallel β–sheets) was observed only in pasta samples. The unfolding of protein during the pasta making process might lead to the appearance of these bands at 1630 – 1610 cm^{-1}. In addition, the intensity of the band at 1630 cm^{-1} tended to decrease in pasta samples after cooking. Georget and Belton (2006) presumed that the lower intensity of the FT–IR second–derivative spectra at 1630 cm^{-1} was the result of a weakening of hydrogen bonds when temperature increased. They also believed that the emergence of the peak at 1630 cm^{-1} together with the band at 1680 cm^{-1} could be due to a β–sheet conformation. Haris (2000) indicated that the FT–IR bands ~ 1680 and 1630 cm^{-1} were associated with an aggregation of polypeptide chains after protein unfolding. The FT–IR spectra obtained from this study show that the signal at 1682 cm^{-1} was stronger for the durum wheat flour than that of the pasta samples. The reason that the FT–IR peak located around 1630 cm^{-1} was appeared plus the intensity of the band at 1650 cm^{-1} was decreased in the pasta spectra was probably rooted from force manipulation applied during kneading pasta durum wheat flour with water. That might promote an alignment of β–structures along with lowering a content of α–helices in pasta matrixes.

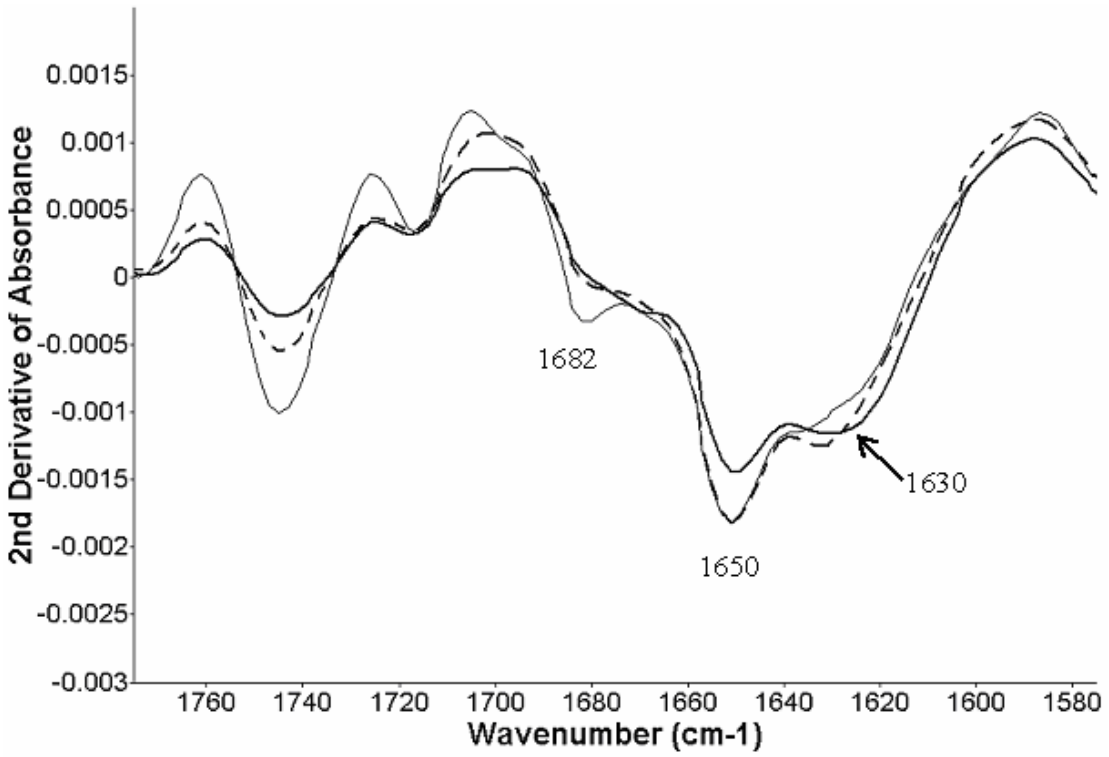

Figure 5.3. FT–IR second–derivative spectra of durum wheat flour (—), pasta before cooking (---), and pasta after cooking (▬) in the amide I region

5.4.2 Raman spectroscopic analysis

The Raman spectra of wheat flour and pasta samples are illustrated in Figures 5.4 A and B. Bouraoui and others (1997) determined effects of processing on surimi and found that cooking decreased intensity of Raman spectra in the region of 3100 – 2800 cm^{-1}, assigned for the C–H stretching, by comparing processed surimi with raw surimi. Similarly, a lower intensity around 3100 – 2800 cm^{-1} (Figure 5.4 A) was found in pasta after cooking than that in uncooked pasta and flour samples. The C–H bending vibrations of aliphatic residues located at 1460 cm^{-1} (Figure 5.4 B) appeared in all samples but the strong sharp bands were observed only in durum wheat flour and uncooked pasta. The changes of the band centered at 1460 cm^{-1} might be a result of cooking effects. The

emergence of a split peak instead of an individual sharp peak at 1340 cm^{-1} region, assigned for C–H vibrations of polysaccharides, might relate to a modification in pasta samples after cooking (Figure 5.4 B). These findings indicated that an alteration in the Raman shift located around 3100 – 2800, 1460, and 1340 cm^{-1} were possible employed for observing changes in pasta matrixes after cooking.

Considering the intensity ratio I_{845}/I_{823} (Figure 5.4 B), Raman spectra obtained from cooked pasta showed a lower I_{845}/I_{823} ratio than that from uncooked pasta. Strong hydrogen bonding to a negative acceptor caused a low I_{845}/I_{823} ratio (0.3 – 1.0), whereas hydrogen bonds between the phenolic OH group and an acid donor led to a higher ratio (0.9 – 2.5) (Li–Chan and others 1994). In this study, the intensity of I_{845}/ I_{823} ratio tended to be high in pasta samples, 1.5 for cooked pasta and 1.8 for uncooked pasta. The high I_{845}/I_{823} ratio in pasta samples might stem from tyrosine residues being exposed in the high polarity environment of the pasta matrix during mixing and kneading of durum wheat flour with water. While a peak at 525 cm^{-1} appeared in both cooked and uncooked pasta, an absence of this region was noted in durum wheat flour samples, indicating the formation of disulfide bonds in pasta matrixes (Figure 5.4 B). However, there was no significant change observed in the region of 2580 – 2550 cm^{-1}, assigned to sulfhydryl (S–H) stretching vibrations, among tested samples (Figure 5.4 A).

A split of the peak at 1260 (α–helix) cm^{-1} was observed in cooked and uncooked pasta samples (Figure 5.4 B). A division of the peak located at this region (1260 cm^{-1}) might reflect on changes of the native state of durum wheat flour during pasta making process. As a result, modification of native state of durum wheat flour in pasta matrixes could decrease α–helical content. A higher Raman intensity of the peaks centered at 1673

cm^{-1} (antiparallel β–pleated sheet) and 1005 cm^{-1} (β–pleated sheet), which was accompanied by an absence of the Raman band at 1260 cm^{-1}, was detected in cooked pasta and uncooked pasta (Figure 5.4 B). The explanation for this finding is that while the content of α–helices decreased, an increase of β structures was observed in pasta matrixes. Therefore, mixing durum wheat flour with water, together with kneading and rolling the gluten dough during making pasta, might cause the formation of β–structures and then lead to a simultaneous reduction of α–helical content in pasta matrixes. These results agree with the previous explanation observed in FT–IR measurement as well as the findings reported by Pezolet and others (1992) and Popineau and others (1994), which indicated that as intermolecular β–sheets increased, the α–helix content decreased.

The band at 480 cm^{-1}, assigned for the vibrations of C–C bonds of amylose and amylopectin chains, has been used to evaluate the distribution of starch (Celedon and Aguilera 2002; Baranska and others 2005). Celedon and Aguilera (2002) indicated that the bigger width of the 480 cm^{-1} band was related to the conformations of amylose and amylopectin after the disruption of the starch granule structure. In this study, the strongest and widest signal at the 480 cm^{-1} region (Figure 5.4 B) was obtained from Raman spectra of durum wheat flour, followed by that of uncooked pasta, and that of cooked pasta, respectively. Moreover, the intensity of the Raman signal obtained from cooked pasta was noticeably different from the other two. The proposed explanation for this finding is simply the gelatinization of starch during the boiling of pasta. This phenomenon would also favor unfolded protein to form networks with gelatinized wheat starch, and consequently, interfered with the interactions between amylose and amylopectin, correlating to a manifestly lower intensity of the 480 cm^{-1} band observed in

cooked pasta. This tentative explanation agrees well with the explanations by Marshall and Chrastil (1992).

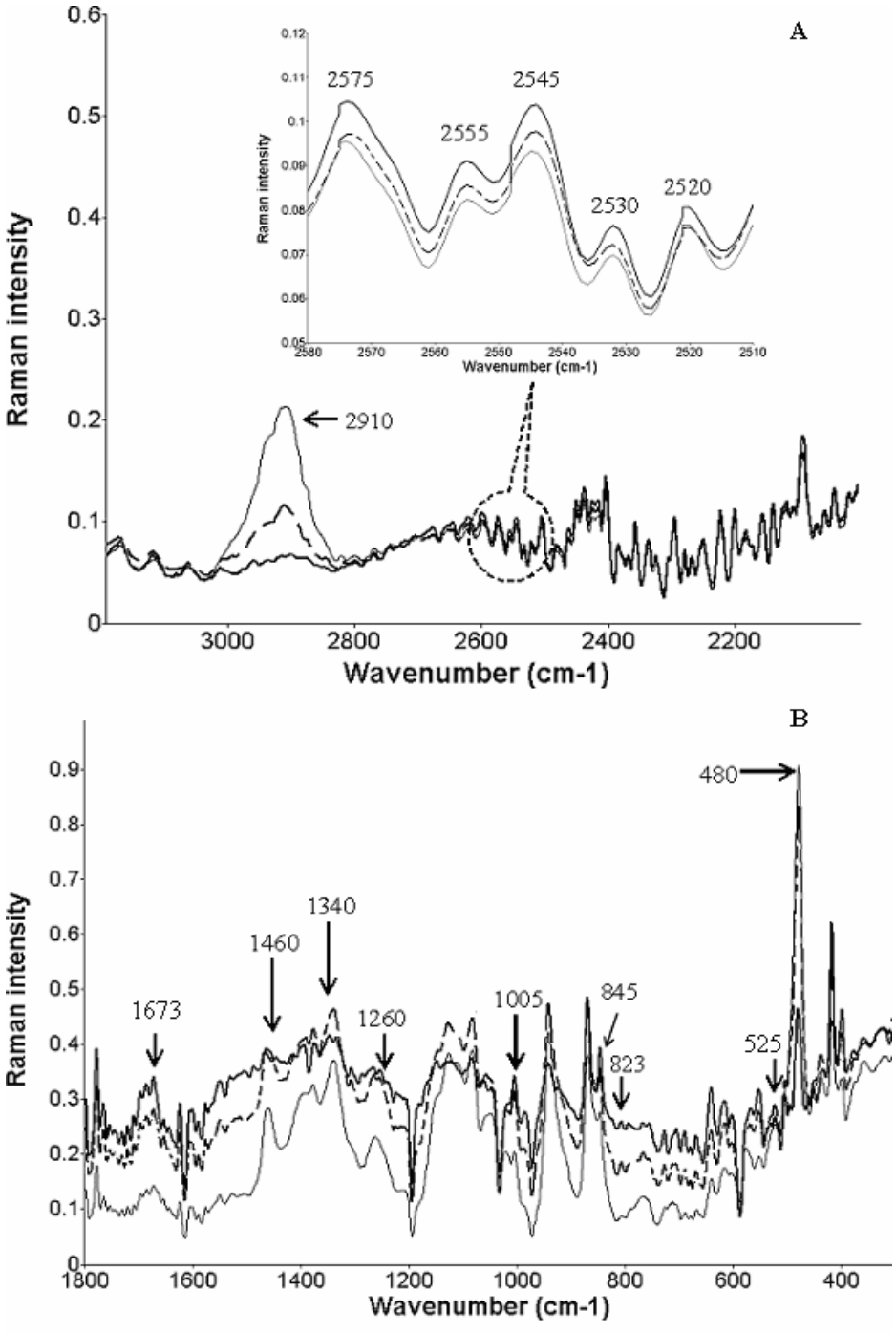

Figure 5.4. Raman spectra of durum wheat flour (—), pasta before cooking (---), and pasta after cooking (▬) in A.) the 3200 – 2000 cm^{-1} region and B.) the 1800 – 300 cm^{-1} region

5.4.3 PCA analysis

The PCA plots of the FT–IR spectra and Raman spectra are shown in Figures 5.5 A and B, respectively.

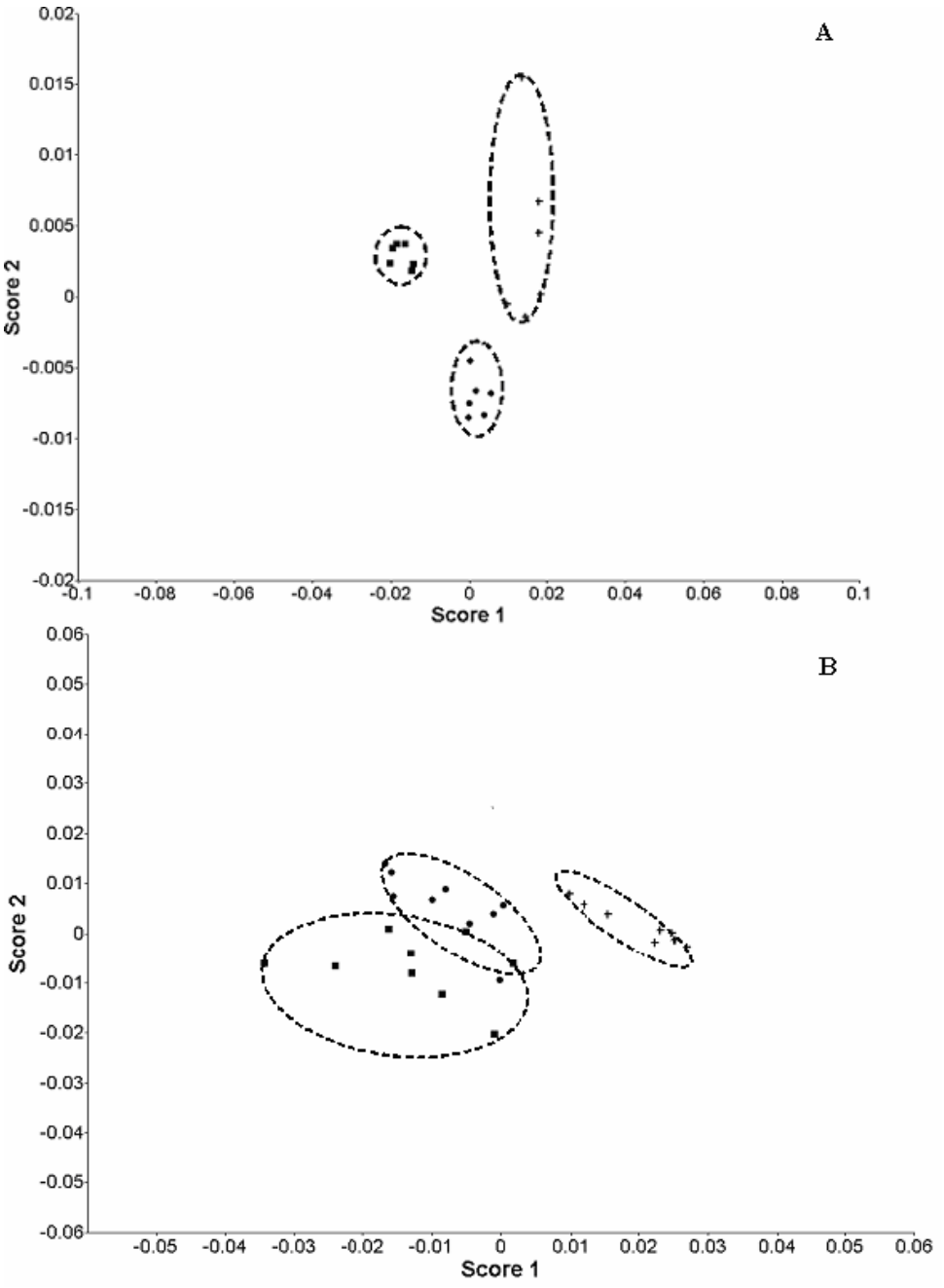

Figure 5.5. PCA plots using A.) FT–IR spectra and B.) Raman spectra of durum wheat flour (■), pasta before cooking (●), and pasta after cooking (+)

A distinct difference was observed in the PCA plot of the FT–IR spectra between durum wheat flour samples and the pasta samples before and after cooking (Figure 5.5 A). In order to describe factors that contributed to variation in the FT–IR spectral data of three different samples, the loading plots of the principal components (PCs) from PCA analysis were achieved (Figure 5.6). The results indicated that variables mainly taking place in the wavenumber of 1750 – 950 cm^{-1} contributed to the variation in the FT–IR spectra, which possibly related to differences in conformations of gluten protein and protein–lipid interactions due to changes of the native state of durum wheat flour during the pasta making process. The first, second, and third loadings ($PC_{1,}$ $PC_{2,}$ and PC_{3}) reflected around 49.96%, 25.76%, and 4.85% on the total variation in the FT-IR spectral data of pasta matrixes, respectively.

Considering PCA results of Raman spectra, an overlapping between the PCA clusters of uncooked pasta and durum wheat flour was noted (Figure 5.5 B). However, the cooked pasta was clearly separated from uncooked pasta and durum wheat flour, which might be primarily due to the cooking effect in the pasta matrixes. The PCs obtained from the second–derivative of the Raman spectra were also plotted and the results showed that large variations in the Raman shift were established around the districts of 1800 – 900 cm^{-1} and 750 – 460 cm^{-1}, which probably were main reasons of a differentiation among the tested samples (Figure 5.7). The first three loadings, including PC_1 (48.48%), PC_2 (17.87%), and PC_3 (5.18%), have a total effect on a variation of Raman spectra of pasta matrixes up to 70%. These findings interpreted that effects of cooking, gluten protein conformations, and changes of starch polymerization might be

accounted in the segregation of the Raman spectral data obtained from durum wheat flour, uncooked pasta, and cooked pasta samples.

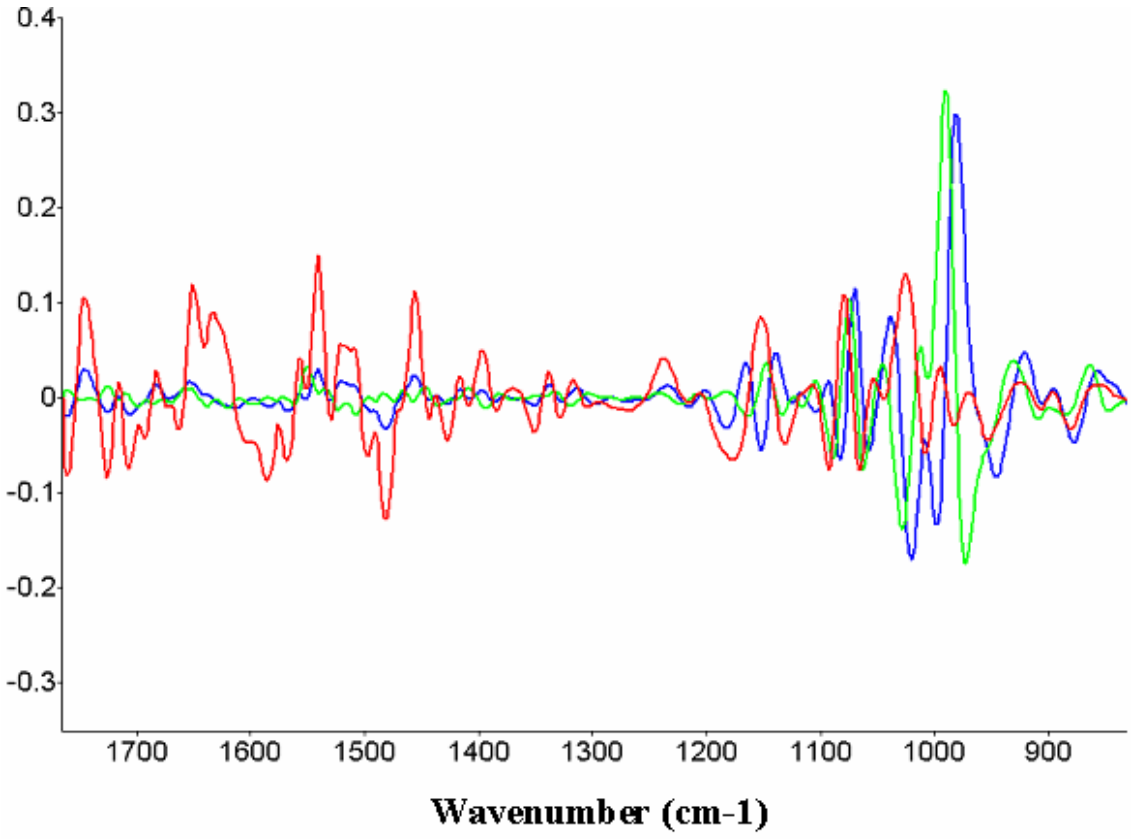

Figure 5.6. Loading plots of the principal components (PCs), including PC_1 (—), PC_2 (—), and PC_3 (—), that were derived from second–derivative transformation of the FT–IR spectra

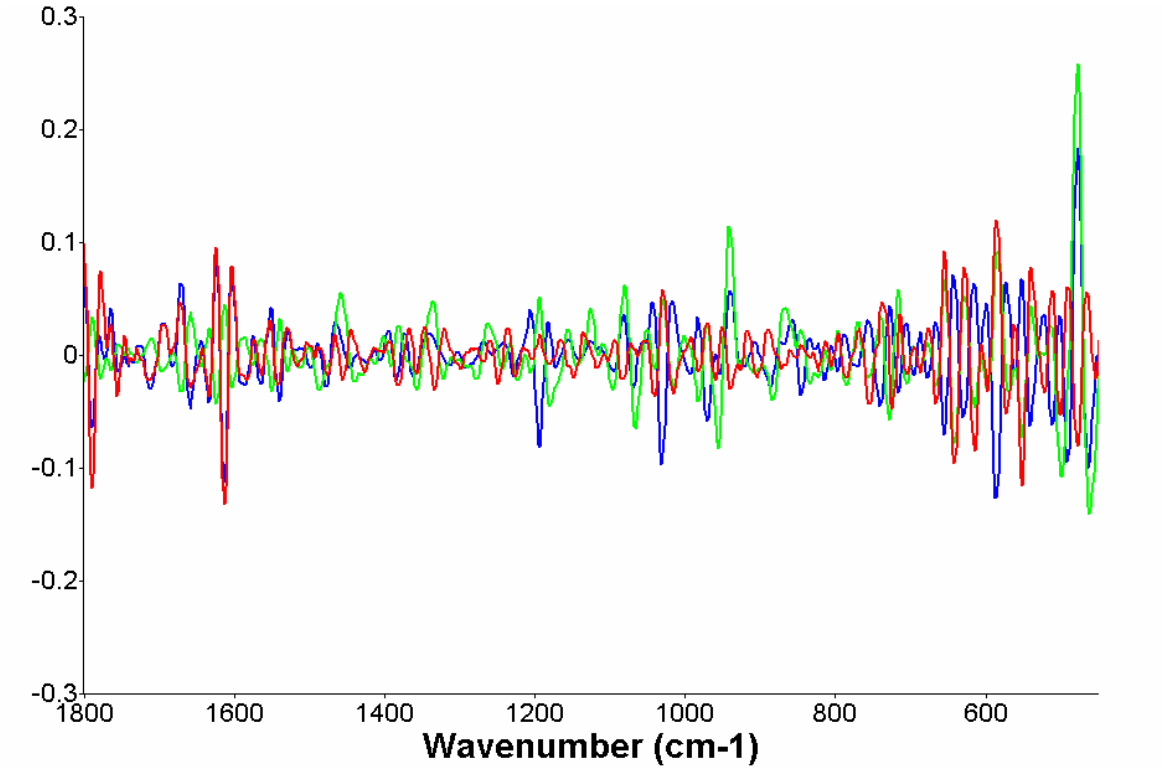

Figure 5.7. Loading plots of the principal components (PCs), including PC_1 (—), PC_2 (—), and PC_3 (—), that were derived from second–derivative transformation of the Raman spectra

5.5 Conclusions

The results demonstrate that FT–IR and Raman spectroscopy could be a potential quick and non–destructive approach to investigate physiochemical changes that take place in pasta. Once measurement, their spectral data offers useful information for studying changes of many food components, such as protein, carbohydrate, and lipid, at the same time. While the interpretation of the FT–IR and Raman spectra is ambiguous for some regions of absorbance, this study contributes to the limited amount of knowledge of physiochemical changes in the manufacture of complex food systems. Nonetheless, further research is needed to use these vibrational spectroscopic methods to investigate a

wider range of food matrixes and explore their potential applications in food scientific research including food industries.

CHAPTER 6

PHYSIOCHEMICAL CHANGES IN PASTA MATRIXES AFTER PARTIALLY REPLACING DURUM WHEAT FLOUR WITH BEEF HEART INVESTIGATED BY FT−IR AND RAMAN SPECTROSCOPY

6.1 Abstract

New pasta products were developed by partially replacing durum wheat flour with beef heart. Physiochemical changes of the pasta were investigated by vibrational spectroscopy, namely Fourier transform infrared (FT−IR) and Raman spectroscopy. Relationships between pasta texture and the intensity of vibrational spectra were established. Lipid−protein complex formation, β−sheet arrangement, degree of polysaccharide polymerization, and cysteine thiol group are proposed to possibly be related to hardness and chewiness of pasta. The lipid portion and β−sheet structure might be significant parameters for explaining pasta adhesiveness, while pasta firmness might be related to β−sheet alignment and the polysaccharide network. Pasta cohesiveness might involve the α−helical structures and hydrogen bonding formation in the gluten network. However, no variable met the 0.1 significant level for inclusion into the model to explain pasta springiness. These results revealed that FT−IR and Raman spectroscopy could be employed to evaluate physical chemistry of pasta and showed a potential use for quality assessment in pasta products.

Keywords: Pasta; Physical chemistry; Beef heart; Texture; FT−IR; Raman

6.2 Introduction

In pasta products, cooking quality is considered as the most vital parameter affecting organoleptic attributes, and cooked pasta could turn out to be sticky if the wheat protein network is not strong enough to hold the gelatinized starch (Smith 1999). Acceptability of cooked pasta is historically based on three organoleptic properties, including appearance, flavor, and texture. According to Bourne (2002b), changes of textural properties are likely related to the physical chemistry of food components. As a result, understanding the effect of food component interactions and food structural conformations on pasta texture profiles could provide useful information for controlling quality of pasta products, particularly after incorporating additional ingredients into the pasta matrixes. In this study, beef heart was used as an additional ingredient in the pasta in order to increase the economic value of beef heart and also to enhance the nutritional value of the newly formulated pasta products. However, incorporation of beef heart in the pasta can lead to obvious changes in organoleptic attributes of pasta. In particular, the texture attributes are the main concern for consumers' acceptability. Vibration spectroscopy is a promising technique that can be applied to investigate changes of many food components, such as protein, carbohydrate, and lipid, with just one measurement. Therefore, in this study, vibration spectroscopy was the analytical method used to monitor physiochemical changes in the formulated pasta.

Vibrational spectroscopy is an analytical technique that associates the interaction of molecules with the radiation in the vibrational region of the electromagnetic spectrum. Fourier transform infrared spectrometer (FT−IR) is one of the vibrational spectroscopy methods and managed under a mathematical system called Fourier transform (FT) (Pavia

and others 2001). In Raman spectroscopy, the electromagnetic radiation is scattered by the molecules, and the spectrum of the scattered radiation is then collected at a particular angle, normally 90°. An important advantage of Raman spectroscopy over FT−IR is that water does not cause interference, consequently, Raman spectroscopy can be applied in aqueous solutions (Skoog and others 1998).

FT−IR and Raman spectroscopy have been successfully used for qualitative and quantitative studies of organic compounds, inorganic components, and biological materials. Since FT−IR and Raman spectroscopy provide information on molecular vibrations and structures, these vibrational spectroscopic methods have, therefore, great potential as general methods to determine physiochemical changes of food systems (Li−Chan 1996; Thygesen and others 2003). In the past decade, vibrational spectroscopic methods, including FT−IR and Raman spectroscopy, have been prevalently introduced to food science research as promising techniques for the quality assessment of food products. For example, Ellis and others (2005) successfully employed FT−IR and Raman spectroscopy to distinguish chicken meat from turkey meat, and also to differentiate leg muscle from the pricier breast muscle. Their study pointed out that FT−IR and Raman spectroscopy could be useful in food regulation for quickly identifying adulterated poultry products. FT−IR was successfully implemented in the quality control of alcoholic beverages by showing a strong correlation to traditional analytical methods of relative density, ethanol, original gravity, and lactic acid (Lachenmeier 2007). Herrero (2008) showed good correlation between Raman spectroscopy and traditional evaluation methods of muscle food quality, such as protein solubility, water holding capacity, and instrumental texture analysis, and also predicted that Raman spectroscopy would be

implemented for measuring muscle food quality in the near future as a direct and nondestructive technique because it requires only small sample sizes. Ozaki and others (1992) applied Raman spectroscopy to monitor quality changes in Japanese tea by comparing the carotenoid content of old leaves with that of new leaves. Other studies showed that the quantitative analysis of unsaturated acyclic components in garlic oil was considerably equivalent to the results obtained from an existing GC analytical technique (Kimbaris and others 2006). However, application of FT−IR and Raman spectroscopy to assess quality of wheat protein−based food products, such as pasta, has not been published yet.

The objective of this study was to examine food component interactions and food structural conformations in cooked home–made pasta made with durum wheat flour and also in pasta made with partially replacing durum wheat flour with 10% and 30% freeze–dried beef heart using FT−IR and Raman spectroscopy combined with principal component analysis (PCA). In addition, the effect of physiochemical changes on pasta texture was investigated using regression analysis to evaluate correlations between the changes observed from these spectroscopic methods and pasta texture, which was measured by instrumental texture analysis.

6.3 Materials and methods

6.3.1 Freeze−dried beef heart preparation

Beef hearts were purchased from the meat laboratory of the University of Missouri, Columbia. The beef hearts were cleaned with distilled water, any non–edible portions were removed, and then they were cut into small pieces. After homogenizing in a general–purpose electric blender (Osterizer, Oster Corporation, Wis.), the hearts were freeze–dried in a freeze–dryer (LabConCo Corp., Kansas City, Mo.) for ~ 48 h. Freeze–dried beef hearts were subsequently blended into fine powders and kept in a Ziploc® plastic freezer bag (S.C. Johnson & Son, Inc., Racine, Wis.) that was purged with nitrogen gas before storage in a freezer (~ –20˚C) for further use.

6.3.2 Pasta preparation

Home–made pastas were prepared in three different formulas, by partially replacing durum wheat flour with beef heart at 0%, 10%, and 30% levels of substitution, with three replications. Durum wheat flour (semolina) (Bob's Red Mill Natural Foods, Milwaukie, Ore.) and freeze–dried beef heart were mixed well together with 120 mL of tap water and kneaded for approximately 10 min until a smooth dough was obtained. The dough was then wrapped with a plastic film and rested in a refrigerator at 5ºC for 60 min. Afterwards, the rested dough was flattened using a rolling machine (Al Dente from Villaware®, Cleveland, Ohio) by starting at the widest setting (number 7) and repeating consecutively at narrower settings (numbers 6, 5, 4 and 3, respectively) in order to get a thin pasta sheet. Next, pasta sheets were cut through a spaghetti cutter attachment. The pasta strands were dried on kitchen towels at room temperature for 90 min. After that,

fifty grams of pasta strands were cooked in 1 L of boiling water for 2 min. The pasta was drained and rinsed with tap water. The cooked pasta was kept in a Ziploc® plastic freezer bag for further analysis.

6.3.3 Texture measurement

Methods used for determination of texture profiles and firmness of cooked formulated pasta were slightly altered from Tang and others (1999) by using a TA–HDi ® texture analyzer (Texture Technologies Corp., Scarsdale, N.Y.). The measurement was performed in triplicate for each replication of cooked pastas. The results obtained from the measurements were expressed in terms of firmness, hardness, cohesiveness, adhesiveness, springiness, and chewiness. For texture profile analysis (TPA), a pasta stand was placed on a sample holder, which was fixed with a surface serrated by 90 ºvee grooves, 1.5 mm deep, spaced at 3.6 mm. A flat cylindrical plexiglass plunger (25 mm in a diameter), which was connected to a 5 Kg load cell, was attached to the texture analyzer. A cooked pasta strand was compressed twice to 70% fixed strain using a cross head speed of 0.2 mm/s. For performing the firmness test, a plexiglass blade was employed instead of a flat cylindrical plexiglass plunger. A cooked pasta strand was then sheared crosswise by the blade to 75% fixed strain by using the same head speed as TPA (0.2 mm/s). All data obtained from the texture measurements were collected using Texture Expert Exceed (version 2.61, Texture Technologies Corp., Scarsdale, N.Y.).

6.3.4 FT–IR spectroscopy measurements

FT–IR analysis was conducted at room temperature using a Thermo Nicolet 380 FT–IR Spectrometer (Thermo Electron Corporation, Madison, Wis.) in duplicate. The pasta samples were placed directly onto the attenuated total reflectance (ATR) diamond crystal. FT–IR spectra were collected at the range of 3800 − 900 cm^{-1} and recorded in absorbance units at a resolution of 4 cm^{-1}. Each measurement was an average value of 64 separate scans. Spectral data were collected using OMNIC^{TM} software, version 7.0 (Thermo Electron Corporation, Madison, Wis.).

6.3.5 Raman spectroscopy measurements

Raman spectroscopic analysis was conducted in triplicate and accomplished by using a Renishaw RM1000 Raman Spectrometer System (Renishaw plc, UK), which was equipped with a Leica DMLB microscope from Leica Microsystems (Wetzlar, Germany) and a diode laser source with a power of 300 mW at 785 nm. Silica was used as a standard to calibrate Raman frequency and intensity. In order to perform the analysis, small pieces of cooked pasta samples were placed on a gold coated micro slide (Thermo Electron Corporation, Madison, Wis.). Spectral data were collected with 10 sec exposure time by the Renishaw WiRE 1.3 software (Renishaw plc, UK). Raman spectra were obtained in the Raman shift range from 3200 to 300 cm^{-1} in the extended mode.

6.3.6 Data analysis

Pretreatment of both FT−IR and Raman spectra were operated by using OMNIC version 7.3 (Thermo Electron Inc., Waltham, Mass.). The spectra were corrected their baseline shifts and normalized their scales. The normalized spectra were then processed using the Delight software, version 3.2.1 (D−Squared Development Inc., LaGrande, Ore.), including smoothing with a Gaussian function over 6 cm^{-1}, binning with the width of 2 cm^{-1} and second derivative transformation over the gap value of 12 cm^{-1}.

Principal component analysis (PCA) was conducted using the Delight software with 5 latent variables which is based on the least squares techniques for performing linear fitting to a series of orthogonal eigenvectors (loadings). An array of vectors obtained from a data set (a set of spectra) was extracted to find the best fit product of scores and loadings. The best reproduction of the spectra from the reduced data set was obtained afterward. To avoid confounding effects of water stretching bands in the FT−IR dataset, the region of 2000 − 4000 cm^{-1} was not selected in the PCA analysis.

Relationships between texture attributes (response variables) and intensities of major bands in both FT−IR and Raman spectra (explanatory variables) of the pasta matrixes were described by performing regression analysis, conducted using the SAS® version 9.00 (SAS Institute Inc., Cary, N.C.). All explanatory variables (regressors) included in the regression models were significant at the 0.10 level. Significant differences on texture attributes among cooked pasta samples were determined using analysis of variance (ANOVA) at $p<0.05$ in the general linear models (GLM) procedure of the SAS® software program. The ANOVA was analyzed as a Randomized Complete

Block Design. Fisher's least significant difference (LSD) was performed as a mean separation method.

6.4 Results and Discussion

6.4.1 FT−IR analysis

The FT−IR spectra in the range of 3800 − 900 cm^{-1} is illustrated in Figure 6.1.

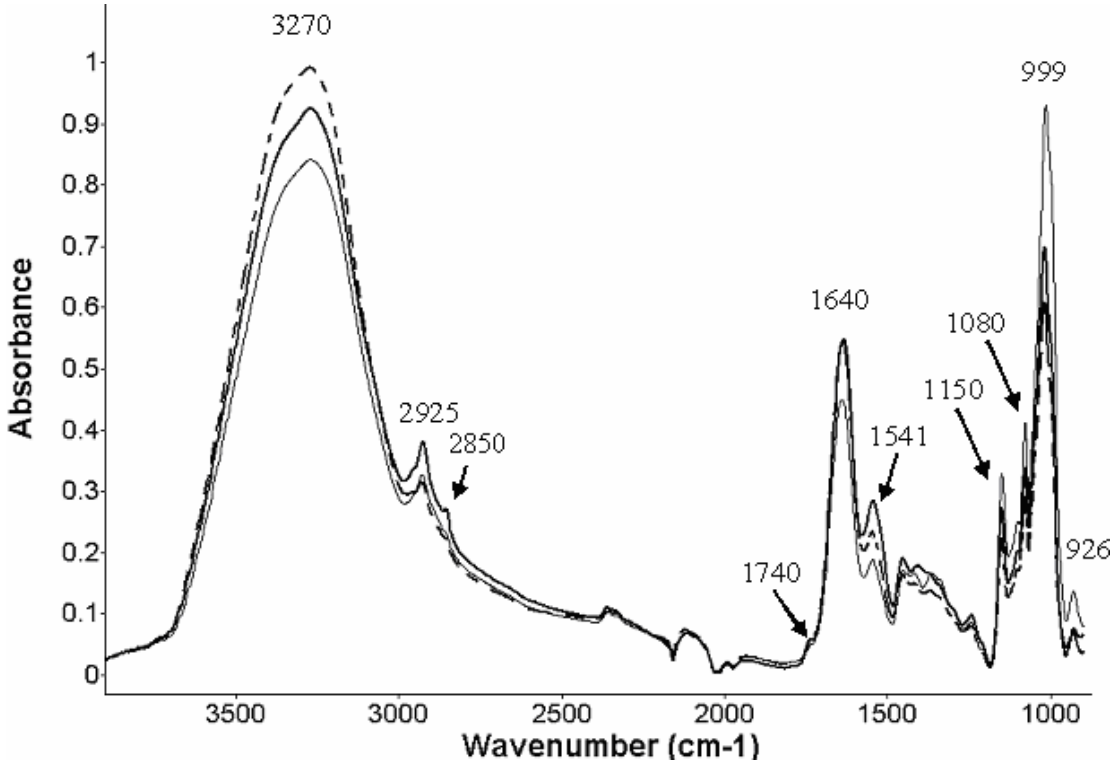

Figure 6.1. FT−IR spectra of cooked pasta; without adding beef heart (—), 10% added beef heart (---), and 30% added beef heart (▬) in the 3800 − 900 cm^{-1} region. Averaged spectra were obtained from three batches of pasta (n = 3) with duplicate analysis.

The highest and broadest peak located around 3270 cm^{-1} in the FT−IR spectra was found in pasta products made with 10% beef heart addition, followed by pasta products made with 30% additional beef heart, and the control (without adding beef heart),

respectively. The prominent peak in the area of 3270 cm^{-1}, assigned for O−H stretching, might relate to water content in the tested pasta. An occurrence of strong broad bands in the vicinity of 3600 − 3000 cm^{-1} has typically been attributed to moisture being presented in food samples, such as a strong wide peak in the 3700 − 3100 cm^{-1} range acquired from cheese (Chen and Irudayaraj 1998). However, Ramesh Yadav and others (2007) believed that a strong broad band of hydrogen−bonded hydroxyl groups (O−H), which is located around 3403 cm^{-1}, might stem from a combination of stretching vibrations of free, inter− and intra−molecular bound hydroxyl groups, which could be linked to gross structures of starch.

FT−IR intensities around the wavenumber of 2925 cm^{-1}, associated to asymmetric stretches of methylene groups, were almost analogous among all pasta samples. However, a small peak located around 2850 cm^{-1}, which was assigned for symmetric stretching vibrations of methylene groups, was found only in the spectra of the 30% added beef heart pasta. Mohamed and others (2005) employed an intensity ratio of 2925 cm^{-1} to 2850 cm^{-1} (I_{2925}/I_{2850}) to describe conformation changes in phospholipids because of interactions with gluten. In this study, the I_{2925}/I_{2850} ratio could be calculated only in pasta samples made with 30% level of beef heart, which was 1.39. A proposed explanation of this finding might be that the 30% added beef heart pasta contained extra amounts of phospholipid to interact with gluten proteins in the matrixes. Similarly, the FT−IR region around 1740 cm^{-1}, where the C═O stretching of the ester functional group is located, was relatively small and the highest intensity in this region was seen in the 30% added beef heart pasta. This finding might be due to the fact that the 30% partially replaced pasta contained the highest fat content among all pasta samples.

The highest peaks in the districts of 1640 cm^{-1} (amide I) and 1541 cm^{-1} (amide II) appeared in the pasta samples with the 30% level of beef heart, which was followed by 10% and 0% substitutions, respectively. However, a strong band near 1640 cm^{-1} might be influenced by the H−O−H bending vibrations of water (Chen and Irudayaraj 1998; Cremer and Kaletunç 2003). According to Wellner and others (2005), a broad band at 1640 cm^{-1} might be caused by overlapping bands, which included bands around 1666 (β−turns), 1650 (α−helix and random), 1630 (β−sheet), and 1620 (intermolecular β−sheet) cm^{-1}. The second−derivatives of the FT−IR spectra were therefore considered in order to stay away from overlapped bands (Figure 6.2). The results demonstrated that β−sheet content was higher in pasta products made with increasing amount of beef heart. Emerging bands at 1650 cm^{-1} might relate to an arrangement of α−helical and random structure in formulated pasta with 0% and 30% levels of beef heart. Ratios of band intensities of amide I to amide II might relate to starch or protein content in tested samples and higher intensity ratios correlated to the higher amounts of starch (Cremer and Kaletunç 2003). The ratios of amide I to amide II obtained from the spectra of pasta made with 0%, 10%, and 30% additional beef heart were 2.4, 2.3, and 1.9, respectively. Cremer and Kaletunç (2003) highlighted that in proteins, the ratio of amide I: amide II classically varies from 3:1 for purely α−helical proteins to 2:1 for β−sheet proteins. The amide I: amide II ratios, which originated from the pasta spectra, were around 2:1 indicating the presence of β−sheets in the pasta samples rather than by influences of starch or moisture contents. Georget and Belton (2006) revealed that β−sheet structures could take place in company with a loss of α−helical structures when dry gluten proteins are exposed to an adequate amount of water as well as heat.

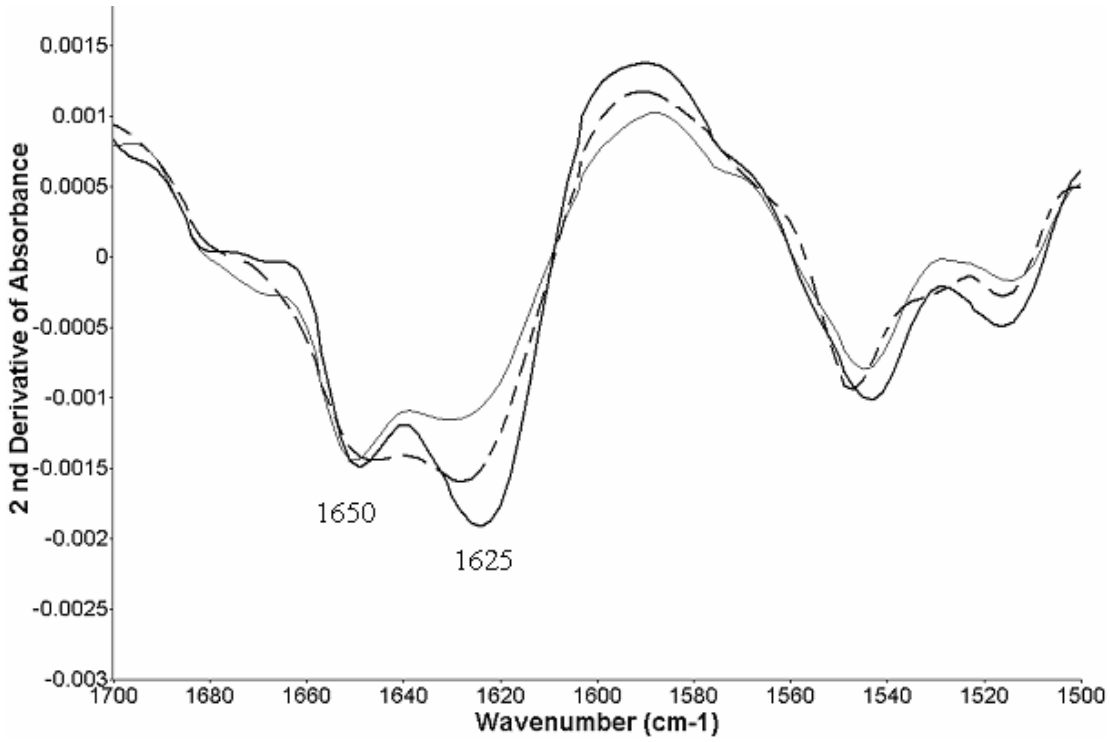

Figure 6.2. FT−IR second−derivative spectra of pasta; without adding beef heart (─), 10% added beef heart (---), and 30% added beef heart (▬) in the region of 1700 − 1500 cm^{-1}

The FT−IR bands that were obtained from the control clearly showed higher intensities than the other two pastas in the regions of 1150, 1080, 999, and 926 cm^{-1}. Cui and others (2007) indicated that the wavenumber range of 1200 – 800 cm^{-1} is fingerprint−like for carbohydrate–based samples. The higher intensity in the region between 1200 and 800 cm^{-1} in 0% added beef heart pasta might, therefore, be associated to the higher carbohydrate content (25%) compared to the 10% beef heart pasta (24%) or the 30% beef heart pasta (22%). In addition, the spectra pattern in this region was equivalent among pasta samples, which might originate from durum wheat carbohydrate.

6.4.2 Raman spectroscopic analysis

The Raman spectra in the region of 2580 − 2510 cm^{-1}, where S−H stretching mode is assimilated, are illustrated in Figure 6.3 and show similar patterns among three different samples, which include 0%, 10%, and 30% substituted beef heart pasta. Normally, cysteine and cystine residues in gluten proteins are key factors in sulfhydryl−disulfide interchange reactions and account for only 2 − 3% of gluten's total amino acid residues (Damodaran 1996). Therefore, comparatively low Raman intensity in this region, which was observed from three different samples, might be due to relatively low amounts of cysteine and cystine residues in gluten proteins. However, slightly higher intensity of 10% and 30% added beef heart pasta in the Raman shift of 2580 − 2510 cm^{-1} might be caused by the extra amounts of S−containing amino acid residues in cardiac proteins that could offer more S−H hydrogen bonding interactions in pasta matrixes.

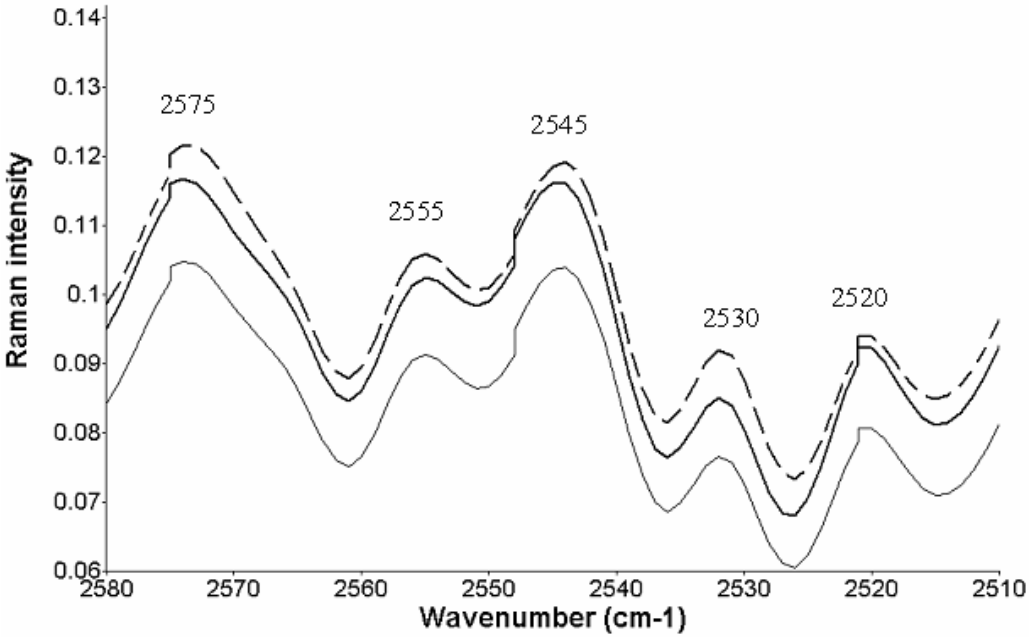

Figure 6.3. Raman spectra of cooked pasta; without adding beef heart (─), 10% added beef heart (---), and 30% added beef heart (▬) in the 2580 − 2510 cm^{-1} region. Averaged spectra were obtained from three batches of pasta (n = 3) with triplicate analysis.

The Raman spectra at the wavenumber range of 1800 − 300 cm^{-1} are depicted in Figure 6.4. The intensities of the peaks at 1673 (assigned for antiparallel *β*−pleated sheet), 1085 (−C−O stretch of carbohydrates), 1005 (*β*−pleated sheet), and 940 (*α*−helix) cm^{-1} were similar between 0% and 10% added beef heart pasta samples, but were considerably different from the Raman intensity in the spectra of 30% additional beef heart pasta. Thus, both 0% and 10% added beef heart pasta might contain a higher proportion of *β*−sheet and *α*−helical structures than pasta made with 30% beef heart addition. The intensity of the stretching bands of carbohydrates (1085 cm^{-1}) that decreased over an increased amount of additional beef heart might be related to starch content in pasta matrixes.

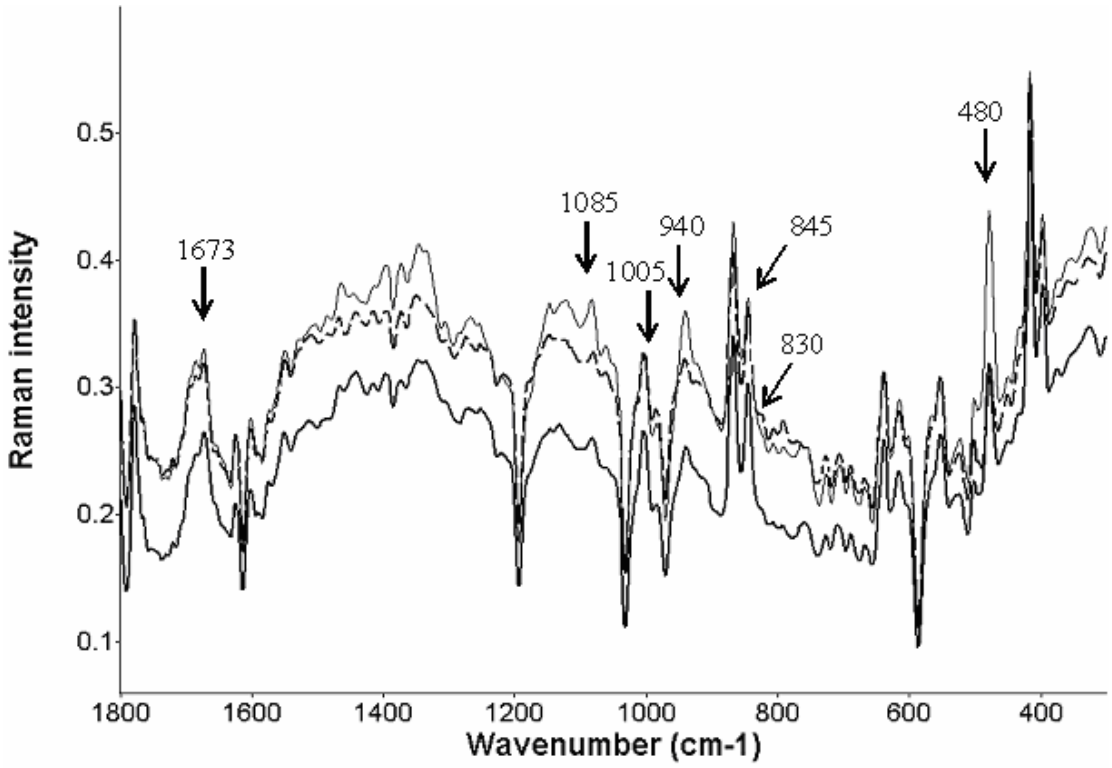

Figure 6.4. Raman spectra of cooked pasta; without adding beef heart (—), 10% added beef heart (---), and 30% added beef heart (▬) in the 1800 − 300 cm^{-1} region

The intensity ratio of the tyrosine doublet bands (I_{845}/I_{830}) could be employed to predict whether tyrosine residues were buried or exposed and also to determine the state of hydrogen bonding of the phenolic −OH group (Spiro and Gaber 1977; Li−Chan and others 1994). The buried tyrosine residues have a tendency to form a strong hydrogen bond between the phenolic (−OH) and a negative acceptor, which is typically carboxylate ions of aspartate or glutamate residues, and then lead to a low I_{845}/I_{830} ratio of 0.3 − 1.0 (Li−Chan and others 1994). On the other hand, when the tyrosine residue is exposed, its phenolic oxygen can interact with a proton (H^+) donor in a hydrophilic environment via hydrogen bonding, in this case, the I_{845}/I_{830} ratio is higher (0.9 − 2.5) (Li−Chan and others 1994). The I_{845}/I_{830} ratios calculated from the spectra of pasta samples made with 0%, 10% and 30% beef heart substitutions were 1.4, 1.4, and 1.6, respectively. These finding explained that tyrosine residues in cooked pasta matrixes were probably exposed to hydrophilic environments and could be able to form hydrogen bonds with acid donors, such as water in the matrixes.

The Raman signal around 480 cm^{-1} has been employed by many researchers to investigate changes of polysaccharides in food systems, such as to investigate distributions of starch in carrot (Baranska and others 2005), and to evaluate rates of retrogradation of potato, maize, and wheat starch (Fechner and others 2005). In this study, the highest Raman intensity in the regions of 480 cm^{-1} (assigned for skeletal vibrations of starch) was observed in pasta samples made without additional beef heart and showed a clear−cut difference from the pasta products made with 10% and 30% beef heart addition. This finding showed that partially substituting durum wheat flour with beef heart caused a reduction of amylose−amylopectin network developments because

decreased intensities of the Raman signals at 480 cm^{-1} were observed in the formulated pasta.

The Raman spectra in the region tentatively assigned for stretching modes of C−S and S−S are demonstrated in Figure 6.5. The peaks located in the areas of 640, 550, 525, and 503 cm^{-1} were almost identical between pasta samples made with 0% and 10% beef heart substitutions but were obviously different from pasta made with 30% beef heart addition. This observation indicated that beef heart at 30% replacement might interrupt disulfide formations in pasta matrixes. Perhaps, cardiac amino acid residues disrupted disulfide bridges that were formed by cysteine and cystine residues of gluten proteins because an inferior intensity of these Raman shifts was observed in the spectra of 30% added beef heart pasta.

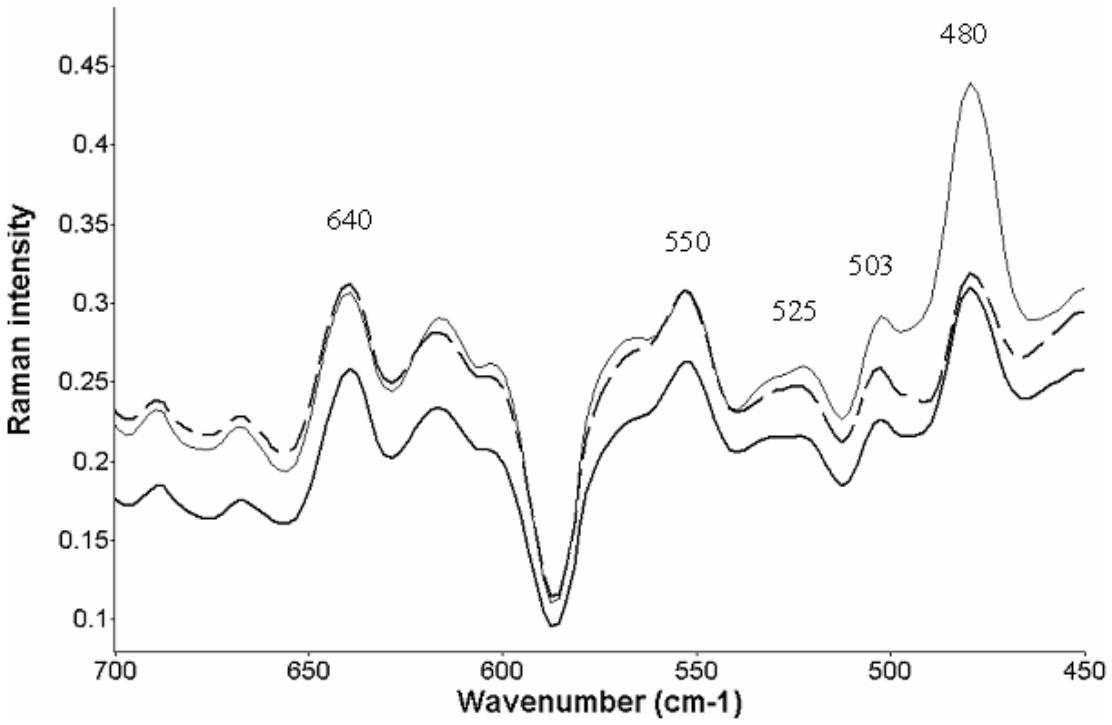

Figure 6.5. Raman spectra of cooked pasta; without adding beef heart (—), 10% added beef heart (---), and 30% added beef heart (▬) in the 700 − 450 cm^{-1} region

6.4.3 PCA analysis

PCA clusters of FT−IR and Raman spectra obtained from cooked pasta samples, which were made from durum wheat flour and three different levels of beef heart (0%, 10%, 30% substitutions), are shown in Figures 6.6 and 6.7, respectively. The PCA plots of the FT−IR spectra indicated that pasta samples made up with 10% and 30% beef heart were actually partially overlapped. A PCA cluster obtained from the Raman spectra of pasta made without any additional beef heart separated well from the other two but the PCA cluster of 10% added beef heart pasta overlapped with the cluster of 30% added beef heart (Figure 6.7). These results indicated that partially replacing durum wheat flour with beef heart could lead to noticeable changes in pasta characteristics, which could be revealed by multivariate statistical analysis such as PCA.

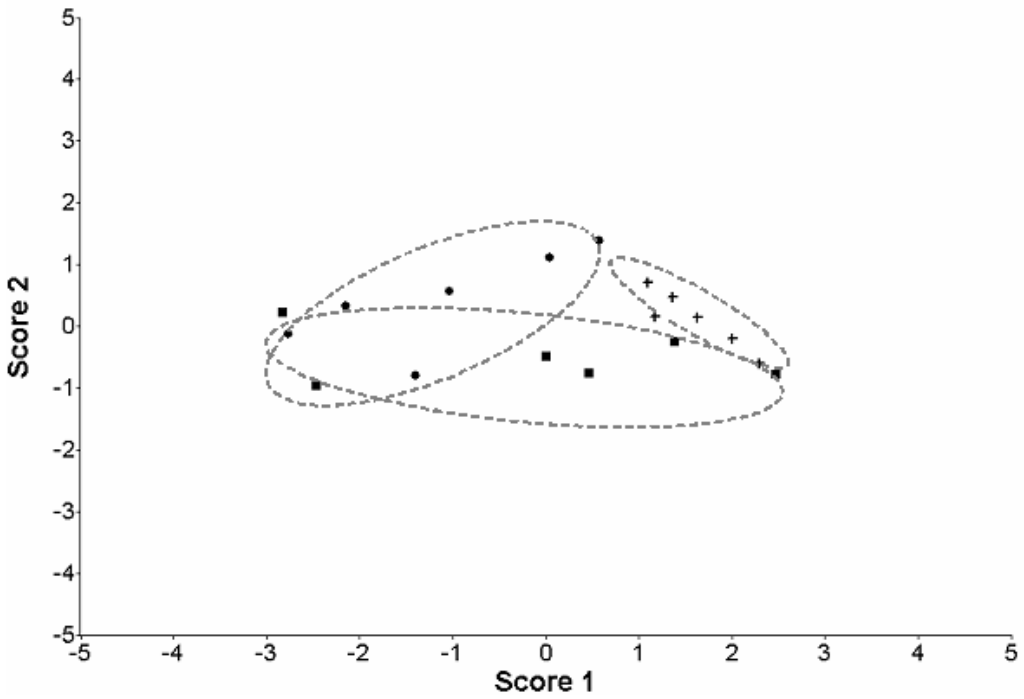

Figure 6.6. PCA plots using FT−IR spectra of cooked pasta obtained from different formulations; without added beef heart (+), 10% added beef heart (●), and 30% added beef heart (■). Number of sample is 3 (n = 3) with duplicate analysis

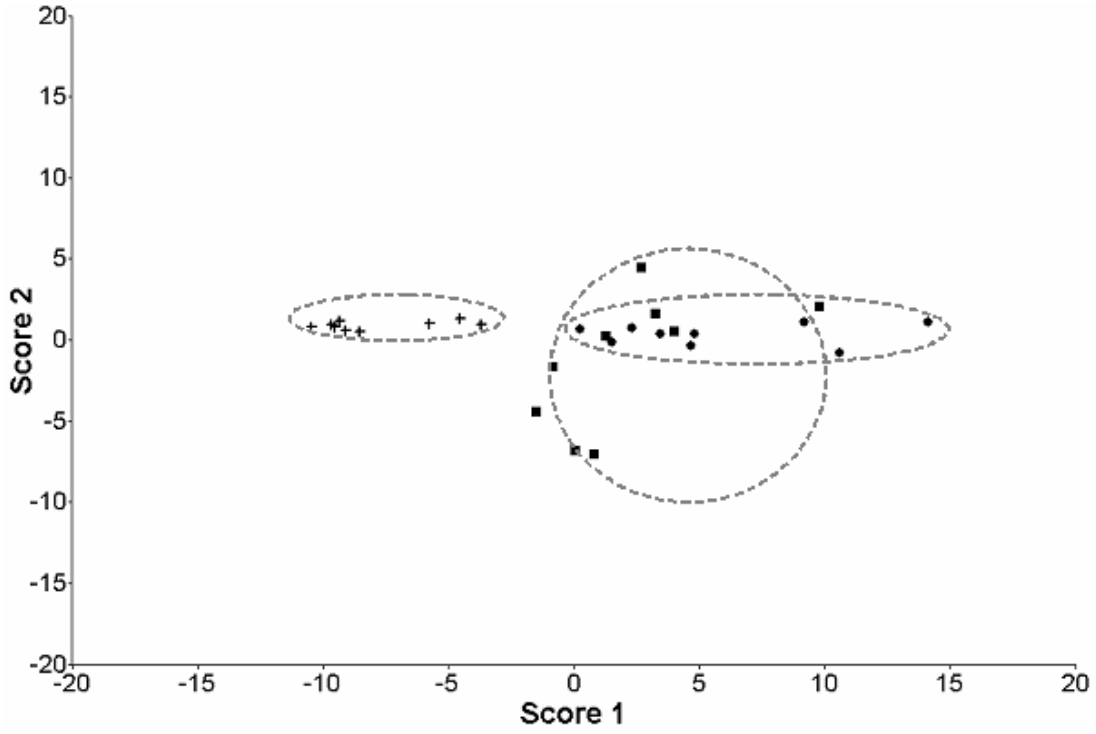

Figure 6.7. PCA plots using Raman spectra of cooked pasta obtained from different formulations; without added beef heart (+), 10% added beef heart (●), and 30% added beef heart (■). Number of sample is 3 (n = 3) with triplicate analysis

6.4.4 Relationships between vibrational spectra' intensities and pasta texture attributes

Texture characteristics of cooked fresh pasta were determined and expressed in terms of hardness, cohesiveness, adhesiveness, springiness, chewiness, and firmness (Table 3.3). Hardness, adhesiveness, chewiness, and firmness showed significant increases between 0% and 30% added beef heart pasta as well as between 10% and 30% additional beef heart pasta. Cohesiveness of pasta at 10% substitution was significantly lower than that of pasta at 30% substitution, but both pasta samples were not significantly different from pasta made without beef heart addition. However, no substantial difference among pasta samples was observed for springiness. Wrigley (1996) believed that the

similarity between glutenin in the gluten network and titin, which is the longest single−chain polypeptide in heart muscle, was not only due to their massive protein size, but both of them also constructed a functional feature of springiness in their domains. As a result, incorporating beef heart into pasta did not cause a significant change of springiness in cooked pasta samples, compared among 0%, 10%, and 30% additional beef heart pasta.

Relationships between texture characteristics and physiochemical changes that were measured by vibrational spectroscopic methods (FT−IR and Raman spectroscopy) were analyzed using regression analysis (Table 6.1).

According to the results, an improvement of lipid−protein complex formation (FT−IR band at 2926 cm^{-1}), decreased β−sheets (FT−IR intensity ratio of 1640 and 1541 cm^{-1}; Raman band at 1673 and 1005 cm^{-1}), a reduction of polysaccharide network (FT−IR band at 999 cm^{-1}; Raman band at 1085 cm^{-1}), and increased sulfhydryl groups (Raman band at 2530 cm^{-1}) corresponded to an increase in pasta hardness and chewiness. Beattie and others (2004) found a negative correlation between the Raman band at 1006 cm^{-1} and toughness of cooked beef and concluded that a reduction of β−sheet formation led to an increase in toughness. Increases of lipid portions (FT−IR band at 1740 cm^{-1}) and β−sheet structures (FT−IR band at 1541 cm^{-1}) as well as decreased starch complex formation (Raman band at 1085 cm^{-1}) significantly increased pasta adhesiveness. A reduction in the amylose−amylopectin network formation (FT−IR band at 999 cm^{-1}; Raman band at 1085 cm^{-1}) and a declination of β−sheet arrangement (FT−IR intensity ratio of 1640 and 1541 cm^{-1}) were correlated with increased firmness in the pasta matrixes. Alpha−helix alignment (Raman spectra at 940 cm^{-1}) and hydrogen bonding formation (Raman spectra

at 845 cm^{-1}) in the pasta matrixes exhibited a negative correlation with pasta cohesiveness. This finding was in agreement with Damodaran (1996) who believed that hydrogen bonding in gluten network made a contribution to cohesion−adhesion of wheat protein−based products. Thus, increased cardiac amino acid residues in the pasta matrixes might break up the development of hydrogen bridges in the gluten network and likely altered pasta cohesiveness. Beattie and others (2004) found that decreased α−helices (Raman spectra at 940 cm^{-1}) correlated to increased juiciness of cooked beef matrixes, and increased hydrogen bonding of the tyrosine residues (Raman spectra at 860 cm^{-1}) contributed to a reduced degree of tenderness of cooked beef. There was no variable (vibrational spectra) that fit into the regression models for springiness of pasta products at the 0.1 significant levels.

Table 6.1. Prediction models of texture attributes investigated by regression analysis: relationships between texture attributes and intensities of major bands in FT−IR and Raman spectra

Texture attributes	**Vibrational spectra data fit in a prediction model of texture attributes (wavenumber cm^{-1})**
FT−IR spectroscopy	
Hardness	I_{2926}, I_{1640}, I_{1541}, and I_{999}
Cohesiveness	no variable met the 0.1 significant levels
Adhesiveness	I_{1740} and I_{1541}
Springiness	no variable met the 0.1 significant levels
Chewiness	I_{2926}, I_{1640}, I_{1541}, and I_{999}
Firmness	I_{1640}, I_{1541}, and I_{999}
Raman spectroscopy	
Hardness	I_{2530}, I_{1673}, I_{1085}, and I_{1005}
Cohesiveness	I_{940} and I_{845}
Adhesiveness	I_{1085}
Springiness	no variable met the 0.1 significant levels
Chewiness	I_{2530}, I_{1085}, and I_{1005}
Firmness	I_{1085}

6.5 Conclusions

The prediction model for texture attributes obtained from FT−IR spectra was comparable and complimentary to that obtained from Raman spectroscopy. Based on the finding of this study, both FT−IR and Raman spectroscopy could be implemented to examine physiochemical changes of pasta matrixes and to assess the quality of pasta texture as well. Although vibrational spectroscopic methods, including FT−IR Raman spectroscopy, have been proposed as novel techniques for quality assessment in many food products, further research on a wider range of food matrixes is still needed. Correlating vibrational spectroscopy and pasta organoleptic characteristics, such as flavor and sensory attributes, should also be considered for use in pasta quality control.

CHAPTER 7

VIBRATIONAL SPECTROSCOPIC CHARACTERIZATION OF FREEZE–DRIED BEEF HEART

7.1 Abstract

The freeze–dried beef heart used in this study was also examined using FT–IR and Raman spectroscopy. The results showed that beef heart proteins mainly consisted of α–helix and β–sheet structures. By comparing spectral data of beef heart to spectral data of pasta made with 0%, 10%, and 30% added beef heart, the additional amounts of lipids and proteins, which were supplied by beef heart, caused a modification in pasta matrixes. The spectral data of beef heart obtained from this study is an initial step of using FT–IR and Raman spectroscopy for evaluation meat products for adulteration.

Keywords: Vibrational spectroscopy; FT–IR; Raman spectroscopy; Beef heart; Secondary structure

7.2 Introduction

Beef heart is one of the most economical edible beef muscles due to a low cost of approximately 65 dollars per 100 pounds (U.S. Department of Agriculture, the Agricultural Marketing Service 2008). Therefore, many meat food products, such as beef jerky (Miller and others 1988), surimi (Wang and Xiong 1998), and frankfurters (Desmond and Kenny 1998), were reformulated with beef heart with the purposes of increasing values of beef heart, enhancing nutritional values of newly formulated food products, and also reducing costs of productions. In regard to food regulations, vibrational spectroscopy, including FT–IR and Raman spectroscopy, has recently become a promising tool for rapidly identifying adulterated meat products. However, there is insufficient data on the spectroscopic characterization of edible meat muscles. Therefore, the objective of this study was to examine beef heart spectrospcopically.

7.3 Materials and methods

7.3.1 Freeze–dried beef heart preparation

Beef hearts were obtained from the meat laboratory of the University of Missouri, Columbia. The beef hearts were cleaned with distilled water and their non–edible portions were removed. Afterwards, the beef hearts were chopped into small pieces and then homogenized in a general–purpose electric blender (Osterizer, Oster Corporation, Wis.). The beef hearts were dried in a freeze–dryer (LabConCo Corp., Kansas City, Mo.) for ~48 h. Afterwards, the freeze–dried beef hearts were ground into fine powders and stored under nitrogen in plastic bags at –20°C until use.

7.3.2 FT–IR spectroscopy measurements

FT–IR spectroscopic characterization of freeze–dried beef hearts was performed using a thermo Nicolet 380 FT–IR Spectrometer (Thermo Electron Corporation, Madison, Wis.) at room temperature. The freeze–dried beef hearts were placed directly on the top of the ATR diamond crystal. FT–IR measurements were analyzed for the wavenumber of 4000 to 900 cm^{-1}. The FT–IR spectroscopic outcomes were expressed in term of FT–IR spectra in which frequencies of radiation (wavenumber cm^{-1}) are recorded as absorbance units at a resolution of 4 cm^{-1}. Each spectrum is the average value of 64 separate scans and was collected using OMNIC^{TM} software, version 7.0 (Thermo Electron Corporation, Madison, Wis.). Measurements were done in duplicate.

7.3.3 Raman spectroscopy measurements

A Renishaw RM1000 Raman Spectrometer System (Renishaw Ramascope from Renishaw plc, UK) equipped with a Leica DMLB microscope from Leica Microsystems (Wetzlar, Germany) was employed for characterizing the freeze–dried beef hearts. A diode laser with a power of 300 mW at 785 nm together with an integral plasma filter was used as a laser source. The freeze–dried beef hearts were placed directly on a gold coated micro slide (Thermo Electron Corporation, Madison, Wis.) and viewed through the Leica DMLB microscope with a 50× objective at room temperature. Raman spectral data were collected with 10 sec exposure time by the Renishaw WiRE 1.3 software (Renishaw plc, UK) and the extended mode of the Raman shift (wavenumber cm^{-1}) within the range of 3200 – 350 cm^{-1} was considered. Each measurement was done in three replications and average results were obtained.

7.3.4 Spectral treatment

Baseline corrections and scale normalizations of spectral data obtained from the FT–IR and Raman analyses were processed by using OMNIC version 7.3 (Thermo Electron Inc., Waltham, Mass.). Afterwards, the normalized spectra were treated using the Delight software, version 3.2.1 (D–Squared Development Inc., LaGrande, Ore.) by smoothing the spectra with a Gaussian function over 6 cm^{-1} and binning the spectra with the width of 2 cm^{-1}. The spectra were transformed to their second derivative points over the gap value of 12 cm^{1} in order to ensure overlapped vibrational bands.

7.4 Results and discussion

7.4.1 FT–IR analysis

Figure 7.1 illustrates the FT–IR spectra of freeze–dried beef heart ranging from 4000 – 900 cm^{-1}. A wide–ranging band centered around 3280 cm^{-1} was demonstrated in the FT–IR spectra. The bands of the asymmetric stretches (~ 2925 cm^{-1}) and symmetric stretches (~ 2855 cm^{-1}) of methylene groups were observed in the FT–IR spectra of freeze–dried beef heart. A sharp signal in the wavenumber of 1740 cm^{-1} ,which can be attributed to C=O stretches of ester groups principally from lipids and fatty acids, was visible in the FT–IR spectra, and likely reflects the fat content of the beef heart.

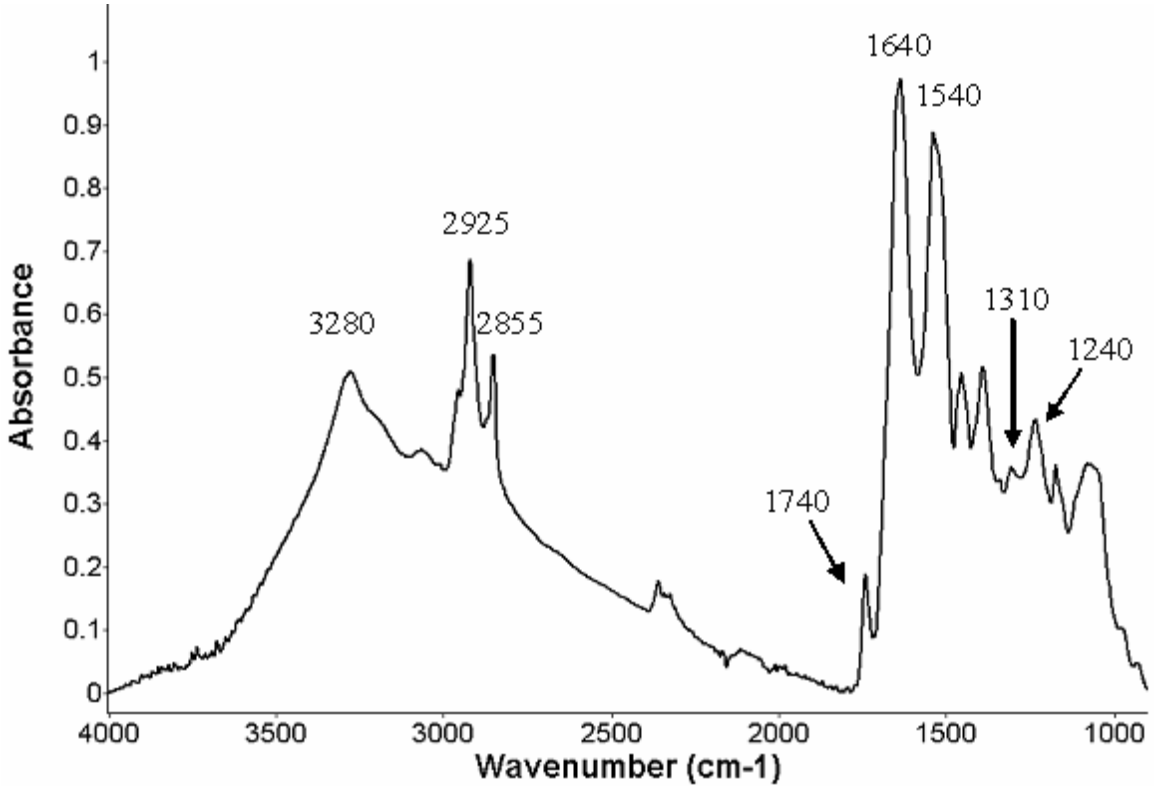

Figure 7.1. FT–IR spectra of freeze–dried beef heart in the 4000 – 900 cm^{-1} region

The spectral ranges where amide I (1640 cm^{-1}), amide II (1541 cm^{-1}), and amide III (1350 – 1200 cm^{-1}) are located, have been widely used to determine the secondary structure of proteins based on the vibrational features of the C=O, C–N, and N–H groups of peptide bond. In this study, the FT–IR spectra of beef heart showed strong sharp bands located around 1640 cm^{-1} and 1541 cm^{-1}. A spiky peak in the wavenumber of 1640 cm^{-1} was possibly caused by the effect of bending vibrations of water (H–O–H) (Chen and Irudayaraj 1998; Cremer and Kaletunç 2003). However, Wellner and others (2005) believed that overlapping bands around the area of 1640 cm^{-1} contributed to a broad band in that area, which included bands of β–turns (1666 cm^{-1}), α–helixes and random coils (1650 cm^{-1}), β–sheets (1630 cm^{-1}), and intermolecular β–sheets (1620 cm^{-1}). Because of

the very low moisture content of freeze–dried beef heart, the strong sharp band in the region of 1640 cm^{-1} was, therefore, more likely due overlapping bands, which were 1682 (β–sheets), 1650, and 1630 cm^{-1} (Figure 7.2), rather than by H–O–H bending.

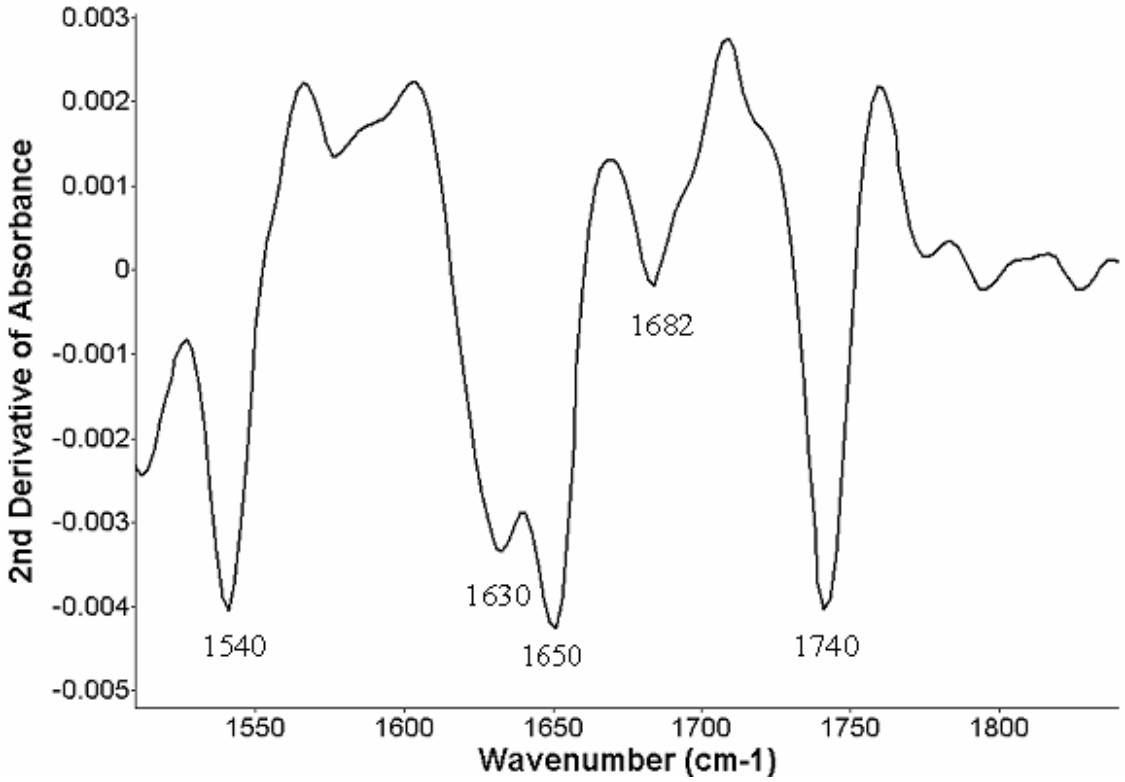

Figure 7.2. FT–IR secondary–derivative spectra of freeze–dried beef heart in the 1500 – 1850 cm^{-1} region

Although the amide III area showed relatively weak signals, O–H vibrations from water do not have an influence on FT–IR spectra in this region. Therefore, investigating the amide III regions has been an effective way for identifying secondary structures of proteins (Singh 2000). The separated peaks in the amide III region were obviously noticeable in the FT–IR spectra of the beef heart. Singh (2000) believed that the peak at 1240 cm^{-1} was indicative of β-sheets of the protein structure, which was also observed in

the FT–IR spectral data of beef heart. Besides, the band for α-helical structures (~ 1310 cm^{-1}) was found in this study. These results indicated that α-helical and β–sheet structures were major components in beef heart protein, which corresponded to the data from spectral analysis in the amide I region.

In order to understand the effects of beef heart addition on physiochemical changes in pasta matrixes, an average spectrum of FT–IR spectra obtained from freeze–dried beef heart was compared to FT–IR spectral data obtained from uncooked pasta made with 0%, 10%, and 30% beef heart substitution (Figure 7.3). The results indicated that the changes in pasta matrixes observed after the fortification with beef heart might be due to the additional proteins and lipids from the beef heart.

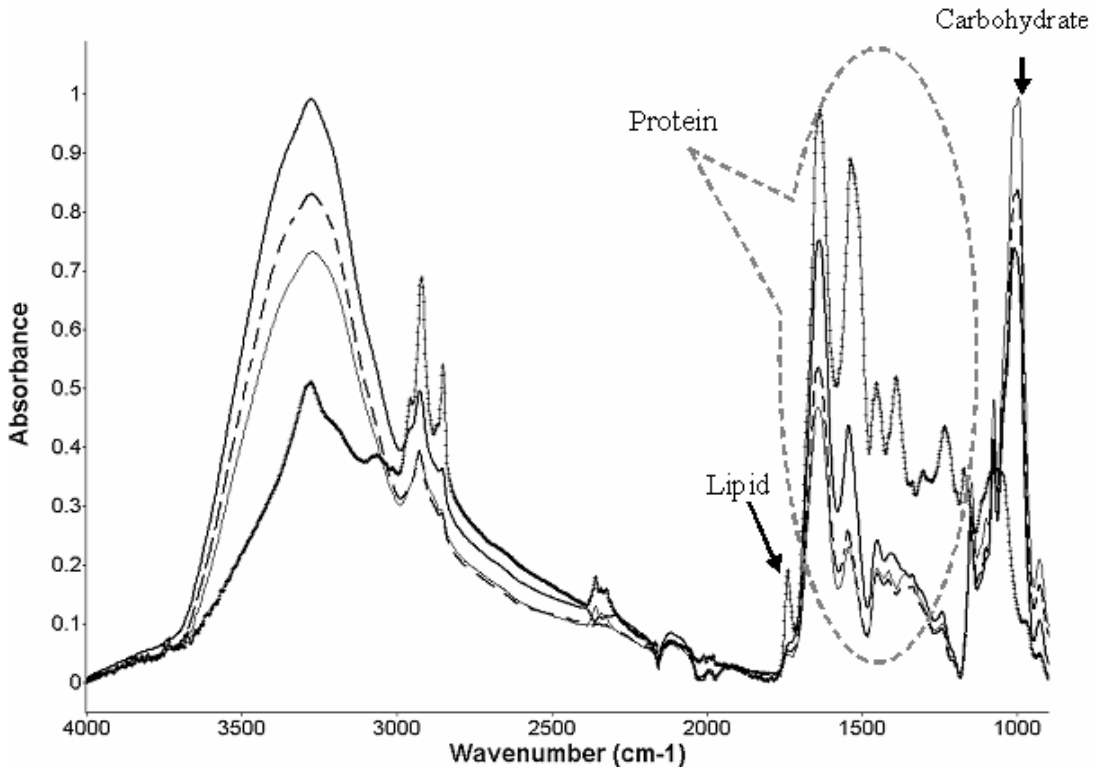

Figure 7.3. An average spectrum of FT–IR spectra obtained from freeze–dried beef heart (+++) compared to FT–IR spectra of uncooked pasta; without adding beef heart (—), 10% added beef heart (- - -), and 30% added beef heart (▬) in the 3800 − 900 cm^{-1} region

7.4.2 Raman spectroscopic analysis

Raman bands tentatively assigned to C–H stretching (3000 – 2800 cm^{-1}), S–H hydrogen bonding interactions (2600 – 2500 cm^{-1}), polypeptide backbone arrangements that included Amide I (1690 – 1650 cm^{-1}) and Amide III (1280– 1230 cm^{-1}), C–H bending (~ 1445 cm^{-1}), C–N and C–C stretching (1120 – 1040 cm^{-1}), phenylalanine (~ 1006 cm^{-1}), α–helical structure (940 cm^{-1}), tyrosine doublet (850 and 830 cm^{-1}), C–S stretching (800 – 600 cm^{-1}), and disulfide bonds (600 – 450 cm^{-1}) were all detected in the Raman spectrum of freeze–dried beef heart (Figures 7.4 and 7.5).

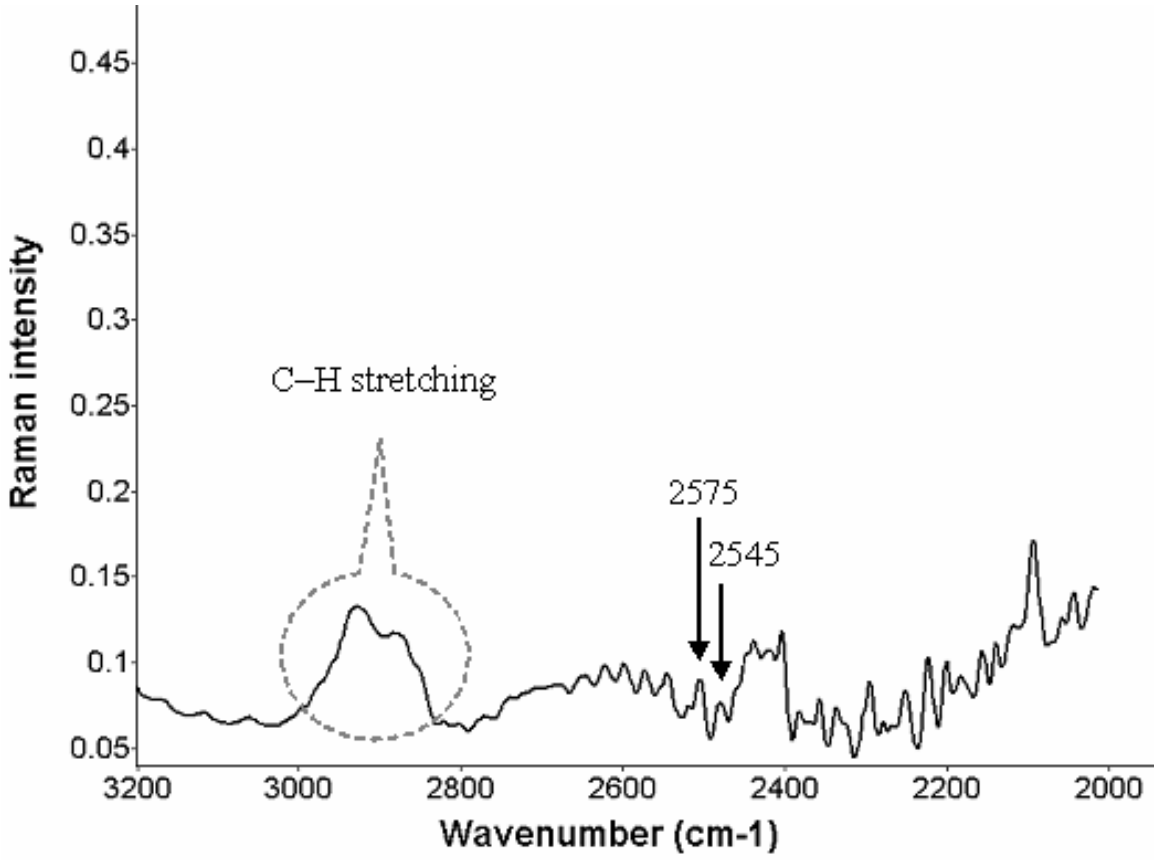

Figure 7.4. Raman spectra of freeze–dried beef heart in the 3200 – 2000 cm^{-1} region

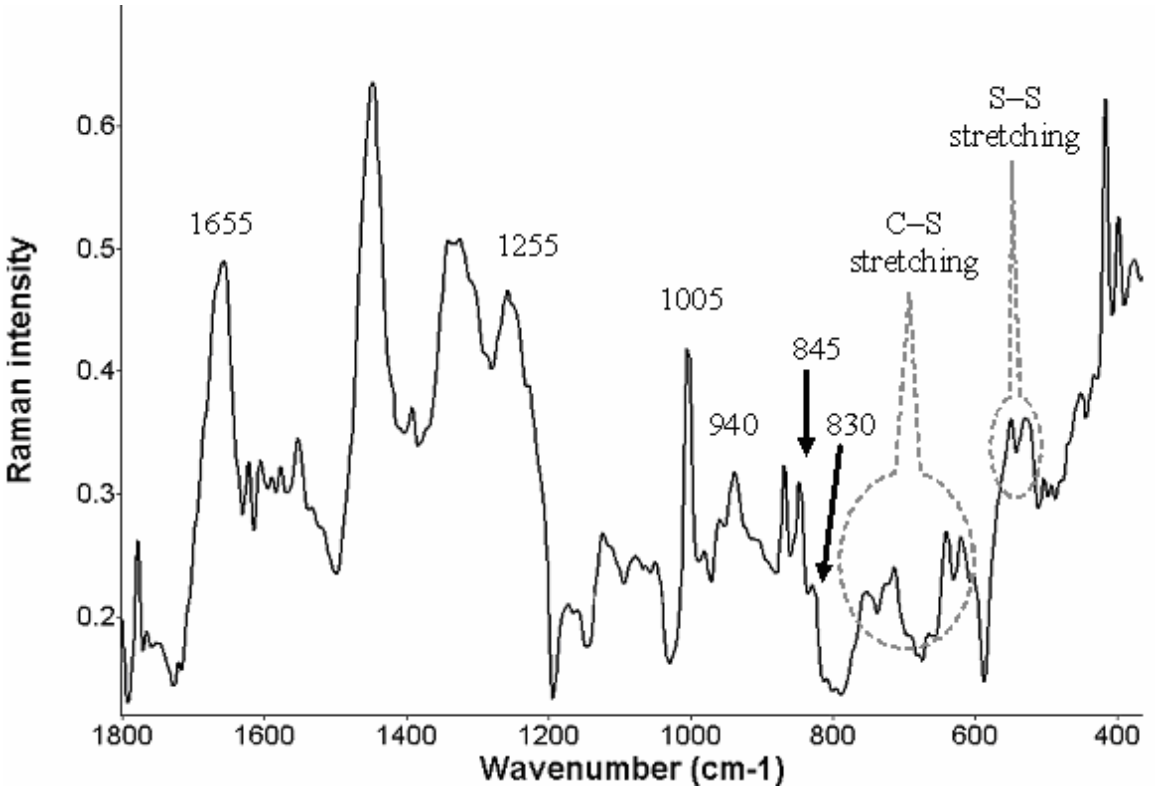

Figure 7.5. Raman spectra of freeze–dried beef heart in the 1800 – 300 cm^{-1} region

The broad band located around 2910 cm^{-1} (Figure 7.4) was assigned to the C–H stretching vibration and might be caused by an overlap of vibrational modes of numerous amino acids (Howell and others 1999). In addition to protein that can cause the C–H stretching vibration, fat and carbohydrate in the beef heart might also cause the vibration bands in this region. Relatively small bands in the Raman shift of 2580 – 2510 cm^{-1}, assigned for S−H stretching, was present in the Raman spectral data of freeze–dried beef heart. This indicated that freeze–dried beef heart includes sulfur containing amino acids, which have the potential to form disulfide bonds with other sulfur containing compounds. The existence of the sulfur containing amino acids was also supported by emerging bands in the regions assigned to C–S stretching and S–S stretching (Figure 7.5).

The presence of an outstanding sharp Amide I band located around 1655 cm^{-1} in the beef heart spectra probably indicated that α–helix was a predominant structure found in beef heart proteins (Figure 7.5). This assumption was also confirmed by an appearance of the Amide III band centered on 1255 cm^{-1} (α–helix) and that of the Raman band in the region of 940 cm^{-1}, assigned for α–helical arrangements. In addition, a sharp peak that was centered around 1005 cm^{-1} (assigned to β–pleated sheet) appeared in the Raman spectra of freeze–dried beef heart. As a result, α–helices and β–sheets were possibly major arrangements of polypeptides found in freeze–dried beef heart, a result that is congruent with the FT-IR analysis.

Bouraoui and others (1997) employed the vibrational bands of the para–substituted benzene ring of tyrosine residues to monitor hydrogen bonds between surimi protein molecules and an aqueous environment. If tyrosine residues were exposed to a polar environment such as in an aqueous solution, in which the tyrosine residues were able to form moderate to weak hydrogen bonds, the intensity ratio of the tyrosine doublet band (~ I_{845}/I_{823}) generally ranged from 0.9 to 2.5 (Li–Chan and others 1994). On the other hand, if the tyrosine residues were buried in a hydrophobic environment and tended to participate in strong hydrogen bonding to a negative acceptor, a low I_{845}/I_{823} ratio (0.3 – 1.0) would be obtained (Li–Chan and others 1994). The I_{845}/I_{830} ratio obtained from freeze–dried beef heart spectra was 1.5, which implied that the tyrosine residues of beef heart samples were exposed and capable to be involved in hydrogen bond formations in a polar environment.

In order to identify effects of beef heart addition on the physical chemistry of pasta matrixes, an average Raman spectrum obtained from freeze–dried beef heart was also compared to Raman spectral data obtained from uncooked pasta fortified with beef heart at 0%, 10%, and 30% level (Figure 7.6). The results showed that a protein portion in beef heart might be responsible for physiochemical changes in the fortified pasta matrixes.

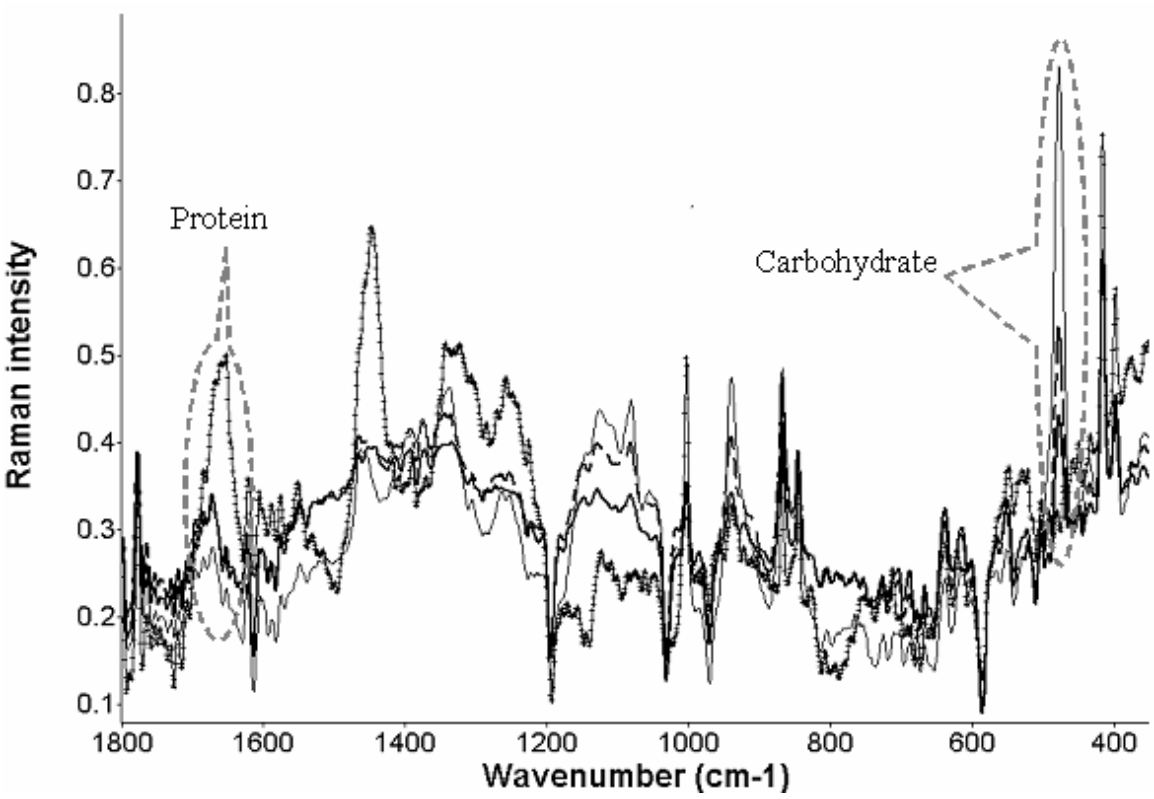

Figure 7.6. An average spectrum of Raman spectra obtained from freeze–dried beef heart (+++) compared to Raman spectra of uncooked pasta; without adding beef heart (—), 10% added beef heart (---), and 30% added beef heart (▬) in the 1800 − 300 cm^{-1} region

7.5 Conclusion

FT–IR and Raman spectroscopy were used to characterize beef heart by vibrational spectroscopy. The spectral data of beef heart obtained from both FT–IR and Raman spectroscopy clearly showed that cardiac polypeptides contained considerable amounts of α–helical and β–sheet–type structures. Lipid and protein portions in beef heart were a key explanation of physiochemical changes in pasta matrixes. Characteristic vibrational spectroscopic data of beef heart could be useful for identifying adulteration of meat products, such as ground beef patties and beef sausages, with beef heart. In addition, the result of this study is an important contribution to developing a vibrational spectral database of food components, which can be used as a reference in food regulation. However, vibrational spectroscopic characterizations of a wide range of different edible muscles are needed in order to be able to use vibrational spectroscopy as a rapid tool in the quality control of meat products.

APPENDIX 1

SAMPLE SAS INPUT FILE

1.1 Texture profile analysis in the cooked pasta samples

```
options ls=100 ps=70;
data one;
input trt TestID$ rep    Hardness    Cohesiveness    Adhesiveness
Springiness Gumminess   Chewiness   Firmness;
datalines;
0   C002          1   809.82  0.51    -63.01  0.67    415.75  278.83
78.98
0   C003          1   1306.59 0.49    -144.15 0.84    645.45  544.39
76.55
0   C004          1   997.46  0.45    -132.14 0.81    453.20  368.16
90.05
0   2CACT001      2   1477.04 0.48    -121.12 0.91    708.77  642.30
61.99
0   2CACT002      2   1317.88 0.47    -87.59  0.95    613.82  580.70
66.18
0   2CACT003      2   1484.37 0.47    -128.81 0.94    695.78  653.00
61.32
0   3CACT001      3   1170.80 0.43    -99.88  0.95    506.19  478.96
48.81
0   3CACT002      3   1091.52 0.43    -152.16 0.86    474.70  406.75
59.46
0   3CACT003      3   1022.46 0.44    -164.22 0.87    450.35  392.91
58.17
10  10H1ACT1      1   1120.90 0.39    -36.91  0.92    432.31  396.11
65.66
10  10H1ACT2      1   1400.06 0.40    -43.27  0.94    560.56  529.26
58.08
10  10H1ACT3      1   1335.21 0.41    -55.33  0.92    545.38  503.61
77.44
10  10H2ACT1      2   2104.28 0.42    -89.13  0.84    882.98  737.68
97.52
10  10H2ACT2      2   1871.38 0.43    -73.45  0.87    813.51  704.66
106.67
10  10H2ACT3      2   1589.83 0.43    -71.63  0.92    680.17  625.01
116.98
10  10H3ACT1      3   2272.66 0.45    -169.67 0.87    1015.34 882.64
96.51
10  10H3ACT2      3   1597.14 0.42    -99.91  0.84    677.28  571.90
99.98
10  10H3ACT3      3   1830.98 0.43    -142.82 0.82    787.67  644.53
90.50
30  30H2ACT1      1   4113.82 0.47    -7.19   0.94    1931.39 1806.27
113.94
30  30H2ACT2      1   4482.29 0.47    -4.96   0.95    2119.57 2011.46
316.61
```

```
30  30H2ACT3    1   3989.59 0.46    -2.76   0.93    1838.68 1705.82
280.11
30  30H1001     2   4066.50 0.48    -6.21   0.83    1955.60 1617.55
304.29
30  30H1002     2   3647.93 0.50    -0.74   0.78    1809.94 1416.29
301.57
30  30H1003     2   3854.87 0.48    -1.42   0.83    1858.59 1550.65
277.61
30  30H3ACT1    3   3374.06 0.46    -19.21  0.96    1549.10 1482.49
239.21
30  30H3ACT2    3   3428.21 0.46    -32.12  0.96    1586.04 1520.37
204.86
30  30H3ACT3    3   3850.67 0.47    -39.23  0.93    1795.63 1676.49
197.82

proc print;
proc glm; class trt rep;
model Hardness  Cohesiveness    Adhesiveness    Springiness Gumminess
Chewiness   Firmness=rep trt rep*trt;
test h=trt e=rep*trt;
means trt;
lsmeans trt/s p e=rep*trt;
run;
```

1.2 Color measurement in the cooked pasta samples

```
options ls=100 ps=70;
data one;
input trt$ TestID$ rep    l      a    b;
datalines;
0     C002        1     74.82 -2.01 18.49
0     C003        1     75.77 -1.99 18.61
0     C004        1     75.06 -2.1  18.46
0     2CACT001    2     74.19 -1.13 19.48
0     2CACT002    2     73.25 -0.96 19.54
0     2CACT003    2     73.16 -0.91 19.39
0     3CACT001    3     78.46 -3.4  21.77
0     3CACT002    3     78    -3.27 20.86
0     3CACT003    3     78.6  -3.51 21.23
10    10H1ACT1    1     50.66 9.01  13.79
10    10H1ACT2    1     50.69 9.04  13.83
10    10H1ACT3    1     51.31 8.88  13.69
10    10H2ACT1    2     50.62 8.94  11.6
10    10H2ACT2    2     52.12 9.18  12.93
10    10H2ACT3    2     51.17 9.29  12.5
10    10H3ACT1    3     52.47 8.09  14.55
10    10H3ACT2    3     51.99 8.03  14.49
10    10H3ACT3    3     52.79 8     14.41
30    30H2ACT1    1     33.6  7.83  7.3
30    30H2ACT2    1     34.08 7.94  7.45
30    30H2ACT3    1     33.99 7.97  7.68
30    30H1001     2     36.07 6.23  5.82
30    30H1002     2     37.92 5.7   6.13
```

```
30    30H1003     2     36.57 6.01  5.81
30    30H3ACT1    3     37.65 6.72  7.29
30    30H3ACT2    3     38    6.59  7.27
30    30H3ACT3    3     37.33 6.87  7.35
H     .           1     52.76 11.87 7.71
H     .           1     53.11 11.77 7.65
H     .           1     52.84 11.82 7.81
H     .           2     49.57 10.87 6.41
H     .           2     49.85 10.86 6.4
H     .           2     48.89 10.56 6.17
H     .           3     47.74 12.58 7.15
H     .           3     47.12 12.97 7.2
H     .           3     47.27 12.78 7.07
F     .           1     82.76 -1.29 22.85
F     .           1     82.57 -1.28 22.85
F     .           1     82.07 -1.26 22.85
F     .           2     83.98 -1.34 23.12
F     .           2     84.01 -1.3  23.2
F     .           2     84.32 -1.48 23.65
F     .           3     84.1  -1.47 23.49
F     .           3     84.05 -1.45 23.55
F     .           3     83.68 -1.42 23.52
proc print;
proc glm; class trt rep;
model l a b= rep trt rep*trt;
test h=trt e=rep*trt;
means trt;
lsmeans trt/s p e=rep*trt;
run;
```

1.3 Proximate and cholesterol content analysis in the cooked pasta samples

```
options ls=100 ps=70;
data one;
input trt TestID$ rep    Moisture   Fat   Ash   Prot  Cholesterol CHO;
datalines;
trt    Test ID    rep   Moisture    Fat   Ash   Prot  Cholesterol CHO
0     C002        1     68.73       0.10  0.24  5.10  0.74  25.84
0     C003        2     68.43       0.10  0.21  5.08  0.00  26.18
0     C004        3     71.47       0.27  0.20  4.66  0.00  23.40
10    10H1ACT1    1     71.03       0.26  0.24  6.74  6.89  21.74
10    10H1ACT2    2     67.72       0.19  0.30  7.21  7.64  24.57
10    10H1ACT3    3     65.12       0.53  0.30  7.36  6.84  26.69
30    30H2ACT1    1     62.95       1.17  0.71  14.19 30.72 20.99
30    30H2ACT2    2     63.07       0.62  0.60  13.64 30.53 22.08
30    30H2ACT3    3     61.06       2.11  0.51  12.27 23.58 24.05
proc print;
proc glm; class trt rep;
model Moisture    Fat   Ash   Prot  Cholesterol CHO=rep trt rep*trt;
test h=trt e=rep*trt;
means trt;
lsmeans trt/s p e=rep*trt;
run;
```

1.4 Coenzyme Q_{10} content in the newly formulated pasta samples (before and after cooking)

```
options ls=100 ps=70;
data one;
input Sample$     MC    Q101  Q10;
conc=substr(sample,1,2);
TM=substr(sample,3,2);
rep=substr(sample,5,1);
datalines;
30BC1       2.825 13.8  14.20
30BC1       2.825 13.5  13.89
30BC2       1.96  9     9.18
30BC2       1.96  8.9   9.08
30BC3       2.83  13.3  13.69
30BC3       2.83  12.1  12.45
10BC1       2.07  4.2   4.29
10BC1       2.07  3.4   3.47
10BC2       2.405 4.7   4.82
10BC2       2.405 4.9   5.02
10BC3       1.615 4.8   4.88
10BC3       1.615 5.7   5.79
30AC1       3.83  13.5  14.04
30AC1       3.83  12.9  13.41
30AC2       1.37  8.2   8.31
30AC2       1.37  8.2   8.31
30AC3       1.43  11.4  11.57
30AC3       1.43  11.9  12.07
10AC1       1.1   3.7   3.74
10AC1       1.1   3.8   3.84
10AC2       2.575 4.1   4.21
10AC2       2.575 4.9   5.03
10AC3       1.77  4.6   4.68
10AC3       1.77  4     4.07
proc print;
proc glm; class rep conc tm;
model q10=rep conc|tm;
means conc|tm;
lsmeans conc|tm/s p;
run;
```

1.5 Vibrational spectral data and texture attributes

1.5.1 FT–IR analysis

```
options ls=100 ps=70;
data one;
input trt   ID$         p2926 p1740 p1640 p1541 p1417 p1242 p1150 p1080
      p999  p926 Hardness     Cohesiveness      Adhesiveness
      Springiness Chewiness   Firmness;
datalines;
0     C001        0.2976      0.0524      0.5227      0.2058
      0.1517      0.0715      0.2592      0.3282      0.4914      0.075
      1037.96     0.49        -113.10     0.78
      397.12      81.86
0     C002        0.3188      0.0457      0.4184      0.179 0.1652
      0.0865      0.3553      0.4446      0.9079      0.1346
      1037.96     0.49        -113.10     0.78        397.12      81.86
0     2CACT001    0.3707      0.0594      0.4256      0.2016
      0.1806      0.0959      0.3687      0.4694      0.9312
      0.1559      1426.43     0.47        -112.51     0.93  625.33
      63.16
0     2CACT002    0.3035      0.042       0.3873      0.1707
      0.1627      0.0848      0.3444      0.4388      0.9324      0.15
      1426.43     0.47        -112.51     0.93  625.33      63.16
0     3CACT001    0.3478      0.0473      0.5044      0.1984
      0.1874      0.0966      0.3826      0.4859      0.8293      0.151
      1094.92     0.44        -138.75     0.89  426.20      55.48
0     3CACT002    0.3232      0.0442      0.443       0.1709
      0.1696      0.0869      0.3626      0.4614      0.8656
      0.1431      1094.92     0.44        -138.75     0.89  426.20
      55.48
10    10H1ACT1    0.3599      0.0639      0.4759      0.1805
      0.1677      0.0915      0.3535      0.4559      0.7853
      0.1138      1285.39     0.40        -45.17      0.93  476.33
      67.06
10    10H1ACT2    0.3447      0.0546      0.5019      0.2031
      0.1692      0.0909      0.3466      0.4259      0.6634
      0.1041      1285.39     0.40        -45.17      0.93  476.33
      67.06
10    10H2ACT1    0.3513      0.0437      0.6445      0.299 0.1618
      0.0874      0.1867      0.2558      0.3945      0.0502
      1855.16     0.43        -78.07      0.87        689.12
      107.06
10    10H2ACT2    0.2604      0.0399      0.5248      0.1986
      0.1197      0.0594      0.1723      0.2259      0.2823
      0.0463      1855.16     0.43        -78.07      0.87  689.12
      107.06
10    10H3ACT1    0.3209      0.0487      0.5733      0.2334
      0.1565      0.0865      0.2265      0.322       0.5221      0.106
      1900.26     0.43  -137.46           0.84  699.69      95.66
10    10H3ACT2    0.2511      0.0478      0.5556      0.2467
      0.1251      0.0732      0.1391      0.1679      0.172 0.0425
      1900.26     0.43        -137.46     0.84        699.69      95.66
30    30H1001     0.4335      0.0567      0.5927      0.3407
      0.2043      0.1212      0.3236      0.4189      0.5673
```

```
      0.0514      3856.43     0.49        -2.79       0.81  1528.16
      236.89
30    30H1002     0.4387      0.0483      0.5887      0.3245
      0.1969      0.1027      0.3292      0.4232      0.6293      0.048
      3856.43     0.49        -2.79 0.81  1528.16     236.89
30    30H2ACT1    0.2521      0.0403      0.558       0.2727
      0.1318      0.0763      0.1485      0.1858      0.1932      0.043
      4195.24     0.47        -4.97       0.94  1841.18     294.49
30    30H2ACT2    0.2983      0.044       0.6575      0.3719
      0.1779      0.1162      0.1644      0.2039      0.186 0.0403
      4195.24     0.47        -4.97       0.94        1841.18
      294.49
30    30H3ACT1    0.4313      0.078       0.4608      0.2306
      0.1734      0.0841      0.3695      0.4505      0.7985
      0.0772      3550.98     0.46        -30.19      0.95  1559.78
      213.96
30    30H3ACT2    0.4503      0.0834      0.4006      0.1982
      0.1869      0.0985      0.391       0.479       0.9283
      0.1565      3550.98     0.46        -30.19      0.95  1559.78
      213.96

proc print;
proc reg;
model hardness=   p2926 p1740 p1640 p1541 p1417 p1242 p1150 p1080 p999
      p926/selection=rsquare cp;
run;
proc reg;
model hardness=   p2926 p1740 p1640 p1541 p1417 p1242 p1150 p1080 p999
      p926/selection=stepwise ;
run;

proc reg;
model Cohesiveness =    p2926 p1740 p1640 p1541 p1417 p1242 p1150 p1080
      p999  p926/selection=rsquare cp;
run;
proc reg;
model Cohesiveness =    p2926 p1740 p1640 p1541 p1417 p1242 p1150 p1080
      p999  p926/selection=stepwise ;
run;

proc reg;
model Adhesiveness =    p2926 p1740 p1640 p1541 p1417 p1242 p1150 p1080
      p999  p926/selection=rsquare cp;
run;
proc reg;
model Adhesiveness =    p2926 p1740 p1640 p1541 p1417 p1242 p1150 p1080
      p999  p926/selection=stepwise ;
run;

proc reg;
model Springiness =     p2926 p1740 p1640 p1541 p1417 p1242 p1150 p1080
      p999  p926/selection=rsquare cp;
run;
```

```
proc reg;
model Springiness =     p2926 p1740 p1640 p1541 p1417 p1242 p1150 p1080
      p999  p926/selection=stepwise ;
run;

proc reg;
model Chewiness = p2926 p1740 p1640 p1541 p1417 p1242 p1150 p1080 p999
      p926/selection=rsquare cp;
run;
proc reg;
model Chewiness = p2926 p1740 p1640 p1541 p1417 p1242 p1150 p1080 p999
      p926/selection=stepwise ;
run;

proc reg;
model Firmness =  p2926 p1740 p1640 p1541 p1417 p1242 p1150 p1080 p999
      p926/selection=rsquare cp;
run;
proc reg;
model Firmness =  p2926 p1740 p1640 p1541 p1417 p1242 p1150 p1080 p999
      p926/selection=stepwise ;
run;
```

1.5.2 Raman analysis

```
options ls=100 ps=70;
data one;
input trt   ID$   p480  p823  p845  p870  p940  p1005 p1085 p1127 p1260
      p1340 p1460 p1653 p1673 p1685 p503  p525  p550  p640  p2520 p2530
      p2545 p2555 p2575 Hardness    Cohesiveness      Adhesiveness
      Springiness Gumminess   Chewiness   Firmness;
datalines;
0     C002  0.442 0.2668      0.4727      0.6807      0.353 0.385
      0.3964      0.376       0.3559      0.3701      0.381 0.337
      0.3485      0.3861      0.3337      0.2833      0.3234
      0.3893      0.094       0.0837      0.0926      0.111 0.114
      809.82      0.51        -63.01      0.67        415.75
      278.83      78.98
0     C003 0.4442 0.2586      0.4605      0.6506      0.3576
      0.3618      0.3633      0.304       0.3284      0.3747
      0.3831      0.2848      0.3412      0.3329      0.3552
      0.2551      0.2958      0.3522      0.1003      0.0839
      0.1213      0.0878      0.0979      1306.59     0.49  -144.15
      0.84        645.45      544.39      76.55
0     C004 0.4477 0.2862      0.4727      0.676       0.3642
      0.3912      0.3641      0.356       0.3722      0.367 0.3808
      0.3377      0.3473      0.3574      0.3422      0.2597
      0.3315      0.3927      0.1335      0.0892      0.1399
      0.1138      0.1272      997.46      0.45        -132.14     0.81
      453.20      368.16      90.05
0     2CACT001    0.5012      0.2887      0.4739      0.7012      0.428
      0.4491      0.4554      0.3977      0.3429      0.401
      0.3984      0.3262      0.3555      0.3772      0.3251
      0.2597      0.3105      0.3734      0.1279      0.1069
```

```
      0.1282      0.1094      0.1296      1477.04     0.48        -
121.12      0.91        708.77      642.30      61.99
0     2CACT002    0.5051      0.281       0.4753      0.6567
      0.3365      0.3993      0.3935      0.3502      0.3324
      0.3917      0.4062      0.302       0.3534      0.3376
      0.3715      0.2601      0.339       0.3968      0.1312
      0.1114      0.1443      0.1249      0.1206      1317.88     0.47
      -87.59      0.95        613.82      580.70      66.18
0     2CACT003    0.5218      0.256       0.5153      0.6832
      0.4022      0.3966      0.3762      0.3688      0.3237
      0.3797      0.3876      0.3191      0.3622      0.3673
      0.3646      0.2506      0.3119      0.4124      0.1031
      0.0974      0.1398      0.1092      0.1351      1484.37     0.47
      -128.81     0.94        695.78      653.00      61.32
0     3CACT001    0.5051      0.281       0.4753      0.6567
      0.3365      0.3993      0.3935      0.3502      0.3324
      0.3917      0.4062      0.302       0.3534      0.3376
      0.3715      0.2601      0.339       0.3968      0.0908
      0.0751      0.0791      0.0706      0.1039      1170.80     0.43
      -99.88      0.95        506.19      478.96      48.81
0     3CACT002    0.5051      0.281       0.4753      0.6567
      0.3365      0.3993      0.3935      0.3502      0.3324
      0.3917      0.4062      0.302       0.3534      0.3376
      0.3715      0.2601      0.339       0.3968      0.0875
      0.0713      0.0809      0.0765      0.0658      1091.52     0.43
      -152.16     0.86        474.70      406.75      59.46
0     3CACT003    0.5051      0.281       0.4753      0.6567
      0.3365      0.3993      0.3935      0.3502      0.3324
      0.3917      0.4062      0.302       0.3534      0.3376
      0.3715      0.2601      0.339       0.3968      0.0631
      0.0455      0.0751      0.0584      0.0691      1022.46     0.44
      -164.22     0.87        450.35      392.91      58.17
10    10H1ACT1    0.3549      0.2707      0.4544      0.623 0.294
      0.3725      0.2883      0.2713      0.2857      0.3403      0.347
      0.3017      0.3345      0.3281      0.2991      0.2276
      0.3031      0.3709      0.0593      0.0305      0.0513
      0.0553      0.0497      1120.90     0.39  -36.91      0.92
      432.31      396.11      65.66
10    10H1ACT2    0.2568      0.2863      0.4927      0.6376
      0.2702      0.3747      0.3264      0.2948      0.3195
      0.2931      0.3204      0.3025      0.3298      0.3419
      0.3213      0.2149      0.3203      0.3753      0.0872
      0.0754      0.0781      0.0661      0.0865      1400.06     0.40
      -43.27      0.94        560.56      529.26      58.08
10    10H1ACT3    0.2915      0.279       0.4499      0.6027
      0.2962      0.3658      0.2875      0.3017      0.2808
      0.3191      0.315       0.2914      0.3325      0.3304
      0.2876      0.2228      0.2859      0.3807      0.1031
      0.0913      0.1222      0.1111      0.1082      1335.21     0.41
      -55.33      0.92        545.38      503.61      77.44
10    10H2ACT1    0.3413      0.2071      0.4409      0.5938
      0.2759      0.3217      0.2714      0.2193      0.291 0.3599
      0.2975      0.2528      0.2392      0.2681      0.2512
      0.1863      0.2413      0.3346      0.1251      0.1177
```

```
      0.1369      0.1415      0.1464      2104.28     0.42  -89.13
      0.84        882.98      737.68      97.52
10    10H2ACT2    0.3751      0.2668      0.477       0.6425
      0.3336      0.3361      0.3416      0.3596      0.3184
      0.3282      0.309       0.2837      0.2961      0.326 0.2665
      0.2671      0.3358      0.3824      0.1446      0.1296
      0.1626      0.1388      0.1596      1871.38     0.43  -73.45
      0.87        813.51      704.66      106.67
10    10H2ACT3    0.397       0.3194      0.5156      0.7184
      0.3388      0.4179      0.3761      0.3582      0.3927
      0.3729      0.4126      0.3537      0.3791      0.3871
      0.3529      0.2554      0.3743      0.4351      0.1378
      0.1228      0.1636      0.1482      0.1538      1589.83     0.43
      -71.63      0.92        680.17      625.01      116.98
10    10H3ACT1    0.3992      0.3604      0.534       0.6956
      0.4015      0.486       0.4262      0.3867      0.3985
      0.4224      0.4388      0.4115      0.4228      0.3977
      0.3436      0.3223      0.393       0.4651      0.1035
      0.1041      0.0987      0.0869      0.1011      2272.66     0.45
      -169.67     0.87        1015.34     882.64      96.51
10    10H3ACT2    0.3772      0.3417      0.516       0.688 0.374
      0.4174      0.454       0.4238      0.341       0.3458
      0.3643      0.3559      0.3598      0.3487      0.346 0.275
      0.3541      0.3966      0.1517      0.1593      0.1493
      0.1588      0.1997      1597.14     0.42        -99.91      0.84
      677.28      571.90      99.98
10    10H3ACT3    0.3274      0.3073      0.5017      0.64  0.3382
      0.3887      0.3287      0.3342      0.2993      0.3418
      0.3352      0.326       0.3661      0.3542      0.2722
      0.2434      0.3289      0.3596      0.1069      0.131 0.1615
      0.1208      0.1542      1830.98     0.43        -142.82     0.82
      787.67      644.53      90.50
30    30H1001     0.4314      0.1537      0.3584      0.5576      0.206
      0.3453      0.221       0.2668      0.266 0.2756      0.2775
      0.2227      0.2633      0.2352      0.2217      0.2167
      0.2232      0.3466      0.109       0.1038      0.1137
      0.1038      0.1084      4066.50     0.48  -6.21 0.83
      1955.60     1617.55     113.94
30    30H1002     0.3703      0.1679      0.3382      0.53  0.24
      0.2741      0.2185      0.2105      0.2241      0.2834
      0.2308      0.1874      0.1959      0.2128      0.2901
      0.2114      0.2232      0.2978      0.108       0.0835      0.113
      0.1152      0.0977      3647.93     0.50  -0.74 0.78
      1809.94     1416.29     316.61
30    30H1003     0.2527      0.1854      0.4269      0.5992
      0.1965      0.3033      0.1811      0.1779      0.1592
      0.2417      0.2234      0.1951      0.2716      0.2073
      0.1634      0.1567      0.1886      0.3246      0.0999
      0.0812      0.104       0.0795      0.087       3854.87     0.48
      -1.42       0.83        1858.59     1550.65     280.11
30    30H2ACT1    0.2971      0.1475      0.4079      0.5734
      0.1832      0.3641      0.2564      0.2385      0.2682
      0.3231      0.2892      0.2762      0.2941      0.3187
      0.2062      0.1758      0.2819      0.3517      0.0938
```

```
      0.0994      0.1145      0.0963      0.1231      4113.82     0.47
      -7.19       0.94        1931.39     1806.27     304.29
30    30H2ACT2    0.301       0.2489      0.4556      0.6108      0.293
      0.3601      0.2663      0.2825      0.3245      0.352
      0.3543      0.3145      0.3407      0.343 0.3197      0.2252
      0.3159      0.398       0.0983      0.0835      0.1189
      0.1053      0.0938      4482.29     0.47  -4.96 0.95
      2119.57     2011.46     301.57
30    30H2ACT3    0.3147      0.2962      0.4978      0.6645
      0.3152      0.4433      0.3009      0.2962      0.2907
      0.3497      0.334       0.2861      0.3233      0.3268
      0.2949      0.2969      0.3137      0.3856      0.0983
      0.0835      0.1189      0.1053      0.0938      3989.59     0.46
      -2.76 0.93  1838.68     1705.82     277.61
30    30H3ACT1    0.3535      0.2448      0.4579      0.646 0.3122
      0.3458      0.2614      0.2831      0.2635      0.304 0.3045
      0.2863      0.249       0.2642      0.2541      0.1847
      0.2897      0.3228      0.0983      0.0835      0.1189
      0.1053      0.0938      3374.06     0.46  -19.21      0.96
      1549.10     1482.49     239.21
30    30H3ACT2    0.3451      0.2281      0.4776      0.7009      0.32
      0.3823      0.3184      0.3015      0.3077      0.3204
      0.3488      0.2729      0.3058      0.314 0.3113      0.2256
      0.3053      0.3597      0.1318      0.1181      0.1458
      0.1508      0.1499      3428.21     0.46  -32.12      0.96
      1586.04     1520.37     204.86
30    30H3ACT3    0.3949      0.2588      0.4542      0.6954
      0.3157      0.3977      0.2929      0.2933      0.3232
      0.3646      0.3365      0.3461      0.3386      0.3463
      0.3066      0.2279      0.2919      0.3644      0.1336
      0.1336      0.1326      0.1376      0.1286      3850.67     0.47
      -39.23      0.93  1795.63     1676.49     197.82
```

```
proc print;
proc reg;
model hardness=   p480  p823  p845  p870  p940  p1005 p1085 p1127 p1260
      p1340 p1460 p1653 p1673 p1685 p503  p525  p550  p640  p2520 p2530
      p2545 p2555 p2575/selection=rsquare cp;
run;
proc reg;
model hardness=   p480  p823  p845  p870  p940  p1005 p1085 p1127 p1260
      p1340 p1460 p1653 p1673 p1685 p503  p525  p550  p640  p2520 p2530
      p2545 p2555 p2575/selection=stepwise ;
run;

proc reg;
model Cohesiveness =    p480  p823  p845  p870  p940  p1005 p1085 p1127
      p1260 p1340 p1460 p1653 p1673 p1685 p503  p525  p550  p640  p2520
      p2530 p2545 p2555 p2575/selection=rsquare cp;
run;
proc reg;
model Cohesiveness =    p480  p823  p845  p870  p940  p1005 p1085 p1127
      p1260 p1340 p1460 p1653 p1673 p1685 p503  p525  p550  p640  p2520
      p2530 p2545 p2555 p2575/selection=stepwise ;
run;
```

```
proc reg;
model Adhesiveness =    p480  p823  p845  p870  p940  p1005 p1085 p1127
      p1260 p1340 p1460 p1653 p1673 p1685 p503  p525  p550  p640  p2520
      p2530 p2545 p2555 p2575/selection=rsquare cp;
run;
proc reg;
model Adhesiveness =    p480  p823  p845  p870  p940  p1005 p1085 p1127
      p1260 p1340 p1460 p1653 p1673 p1685 p503  p525  p550  p640  p2520
      p2530 p2545 p2555 p2575/selection=stepwise ;
run;


proc reg;
model Springiness =     p480  p823  p845  p870  p940  p1005 p1085 p1127
      p1260 p1340 p1460 p1653 p1673 p1685 p503  p525  p550  p640  p2520
      p2530 p2545 p2555 p2575/selection=rsquare cp;
run;
proc reg;
model Springiness =     p480  p823  p845  p870  p940  p1005 p1085 p1127
      p1260 p1340 p1460 p1653 p1673 p1685 p503  p525  p550  p640  p2520
      p2530 p2545 p2555 p2575/selection=stepwise ;
run;

proc reg;
model Chewiness = p480  p823  p845  p870  p940  p1005 p1085 p1127 p1260
      p1340 p1460 p1653 p1673 p1685 p503  p525  p550  p640  p2520 p2530
      p2545 p2555 p2575/selection=rsquare cp;
run;
proc reg;
model Chewiness = p480  p823  p845  p870  p940  p1005 p1085 p1127 p1260
      p1340 p1460 p1653 p1673 p1685 p503  p525  p550  p640  p2520 p2530
      p2545 p2555 p2575/selection=stepwise ;
run;

proc reg;
model Firmness =  p480  p823  p845  p870  p940  p1005 p1085 p1127 p1260
      p1340 p1460 p1653 p1673 p1685 p503  p525  p550  p640  p2520 p2530
      p2545 p2555 p2575/selection=rsquare cp;
run;
proc reg;
model Firmness =  p480  p823  p845  p870  p940  p1005 p1085 p1127 p1260
      p1340 p1460 p1653 p1673 p1685 p503  p525  p550  p640  p2520 p2530
      p2545 p2555 p2575/selection=stepwise ;
run;
```

APPENDIX 2

THE PREPARATION OF AMMONIUM ACETATE BUFFER, pH 4.4

2.1 Calculation: how much molarity of ammonium acetate and acetic acid are needed to make 1 M buffer at pH 4.4?

2.1.1 Method 1

M of acid + M of salt = M of buffer

$$\text{pH} = \text{p}K_a + \log\frac{[Salt]}{[Acid]}$$

Let y = M of salt

$\therefore$ M of acid = M of buffer $- y$

$= 1 - y$

Since, pH = 4.4, $\text{p}K_a = 4.76$

Therefore,
$$4.4 = 4.76 + \log\frac{[y]}{[1-y]}$$

$$-0.36 = \log\frac{[y]}{[1-y]}$$

$$0.437 = \frac{[y]}{[1-y]}$$

$$y = 0.437 - 0.437y$$

$$y = 0.304$$

$\therefore$ M of ammonium acetate = 0.304

Since, M of acetic acid = $1 - y$

$\therefore$ M of acetic acid = $1 - 0.304 = 0.696$

2.1.2 Method 2

$$\text{pH} = \text{pK}_a + \log\frac{[A]}{[AH]}$$

Therefore, $4.4 = 4.76 + \log\frac{[A]}{AH}$

$$-0.36 = \log\frac{[A]}{AH}$$

$$\frac{[A]}{AH} = 0.437$$

$$[A] = 0.437[AH]$$

Since $[A] + [AH] = [\text{Buffer}]$

$$[AH] + 0.437[AH] = 1$$

$$[AH] = \frac{1}{1.437} = 0.696$$

$$\therefore \quad [A] = 0.437 \times 0.696 = 0.304$$

2.2 Calculation: how many milliliters of acetic acid and how many grams of ammonium acetate must be added to prepare 1 L of the buffer?

$g = M \times MW$; MW of acetic acid = 60.05

$= 0.696 \times 60.05 = 41.7948$

$D = M/V \quad \therefore \quad V = M/D$

$$V = \frac{41.7948}{1.05}$$

$= 39.80$ mL

Therefore, the needed volume of acetic acid to prepare 1 M ammonium acetate buffer is 39.80 mL for making 1 L of the buffer

g	=	M × MW	; MW of ammonium acetate = 77.08
	=	0.304 × 77.08	= 23.432

Therefore, the volume of ammonium acetate needed to prepare 1 M ammonium acetate buffer is 23.432 g for making 1 L of the buffer

2.3 Preparation of 1 M ammonium acetate buffer

Approximately 2.3432 g of ammonium acetate (Sigma–Aldrich, Inc., St. Louis, Mo.) were accurately weighed, transferred into a 100 mL volumetric flask that filled with HPLC grade water (Sigma–Aldrich, Inc., St. Louis, Mo.) around one fourth of the flask, and mixed well. Afterwards, 3.98 mL acetic acid (Glacial, Fisher Scientific, Fairlawn, N.J.) were slowly added into the flask before making to the volume with the HPLC water. The pH of ammonium acetate buffer was ensured at 4.4 using a pH meter (Model 230A, Fisher Scientific, Fairlawn, N.J.). Finally, the buffer was filtered through a filter paper (Whatman #4, Whatman International Ltd., England) before use.

BIBLIOGRAPHY

ADA's Public Relations Team. 2004a. Visualize the right portion size. http://www.eatright.org/cps/rde/xchg/ada/hs.xsl/home_4367_ENU_HTML.htm. Accessed 2008 Oct 13.

ADA's Public Relations Team. 2004b. Pasta in just the right amounts. http://www.eatright.org/cps/rde/xchg/ada/hs.xsl/home_4050_ENU_HTML.htm. Accessed 2008 Oct 13.

Aguilaniu H, Durieux J, Dillin A. 2005. Metabolism, ubiquinone synthesis, and longevity. Genes Dev 19:2399–406.

Alizadeh–Pasdar N, Nakai S, Li–Chan ECY. 2002. Principal component similarity analysis of Raman spectra to study the effects of pH, heating, and *K*–carrageenan on whey protein structure. J Agric Food Chem 50:6042–52.

Anonymous. 2005. About gluten. http://www.perten.com/pages/ProductPage____415.aspx?epslanguage=EN. Accessed 2008 July 15.

Anonymous. 2007. Electron transport phosphorylation. http://trc.ucdavis.edu/biosci10v/bis10v/week3/06electrontransport.html. Accessed 2008 July 15.

AOAC International. 2006. Official methods of analysis of AOAC international, 18th edition. Washington, DC: Association of Official Analytical Chemists.

Arboleda PH, Loppnow GR. 2000. Raman spectroscopy as a discovery tool in carbohydrate chemistry. Anal Chem 72(9):2093–8.

Baranska M, Schulz H, Baranski R, Nothnagel T, Christensen LP. 2005. In situ simultaneous analysis of polyacetylenes, carotenoids and polysaccharides in carrot roots. J Agric Food Chem 53 (17):6565–71.

Barbieri B, Lund B, Lundstrom B, Scaglione F. 1999. Coenzyme Q10 administration increases antibody titer in hepatitis B vaccinated volunteers–A single blind placebo–controlled and randomized clinical study. Biofactors 9:351–7.

Beattie RJ, Bell SJ, Farmer LJ, Moss BW, Patterson D. 2004 Preliminary investigation of the application of Raman spectroscopy to the prediction of the sensory quality of beef silverside. Meat Sci 66(4):903−13.

Bouraoui M, Nakai S, Li–Chan E. 1997. In situ investigation of protein structure in Pacific whiting surimi and gels using Raman spectroscopy. Food Res Int 30 (1):65–72.

Bourne MC. 1978. Texture profile analysis. Food Technol 32(7):62–6, 72.

Bourne MC. 2002a. Principles of objective texture measurement. In: Bourne MC, editor. Food texture and viscosity: concept and measurement. 2nd ed. California: Academic Press. p 107–88.

Bourne MC. 2002b. Texture, viscosity, and food. In: Bourne MC, editor. Food texture and viscosity: concept and measurement. 2nd ed. California: Academic Press. p 1–32.

Bulkin BJ, Kwak Y, Dea ICM. 1987. Retrogradation kinetics of waxy–corn and potato starches; a rapid Raman–spectroscopic study. Carbohyd Res 160:95–112.

Business trend analysis. 2006. [Report] The 2006 U.S. pasta market outlook (with pasta forecasts through 2014). The infoshop's market research reports online catalog home page, http://www.the-infoshop.com/pdf/bta37956.pdf. Accessed 2008 July 22.

Celedon A, Aguilera JM. 2002. Applications of microprobe Raman spectroscopy in food science. Food Sci Tech Int 8(2):101–8.

Chen M, Irudayaraj J. 1998. Sampling technique for cheese analysis by FTIR spectroscopy. J Food Sci 63(1):96−9.

Choi S–M, Ma C–Y. 2007. Structure characterization of globulin from common buckwheat (*Fagopyrum esculentum* Moench) using circular dichroism and Raman spectroscopy. Food Chem 102:150–60.

Choi J–H, Ryu Y–W, Seo JH. 2005. Biotechnological production and applications of coenzyme Q_{10}. Appl Microbiol Biot 68(1):9–15.

Cole ME. 1991. Review: Prediction and measurement of pasta quality. Int J Food Sci Technol 26(2):133–51.

Conklin KA. 2000. Dietary antioxidant during cancer chemotherapy: impact on chemotherapeutic effectiveness and development of side effects. Nutr Cancer 37(1):1–18.

Cremer D, Kaletunç G. 2003. Fourier transform infrared microspectroscopic study of the chemical microstructure of corn and oat flour−based extrudates. Carbohyd Polym 52:53−65.

Cui SW, Phillips GO, Blackwell B, Nikiforuk J. 2007. Characterization and properties of Acacia senegal (L.) Willd. var. senegal with enhanced properties (Acacia (sen) SUPERGUM^{TM}): Part 4. Spectroscopic characterization of Acacia senegal var. senegal and Acacia (sen) SUPERGUM^{TM} arabic. Food Hydrocolloid 21(3):347−52.

Cupp MJ, Tracy TS. 2003. Coenzyme Q10 (ubiquinone, ubidecarenone). In: Cupp MJ, Tracy TS, editors. Dietary supplements: toxicology and clinical pharmacology. New Jersey: Humana Press Inc. p 53–85.

Damodaran S. 1996. Amino acids, peptides, and proteins. In: Fennema OR, editor. Food Chemistry. 3rd ed. New York: Marcel Dekker, Inc. p 321–429.

Department of Horticulture and Crop Science, the Ohio State University. n.d. Seed ID workshop. Members of the *Poaceae* family home page, http://www.oardc.ohio-state.edu/seedid/family.asp?family=Poaceae. Accessed 2008 July 15.

Desmond EM, Kenny TA. 1998. Preparation of surimi–like extract from beef hearts and its utilization in frankfurters. Meat Sci 50(1):81–9.

DiMauro S, Quinzii CM, Hirano M. 2007. Mutations in coenzyme Q_{10} biosynthesis genes. J Clin Invest 117(3):587–9.

Ellis DI, Broadhurst D, Clarke SJ, Goodacre R. 2005. Rapid identification of closely related muscle foods by vibrational spectroscopy and machine learning. Analyst 130(12):1648−54.

Fechner PM, Wartewig S, Kleinebudde P, Neubert RHH. 2005. Studies of the retrogradation process for various starch gels using Raman spectroscopy. Carbohydr Res 340(16):2563–8.

Foegeding EA, Lanier TC, Hultin HO. 1996. Characteristics of edible muscle tissues. In: Fennema OR, editor. Food chemistry, 3rd ed. New York: Marcel Dekker, Inc. p 879–942.

Gelencsér T, Gál V, Hódsági M, Salgó A. 2008. Evaluation of quality and digestibility characteristics of resistant starch–enriched pasta. Food Bioprocess Technol 1(2):171–9.

Georget DMR, Belton PS. 2006. Effects of temperature and water content on the secondary structure of wheat gluten studied by FT–IR spectroscopy. Biomacromolecules 7(2):469–75.

Gujral HS and Pathak A. 2002. Effect of composite flours and additives on the texture of chapati. J Food Eng 55(2):173–9.

Haris PI. 2000. Fourier transform infrared spectroscopic studies of peptides: Potentials and pitfalls. In: Singh BR, editor. Infrared analysis of peptides and proteins: Principles and application. American Chemistry Society Symposium Series 750. District of Columbia: American Chemical Society. p 54–95.

Herrero AM. 2008. Raman spectroscopy a promising technique for quality assessment of meat and fish: A review. Food Chem 107(4):1642−51.

Hodges S, Hertz N, Lockwood K, Lister R. 1999. CoQ10: could it have a role in cancer management? Biofactors 9:365–70.

Howell NK, Arteaga G, Nakai S, Li–Chan ECY. 1999. Raman spectral analysis in the C–H stretching region of proteins and amino acids for investigation of hydrophobic interactions. J Agric Food Chem 47(3):924–33.

Iizuka K, Aishima T. 1999. Tenderization of beef with pineapple juice monitored by Fourier transform infrared spectroscopy and chemometric analysis. J Food Sci 64(6):973–7.

Jones K. 2004. Raman spectroscopy. http://www.chemsoc.org/ExemplarChem/entries/2004/birmingham_jones/raman.html. Accessed 2008 July 15.

Kagan VE, Quinn PJ. 2000. Coenzyme Q: Molecular mechanisms in health and disease. Florida: CRC Press. 390 p.

Kagan VE, Nohl H, Quinn PJ. 1996. Coenzyme Q: its role in scavenging and generation of radicals in membranes. In: Cadenas E, Packer L, editors. Handbook of antioxidants. New York: Marcel Dekker, Inc. p 157–201.

Kamei M, Fujita T, Kanbe T, Sasaki K, Oshiba K, Otani S, Matsui–Yuasa I, Morisawa S. 1985. The distribution and content of ubiquinone in foods. Int J Vit Nutr Res 56:57–63.

Kill RC. 2001. Introduction. In: Kill RC, Turnbull K, editors. Pasta and semolina technology. Iowa: Blackwell Science Company. p 1–10.

Kim S–H, Huang Y–W, Carpenter JA. 1990. Effect of surimi addition to fresh pasta on ultra–structure and cooked firmness. J Food Sci 55(5):1481–2, 1484.

Kimbaris AC, Siatis NG, Pappas CS, Tarantilis PA, Daferera DJ, Polissiou MG. 2006. Quantitative analysis of garlic (*Allium sativum*) oil unsaturated acyclic components using FT−Raman spectroscopy. Food Chem 94(2):287−95.

Kishi T, Takahashi T, Okamoto T. 1999. Coenzyme–Q redox cycle as an endogenous antioxidant. In: Packer L, Hiramatsu M, Yoshikawa T, editors. Antioxidant food supplements in human health. California: Academic Press. p 165–82.

Kitts DD. n.d. Amino acids, proteins and enzymes: wheat protein. http://www.landfood.ubc.ca/courses/fnh/301/protein/protq4.htm. Accessed 2008 July 15.

Knightly WH. 1981. Shortening systems: fats, oils, and surface–active agents – present and future. Cereal Chem 58(3):171–4.

Koning MMG, Visser H. 1992. Protein interactions, an overview. In: Visser H, editor. Protein interactions. New York: VCH Publishers. p 1–24.

Lachenmeier DW. 2007. Rapid quality control of spirit drinks and beer using multivariate data analysis of Fourier transform infrared spectra. Food Chem 101(2):825−32.

Langsjoen PH, Langsjoen AM. 1999. Overview of the use of CoQ10 in cardiovascular disease. Biofactors 9(2–4):273–84.

Lasztity R. 1996. Wheat proteins. In: Lasztity R, editor. The chemistry of cereal proteins. 2nd ed. New York: CRC Press, Inc. p 19–138.

Lawless HT. 1995. Commentaries to Francis FJ; Quality as influenced by color. Food Qual Pref 6(3):149–55.

Lee DC, Haris PI, Chapman D, Mitchell RC. 1990. Determination of protein secondary structure using factor analysis of infrared spectra. Biochemistry 29(39):9185–93.

Leon AE, Ribotta PD, Ausar SF, Fernandez C, Landa CA, Beltramo DM. 2000. Interactions of different carrageenan isoforms and flour components in breadmaking. J Agric Food Chem 48(7):2634–38.

Li–Chan ECY. 1996. The applications of Raman spectroscopy in food science. Trends Food Sci Tech 7(11):361–70.

Li–Chan E, Nakai S, Hirotsuka M. 1994. Raman spectroscopy as a probe of protein structure in food systems. In: Yada RY, Jackman RL, Smith JL, editors. Protein structure–function relationships in foods. New York: Blackie Academic & Professional, an imprint of Chapman & Hall. p 163–97.

Lin M, Al–Holy M, Chang S–S, Huang Y, Cavinato AG, Kang D–H, Rasco BA. 2005. Detection of *Alicyclobacillus* isolates in apple juice by Fourier transform infrared spectroscopy. Int J Food Microbiol 105(3):369–76.

Liu Q, Charlet G, Yelle S, Arul J. 2002. Phase transition in potato starch–water system I. Starch gelatinization at high moisture level. Food Res Int 35(4):397–407.

Lucisano M, Casiraghi EM, Barbieri R. 1984. Use of defatted corn germ flour in pasta products. J Food Sci 49(2):482–4.

Marcotte, E. 2005. Electron transport & oxidative phosphorylation. http://courses.cm.utexas.edu/emarcotte/ch339k/fall2005/Lecture-Ch19-1.html. Accessed 2008 July 15.

Marshall WE, Chrastil J. 1992. Interaction of food proteins with starch. In: Hudson BJF, editor. Biochemistry of Food Proteins. New York: Elsevier Science Publishers Ltd. p 75–97.

Mattila P, Kumpulainen J. 2001. Coenzyme Q_9 and Q_{10}: contents in foods and dietary intake. J Food Comp Anal 14(4):409–17.

Mattila P, Lehtonen M, Kumpulainen J, 2000. Comparison of in–line connected diode array and electrochemical detectors in the high–performance liquid chromatographic analysis of coenzymes Q9 and Q10 in food materials. J Agric Food Chem 48:1229–33.

Meng G, Chan JCK, Rousseau D, Li–Chan ECY. 2005. Study of protein–lipid interactions at the bovine serum albumin/oil interface by Raman microspectroscopy. J Agric Food Chem 53(4):845–52.

Miller MF, Keeton JT, Cross HR, Leu R, Gomez F, Wilson JJ. 1988. Evaluation of the physical and sensory properties of jerky processed from beef heart and tongue. J Food Qual 11(1):63–70.

Mohamed A, Gordon SH, Harry–O'Kuru RE, Palmquist DE. 2005. Phospholipids and wheat gluten blends: Interaction and kinetics. J Cereal Sci 41(3):259–65.

Munkholm H, Hansen HHT, Rasmussen K. 1999. Coenzyme Q10 treatment in serious heart failure. Biofactors 9:285–9.

National Academy of Sciences, Institute of Medicine, Food and Nutrition Board. 1997 − 2005. Dietary Reference Intakes: Recommended Intakes for Individuals. http://www.iom.edu/Object.File/Master/21/372/0.pdf. Accessed 2008 August 2.

Nelson DL, Cox MM. 2000. Oxidative phosphorylation and photophosphorylation. In: Nelson DL, Cox MM, editors. Lehninger principles of biochemistry. 3rd ed. New York: Worth Publishers. p 659–721.

O'Donnell CD. 2004a. NUTRA Solution: Functional futures: Exclusive R&D trends survey on functional foods and nutraceuticals. Prepared Foods 173(04):NS1–NS18.

O'Donnell CD. 2004b. NUTRA Solution: 2004 New products annual: Buying into bioactives. Prepared Foods 173(03):NS9–NS13.

Olivera DF, Salvadori VO. 2006. Textural characterization of lasagna made from organic whole wheat. Int J Food Sci Tech 41(Supplement 2):63–9.

Overvad K, Diamant B, Holm L, Holmer G, Mortensen SA, Stender S. 1999. Q_{10} in health and disease. Europ J Clin Nutr 53:764–70.

Ozaki Y, Cho R, Ikegaya K, Muraishi S, Kawauchi K. 1992. Potential of near−infrared Fourier transform Raman spectroscopy in food analysis. Appl Spectrosc 46(10):1503−7.

Papas AM. 1999. Other antioxidants. In: Papas AM, editor. Antioxidant status, diet, nutrition, and health. New York: CRC Press LLC. p 231–48.

Parkington JK, Xiong YL, Blanchard SP, Xiong S. 2000. Functionality changes in oxidatively/antioxidatively washed beef–heart surimi during frozen storage. J Food Sci 65(5):796–800.

Pasta P. 2004. Not only semolina or wheat flour. Professional pasta newsletter 25:34–45.

Pavia DL, Lampman GM, Kriz GS. 2001. Infrared spectroscopy. In: Pavia DL, Lampman GM, Kriz GS, editors. Introduction to spectroscopy. 3rd ed. USA: Thomson Learning, Inc. p 13–101.

Pezolet M, Bonenfant S, Dousseau F, Popineau Y. 1992. Conformation of wheat gluten proteins: comparison between functional and solution states as determined by infrared spectroscopy. FEBS Lett 299(3):247–50.

Pietzsch J. n.d. The importance of protein folding. Horizon Symposia home page, http://www.nature.com/horizon/proteinfolding/background/importance.html. Accessed 2008 July 15.

Popineau Y, Bonenfant S, Cornec M, Pezolet M. 1994. A Study by infrared spectroscopy of the conformations of gluten proteins differing in their gliadin and glutenin compositions. J Cereal Sci 20(1):15–22.

Purchas RW, Rutherfurd SM, Pearce PD, Vather R, Wilkinson BHP. 2004a. Concentrations in beef and lamb of taurine, carnosine, coenzyme Q_{10}, and creatine. Meat Sci 66(3):629–37.

Purchas RW, Rutherfurd SM, Pearce PD, Vather R, Wilkinson BHP. 2004b. Cooking temperature effects on the forms of iron and levels of several other compounds in beef semitendinosus muscle. Meat Sci 68(2):201−7.

Quinn PJ, Fabisiak JP. 1999. Expansion of antioxidant function of vitamin E by coenzyme Q. Biofactors 9(2–4):149–54.

Ramesh Yadav A, Mahadevamma S, Tharanathan RN, Ramteke RS. 2007. Characteristics of acetylated and enzyme–modified potato and sweet potato flours. Food Chem 103(4):1119–26.

Roberts WA Jr. 2004. Prepared for success. Prepared Foods 173(03):77–82.

Rosenthal AJ. 1999. Relation between instrumental and sensory measures of food texture. In: Rosenthal AJ, editor. Food texture: measurement and perception. Maryland: Aspen Publishers, Inc. p 1–17.

Rustin P, Munnich A, Rotig A. 2004. Mitochondrial respiratory chain dysfunction causes by coenzyme Q_{10} deficiency. Method Enzymol. 382:81–8.

Schoppet EF, Sinnamon HI, Talley FB, Panzer CC, Aceto NC. 1976. Enrichment of pasta with cottage cheese whey proteins. J Food Sci 41(6):1297–300.

Shogren RL, Hareland GA, Wu YV. 2006. Sensory evaluation and composition of spaghetti fortified with soy flour. J Food Sci 71(6):S428–32.

Singh BR. 2000. Basic aspects of the technique and applications of infrared spectroscopy of peptides and proteins. In: Singh BR, editor. Infrared analysis of peptides and proteins: Principles and application. American Chemical Society Symposium Series 750. District of Columbia: American Chemical Society. p 2–37.

Skoog DA, Holler EJ, Nieman TA. 1998. Raman spectroscopy. In: Skoog DA, Holler EJ, Nieman TA, editors. Principles of instrumental analysis. 5th ed. Chicago: Harcourt Brace & Company. p 429–44.

Smith A. 1999. Starch−based foods. In: Rosenthal AJ, editor. Food texture: measurement and perception. Maryland: Aspen Publishers, Inc. p 152–84.

Souchet N, Laplante S, 2007. Seasonal variation of co–enzyme Q_{10} content in pelagic fish tissues from Eastern Quebec. J Food Comp Anal 20(5):403–10.

Spiro TG, Gaber BP. 1977. Laser Raman scattering as a probe of protein structure. Ann Rev Biochem 46:553–72.

Strazisar M, Fir M, Golc–Wondra A, Milivojevic L, Prosek M, Abram V, 2005. Quantitative determination of coenzyme Q_{10} by liquid chromatography and liquid chromatography/mass spectrometry in dairy products. J AOAC Int 88(4):1020–7.

Strehle KR, Rosch P, Berg D, Schulz H, Popp J. 2006. Quality control of commercially available essential oils by means of Raman spectroscopy. J Agric Food Chem 54(19):7020–6.

Sultanbawa Y, Li–Chan ECY. 2001. Structural changes in natural actomyosin and surimi from Ling Cod (*Ophiodon elongatus*) during frozen storage in the absence or presence of cryoprotectants. J Agric Food Chem 49(10):4716–25.

Synytsya A, Copikova J, Matejka P, Machovic V. 2003. Fourier transform Raman and infrared spectroscopy of pectins. Carbohyd Polym 54(1):97–106.

Tang C, Hsieh F, Heymann H, Huff HE. 1999. Analyzing and correlating instrumental and sensory data: A multivariate study of physical properties of cooked wheat noodles. J Food Qual 22(2):193–211.

Thygesen LG, Lokke MM, Micklander E, Engelsen, SB. 2003. Vibrational microspectroscopy of food: Raman vs. FT–IR. Trends Food Sci Tech 14(1–2):50–7.

UC Berkeley Wellness Letter. 2003. Wellness guide to dietary supplements: Coenzyme Q_{10}. http://www.berkeleywellness.com/html/ds/dsCoenzymeQ10.php. Accessed 2008 Oct 13.

U.S. Department of Agriculture (USDA). 1996. The food guide pyramid. http://www.cnpp.usda.gov/Publications/MyPyramid/OriginalFoodGuidePyramids/FGP/FGPPamphlet.pdf. Accessed 2008 Oct 13.

U.S. Department of Agriculture, Agricultural Research Service. 2007. USDA national nutrient database for standard reference, release 20. Nutrient data laboratory home page, http://www.ars.usda.gov/ba/bhnrc/ndl. Accessed 2008 July 15.

U.S. Department of Agriculture, the Agricultural Marketing Service. 2008 July. Weekly national carlot meat report. Volume 17(028). Available from: Livestock & Grain Market News. Livestock & Seed Program, Des Moines, Iowa. http://www.ams.usda.gov/mnreports/lswwklyblue.pdf. Accessed 2008 July 20.

Walstra P. 2003. Soft solids. In: Walstra P, editor. Physical chemistry of foods. New York: Marcel Dekker, Inc. p 683–771.

Wang B, Xiong YL. 1998. Evidence of proteolytic activity and its effect on gelation of myofibrillar protein concentrate from bovine cardiac muscle. J Agric Food Chem 46(8):3054–9.

Weber C. 2001. Dietary intake and absorption of coenzyme Q_{10}. In: Kagan VE, Quinn PJ, editors. Coenzyme Q: molecular mechanisms in health and disease. New York: CRC Press LLC. p 209–26.

Weber C, Bysted A, Holmer G. 1997a. The coenzyme Q_{10} content of the average Danish diet. Int J Vit Nutr Res 67:123–9.

Weber C, Bysted A, Holmer G. 1997b. Intestinal absorption of coenzyme Q_{10} administered in a meal or as capsules to healthy subjects. Nutr Res 17(6):941–5.

Weber C, Sejersgard Jakobsen T, Mortensen SA, Paulsen G, Holmer G. 1994. Antioxidative effect of dietary coenzyme Q_{10} in human blood plasma. Int J Vit Nutr Res 64(4):311–5.

Weegels PL, Marseille JP, De Jager AM, Hamer RJ. 1991. Structure–function relationships of gluten proteins. In: Bushuk W, Tkachuk R, editors. Gluten proteins. Minnesota: The American Association of Cereal Chemistry, Inc. p 98–111.

Wellner N, Mills ENC, Brownsey G, Wilson RH, Brown N, Freeman J, Halford NG, Shewry PR, Belton PS. 2005. Changes in protein secondary structure during gluten deformation studied by dynamic Fourier transform infrared spectroscopy. Biomacromolecules 6(1):255–61.

Wiseman G. 2001. Durum wheat. In: Kill RC, Turnbull K, editors. Pasta and semolina technology. Iowa: Blackwell Science Company. p 11–42.

Wrigley CW. 1996. Biopolymers: giant proteins with flour power. Nature 381(6585): 738–9.

Yalcin A, Kilinc E, Sagcan A, Kultursay H. 2004. Coenzyme Q_{10} concentrations in coronary artery disease. Clin Biochem 37:706–9.

Yang H, Irudayaraj J, Paradkar MM. 2005. Discriminant analysis of edible oils and fats by FT–IR, FT–NIR and FT–Raman spectroscopy. Food Chem 93(1):25–32.

Yu Z, Ma C–Y, Yuen S–N, Phillips DL. 2004. Raman spectroscopic determination of extent of O–esterification in acetylated soy protein isolates. Food Chem 87:477–81.

Zhang Z, Inserra PF, Watson RR. 1997. Antioxidants and AIDS. In: Garewal HS, editor. Antioxidants and disease prevention. New York: CRC Press LLC. p 31–43.

Zhao YH, Manthey FA, Chang SKC, Hou H–J, Yuan SH. 2005. Quality characteristics of spaghetti as affected by green and yellow pea, lentil, and chickpea flours. J Food Sci 70(6):S371–76.

VITA

Khwankaew Dhanasettakorn was born in Chonburi, Thailand on April 17, 1978. Kookkik or Kik is her nickname. She was the first daughter of Mr. Prasert and Mrs. Pakatip Dhanasettakorn. She grew up in an amazing family and has one sister who is four years younger that her. She spent her childhood in Chonburi and studied at the Anuban Chonburi School up until 1990. After completing elementary school, she moved to Bangkok and attended TriamUdomSuksa Nomkloa School, Thailand. She earned her Bachelor's degree in Biotechnology from Mahidol University, Thailand, in 1999 and went on to attend the Institute of Nutrition, Mahidol University in Food and Nutrition for Development program. After receiving a Master of Science degree in 2002, she began teaching Food Fermentation at the undergraduate level in the department of Agro-industry at Rajamangala University of Technology, Thailand, where she taught for six months. Then she decided to pursue her doctoral degree in the United States. She started attending the Food Science program at the University of Missouri, Columbia in 2003 and received her doctoral degree in 2008.